

**Development of a Self-Cycling Fermentation Approach to Improve
Productivities for Ethanol Production**

by

Jie Wang

A thesis submitted in partial fulfillment of the requirements for the degree of

Doctor of Philosophy

in

Bioresource and Food Engineering

Department of Agricultural, Food & Nutritional Science

University of Alberta

© Jie Wang, 2020

Abstract

Biofuels have great potential to help secure the global energy supply and reduce greenhouse gas emissions. Taking cellulosic ethanol as an example, it is a biofuel produced from lignocellulosic material (e.g. wood and corn stover), which has the most abundant polymer on the planet. The production process starts with pretreatment and enzymatic hydrolysis, which generates sugars for fermentation into ethanol. The ethanol is then distilled into a high purity product. Despite the extensive technological developments achieved over the years for cellulosic ethanol production, the current industry is still faced with economic challenges, hindering its rapid expansion.

This thesis identifies the current industrial fermentation approach—performed in batch—as one of the primary limiting factors. This process requires extensive labor and long fermentation times, resulting in low productivity. In contrast, a self-cycling fermentation (SCF) approach with significant improvements in productivities were observed compared to conventional processing techniques. SCF is a semi-continuous, cycling fermentation technique that can be operated for a number of cycles; when cells arrive at stationary phase, half of the culture volume is automatically harvested and replaced by fresh medium to start the next cycle. Despite the integration of an SCF operation strategy into many microbial cultivation systems under aerobic conditions, there has been no successful report on its application to stable ethanol production.

This work aims to integrate the SCF approach into ethanol fermentation by automating the process and improving overall productivity. The first study mimicked the SCF approach using synthetic medium in shake flasks, where half of the culture volume was manually removed and replaced with sterile medium for a total number of five cycles. As a

result, stable patterns for glucose consumption and ethanol production were observed for SCF after cycle 1, but using only about 1/3 of the fermentation time of batch fermentation. This proved a proof-of-concept that SCF can help significantly increase ethanol volumetric productivity (the amount of ethanol produced by a cycle per working volume per cycle time) compared to batch fermentations performed under similar conditions.

To apply a real SCF strategy into ethanol production, the process needs to be automatically monitored and driven by a feedback control parameter. The second study successfully identified a real-time sensing parameter—gas flow rate—that revealed the flow rate of gas evolved from the fermenter under anaerobic conditions. With the incorporation of the gas flow meter, an SCF system using synthetic medium was successfully operated for ethanol production in a 5-L fermenter. A stable and robust behavior was observed, and the system was automatically operated for 21 cycles. More importantly, the ethanol volumetric productivity of SCF was substantially improved by over 35%, compared to batch.

Finally, to explore the use of feedstocks that would be more representative of the cellulosic ethanol industry, the enzymatic hydrolysate of wood pulp was fed into the newly established SCF system for ethanol production. The same feedback control parameter, gas flow rate, successfully drove the fermentation for 10 cycles, with remarkable improvement in ethanol volumetric productivity (54-82%) compared to batch. Interestingly, during the operation of SCF, cell flocculation was consistently observed as cycle number increased; this improvement will facilitate the downstream separation process. Taken together, this work demonstrated that an advanced cycling fermentation strategy can significantly improve ethanol productivity, which will contribute to a reduction of production cost for

the cellulosic ethanol industry, thus helping to overcome energy and environmental challenges.

Preface

This thesis is an original work performed by Jie Wang. A part of the thesis has been published, with others chapters submitted or in preparation for publication.

Chapter 3 was published as Wang, J., Chae, M., Sauvageau, D., & Bressler, D. C. (2017). Improving ethanol productivity through self-cycling fermentation of yeast: a proof of concept. *Biotechnology for biofuels* 10, 193. As the primary author, I designed, performed, and analyzed the experiments, and wrote the manuscript. Dr. Michael Chae was involved in experiment design and discussion, and helped write the manuscript. Dr. David C. Bressler and Dr. Dominic Sauvageau were the co-supervisors, and they discussed and designed experiments and proofread the manuscript.

Chapter 4 was published as Wang, J., Chae, M., Bressler, D.C., & Sauvageau, D. (2020). Improved bioethanol productivity through gas flow rate-driven self-cycling fermentation. *Biotechnology for Biofuels* 13, 14. <https://doi.org/10.1186/s13068-020-1658-6>. As the primary author, I designed and performed fermentations, analyzed samples, interpreted data, and wrote the manuscript. Under my guidance, Mr. Les Dean, an electrical advisor from the Department of Chemical and Materials Engineering, helped set up part of the fermentation hardware and launch the LabVIEW® software program. Dr. Michael Chae, Dr. David C. Bressler (supervisor), and Dr. Dominic Sauvageau (supervisor) joined in discussion of experimental plans and troubleshooting, and edited the manuscript.

Chapter 5 will be submitted for publication as Wang, J., Chae, M., Beyene, D., Sauvageau, D., & Bressler, D. C. Application of self-cycling fermentation using wood pulp hydrolysates for improved ethanol productivity. Dr. Tray Sato, a professor at the University of Wisconsin-Madison, provided the yeast *Saccharomyces cerevisiae* Y128 for this study. As the primary author, I was responsible for designing, performing, and analyzing experiments, data analysis, and writing the manuscript. Dr. Michael Chae helped me understand the genetic manipulation of the yeast, provided effective comments on aligning the fermentation strategy with metabolic pathways, and edited the manuscript. Dawit Beyene, a PhD student at the Bressler lab, provided the enzymatic hydrolysate as part of the medium component for the fermentation system. Dr. David C. Bressler and Dr. Dominic

Sauvageau were the supervisory authors who contributed to the experimental design, provided advice, participated in the data interpretation, and edited the manuscript.

“It is not the strongest of the species that survives, nor the most intelligent that survives. It is the one that is the most adaptable to change.”

-Leon C. Megginson’s paraphrase for the Origin of Species (by Charles Darwin)

Acknowledgments

I would like to acknowledge my supervisors Dr. David Bressler and Dr. Dominic Sauvageau for their enormous support and guidance throughout my program. Thank you for providing me with such a wonderful opportunity to work on this multi-disciplinary research project. The high standards on critical thinking abilities, the excellent platform to present to a broad range of audiences, and the freedom to guide my project and explore professional development outside the lab have shaped me into a better scientist. The inspirations I got from your mentorship in science, debate, and communication will keep driving me forward. Your outstanding vision and leadership throughout this process helped me grow and develop into a better person, more than I could have imagined.

I want to express my sincere gratitude to Dr. Lisa Stein and Dr. Jonathan Curtis for their contribution as great supervisory committee members to provide excellent advice and comments on my research from a different perspective. Lisa, thank you for the recommendation letter for my scholarship application, and I want to emphasize that your position as a successful female scientist encouraged me to carry on throughout the journey. Dr. Curtis, thank you for providing me with the opportunities to work with and learn from you as a teaching assistant (AFNS 499/599). It was a great experience! I also appreciate your time and efforts for giving me recommendations for my job applications. Many thanks to Dr. Bipro Dhar and Dr. Mario Jolicoeur for serving as my arm-length and external examiners, respectively. I appreciate the time you spent on reviewing my thesis. Thanks to Dr. John Wolodko for kindly being the Chair for my exam.

I must recognize the countless help I received from Dr. Michael Chae. Mike, with all the exceptional scientific challenges, experimental suggestions, and writing comments, you are truly appreciated as an incredible mentor for me. Thank you for pointing out my strength and weakness at the right times. Your encouraging email letter, gap-bridging efforts, and career suggestions have all made a difference to a young scientist like me. I also want to give special thanks to Dr. Justice Asmoning. Justice, thank you so much for your mental and experimental support during the two-year troubleshooting period of my research, the most difficult and challenging time. I am grateful for your sincere suggestions and kind help in life as well.

This research project was possible due to the financial support from BioFuelNet Canada, Natural Sciences and Engineering Research Council of Canada (NSERC), and Future

Energy Systems. I am also thankful for the travel grants from BioFuelNet Canada and the Department of Agricultural, Food and Nutritional Science (AFNS), as well as the scholarships from AFNS and the Faculty of Graduate Studies Research at the University of Alberta.

I want to give thanks to Dr. Noreen Willows for providing me with the opportunities to assist you for the course NUFS 223. I also appreciate the Government of Alberta for providing funding for the course, *The Entrepreneurship Mindset and Innovation Ecosystems*. Instructed by Dr. Tim Hannigan, the course not only significantly broadened horizons and shaped my mindset for entrepreneurship, but also continues to remind me to be a brave person when facing the unknowns and challenges. Many thanks to Mr. Jingui Lan, Ms. Nian Sun, and Ms. Julia Prochnau for their technical support in the lab. I also want to acknowledge Mr. Les Dean for his technical help on successful setup and debugging of my fermentation system.

I like to thank all my colleagues in the Bressler and Sauvageau labs, including but not limited to Birendra, Catherine, Chengyong, Dawit, Diana, Emily, Francesco, Hector, Janet (Jing), Jesse, Isabel, Lin, Michael, Olga, Roman, Tao, Vadim, Yadong, Yeling, Yeye, Yuko, and new lab mates. I also had a good time working with my summer students, David Leung and Gitanshu Bhatia, as well as with visiting PhD student Jorge Arturo Gonzalez Rios. The support I received from you all and the fun we had in group meetings, lunches, parties, the canoeing trip, soccer games, etc. made my research and life at the University of Alberta treasurable and unforgettable.

Last but not least, I would like to thank my family members, friends, and fiancé. To my family members, I am so proud of being born and raised up in an environment full of love, care, and support. Your passion, optimism, curiosity, friendliness, perseverance, and diligence have strongly influenced who I am today. I couldn't have gone this far without your trust, active listening, and open mind to disagreement. To my great friends, both in China and Canada, thank you for sharing and enriching my life at different stages. To Yeling, you have brought plenty of surprise and happiness to me. Your thoughtful arrangements and delicious meals during my tough times and crazy fermentation schedules have truly brightened up my day. Thank you for being so considerate and supporting me unconditionally.

Table of Contents

Chapter 1 Introduction.....	1
1.1 Background.....	1
1.2 Research objective	3
Chapter 2 Literature review	5
2.1 Biofuels.....	5
2.1.1 Ethanol.....	5
2.1.2 Global ethanol production	6
2.2 Feedstocks for ethanol production.....	8
2.2.1 1 st generation feedstock	8
2.2.1.1 Starch-based feedstocks.....	8
2.2.1.2 Sugar-based feedstocks	12
2.2.2 2 nd generation feedstocks	14
2.3 Ethanol fermentation.....	20
2.3.1 Microorganism and metabolic pathways.....	20
2.3.2 Batch fermentation.....	27
2.3.3 Fed-batch fermentation	30
2.3.4 Continuous fermentation	31
2.4 Self-cycling fermentation (SCF)	33
2.4.1 Feedback control of SCF	34
2.4.2 Productivity improvement.....	36
2.4.3 Cell synchrony	38
2.4.4 Existing cycling approaches for ethanol production.....	38
Chapter 3 Improving ethanol productivity through self-cycling fermentation of yeast: a proof of concept.....	41
3.1 Abstract	41
3.2 Introduction.....	42
3.3 Methods.....	44
3.3.1 Yeast, medium, and inoculum	44

3.3.2	Dynamic study of yeast fermentation	45
3.3.3	Cycling fermentation.....	45
3.3.4	Analytical methods	46
3.3.5	Statistical analysis.....	47
3.4	Results.....	47
3.4.1	Dynamic study of batch fermentation.....	47
3.4.2	Cycling study.....	48
3.4.3	Annual ethanol productivity for potential scale-up.....	53
3.5	Discussion.....	57
3.5.1	Dynamic study.....	57
3.5.2	Cycling study.....	58
3.5.3	Annual ethanol productivity for potential scale-up.....	61
3.6	Conclusions.....	62
3.7	Funding.....	63
Chapter 4 Improved bioethanol productivity through gas flow rate-driven self-cycling fermentation.....		64
4.1	Abstract	64
4.2	Background.....	65
4.3	Methods.....	67
4.3.1	Media and yeast	67
4.3.2	Fermentation system.....	68
4.4	Results.....	71
4.4.1	Identification of a monitoring parameter for SCF	71
4.4.2	Assessing the requirements for ergosterol and Tween 80 in anaerobic SCF	75
4.4.3	Demonstration of automated SCF operation.....	78
4.4.4	Improvements in productivity	85
4.5	Discussion.....	86
4.5.1	The monitoring parameter for anaerobic SCF	86
4.5.2	Assessing the requirements for ergosterol and Tween 80 in anaerobic SCF	88
4.5.3	Demonstration of automated SCF operation.....	89

4.6	Conclusions.....	91
4.7	Acknowledgements.....	91
Chapter 5 Application of self-cycling fermentation using wood pulp hydrolysates for improved ethanol productivity.....		92
5.1	Abstract.....	92
5.2	Introduction.....	92
5.3	Methods.....	94
5.3.1	Medium and yeast.....	94
5.3.2	Fermentation.....	95
5.3.3	Sample analysis.....	97
5.4	Results.....	97
5.4.1	Hydrolysates from wood pulp.....	98
5.4.2	Batch fermentation using wood pulp hydrolysate.....	98
5.4.3	Incorporation of the wood pulp hydrolysate in SCF.....	100
5.4.4	Improvement in productivity.....	104
5.4.5	Second fermentation stage.....	106
5.5	Discussion.....	109
5.5.1	Hydrolysates from wood pulp.....	109
5.5.2	Batch fermentation using the wood pulp hydrolysate.....	109
5.5.3	Incorporation of the wood pulp hydrolysate in SCF.....	111
5.5.4	Improvement in productivity.....	112
5.5.5	Second fermentation stage.....	112
5.6	Conclusions.....	114
5.7	Acknowledgments.....	114
Chapter 6 Summary, conclusion, and future directions.....		115
6.1	Summary and conclusion.....	115
6.2	Future directions.....	116
Bibliography.....		120
Appendix A: supplementary material for Chapter 4.....		135
Appendix B: supplementary material for Chapter 5.....		142

List of Table

Table 3.1 Cycling fermentations and overall productivity improvement.	51
---	----

List of Figures

Figure 2.1 Annual production volume of ethanol in the United States. This figure was produced using data from Bai <i>et al.</i> in 2008 [53] and the Department of Energy in 2019 [54].	7
Figure 2.2 Glucose linkages within starch. The structure was drawn by adapting from Maity in 2015 [66].	9
Figure 2.3 The starch to ethanol production process (dry-grind). This diagram was adapted from Naik <i>et al.</i> in 2010 [62] and Koehler <i>et al.</i> in 2019 [44].	10
Figure 2.4 The production of ethanol from sugarcane. The process described is adapted from Dias <i>et al.</i> in 2010 [81] and Ingledew <i>et al.</i> in 2009 [19].	13
Figure 2.5 Chemical structure of cellulose (a) and a sketch of lignocellulosic material (b). For figure (b), black, red, and blue lines represent cellulose, hemicellulose, and lignin, respectively. Cellulose structure is drawn with crystalline and amorphous regions. Figure (b) was adapted from Mosier <i>et al.</i> in 2005 [96].	15
Figure 2.6 The steps to produce cellulosic ethanol.	16
Figure 2.7 The metabolic pathway for ethanol production using glucose as the carbon source for <i>S. cerevisiae</i> (figure adapted from Jacques <i>et al.</i> in 2003 [65] and Ingledew and Lin in 2011 [60]). “P” represents phosphate, and TCA represents tricarboxylic acid.	22
Figure 2.8 The synthesis of ergosterol in yeast cells. Wine chemistry and biochemistry by Moreno-Arribas, M. Victoria, Polo, M. Carmen [118]. Reproduced with permission of Springer in the format Thesis/Dissertation via Copyright Clearance Center. Minor modification was made for the figure.	23
Figure 2.9 The synthesis of unsaturated fatty acids in yeast cells. Wine chemistry and biochemistry by Moreno-Arribas, M. Victoria, Polo, M. Carmen [118]. Reproduced with permission of Springer in the format Thesis/Dissertation via Copyright Clearance Center. Minor modification was made for the figure.	24
Figure 2.10 Major microbial pathways for converting xylose into xylulose. Adapted from Santos <i>et al.</i> in 2016 [5] and McMillan in 1993 [124].	26

Figure 2.11 Common pathway for xylose fermentation to ethanol. Adapted from Santos *et al.* in 2016 [125] and McMillan in 1993 [124]. Note that the enzymes for glycolysis and ethanol production pathways are not shown here (can be seen on Figure 2.7)..... 27

Figure 2.12 Cell growth during batch fermentation. Adapted from Ingledew *et al.* in 2009 [19]. 28

Figure 2.13 Fermentation process for cellulosic ethanol in a batch mode..... 30

Figure 2.14 Fermentation process in fed-batch mode. Fresh medium is constantly added and the fermentation volume in the reactor increases throughout the run. 31

Figure 2.15 A schematic diagram of continuous fermentation. The flow rate of the input medium and output culture are well controlled to be the same rate. Adapted from Jacques *et al.* in 2003 [65]. 32

Figure 2.16 A schematic presentation of SCF operation. The system uses one fermenter monitored by a feedback control parameter, which automatically triggers the removal and replacement of half of the culture inside the fermenter..... 34

Figure 3.1 Dynamic study of batch fermentation in shake flasks. Optical density (OD₆₀₀), pH, glucose consumption, and ethanol production were monitored over a 46 h period. Error bars represent standard deviation of triplicate experiments..... 48

Figure 3.2 Cycling fermentation experiments in shake flasks. OD₆₀₀ (a), glucose concentration (b), ethanol content (c), and pH (d) of the culture were monitored through 5 cycles over a 47 h period. The cycle numbers are indicated with roman numerals. Error bars represent standard deviation of triplicate experiments, except for the OD₆₀₀ value at 40.9 h in Figure 3.2a (the end of cycle 4), which shows the result of duplicate samples (see Materials and methods). Means that do not share the same letter are statistically different (95% confidence level, Tukey). 50

Figure 3.3 Productivities of cycling fermentation experiments conducted in shake flasks. Ethanol volumetric productivity (a), specific productivity (b), and overall productivity (c) were determined for manual cycling experiments. The horizontal solid line represents the mean values obtained through a dynamic batch study (Figure 3.1), where ethanol production reached a plateau at ~20.5 h. Error bars represent standard deviation of triplicate experiments, except for cycle 4 in Figure 3.3b, which represents duplicate

samples (see materials and methods). Means that do not share the same letter are statistically different (95% confidence level, Tukey)..... 53

Figure 3.4 Annual ethanol productivity derived from experiments using shake flasks. Annual ethanol productivity was calculated assuming the number of consecutive cycles operated for each SCF campaign could range from 1 to 100. The horizontal solid line represents the mean values obtained through a dynamic batch study (Figure 3.1), where ethanol production reached a plateau at ~20.5 h. Error bars were calculated from the errors in ethanol yield and cycle time of SCF cycles and represent standard deviation of triplicate experiments..... 56

Figure 4.1 Bioreactor set up for Self-Cycling Fermentation (SCF). The temperature control and the pH probe are not shown. The control gauge for N₂ pressure from the gas cylinder was set to 4 psig during fermentation. The various components displayed in this schematic are not necessarily represented in their actual locations..... 72

Figure 4.2 Batch fermentation. Samples were taken at different intervals during fermentation to analyze biomass contents (a), as well as glucose and ethanol concentrations (b). The data reported is the average from triplicates, with error bars representing standard deviations. The pH (a) and flow rate of the gas released during fermentation (c) were monitored in real-time, and the slope of the flow rate (d) was automatically calculated. A vertical line was added to all graphs at 23.6 h, corresponding to the sharp minimum in slope of gas flow rate (d). The gas flow rate was reported in cubic centimeter per minute (ccm) at 25 °C and 1 atm, and the slope of the gas flow rate was measured in cubic centimeter per minute per cycle time (ccm/h)..... 74

Figure 4.3 Ergosterol and Tween 80 supplementation. SCF was performed using medium without (cycles 1-4, 9-14, and 19-24) or with (cycles 5-8, 15-18, and 25-28) the supplementation of ergosterol (0.02 g/L) and Tween 80 (0.8 g/L). The cycle time (a), pH of the culture (b), as well as gas flow rate (c) and its slope (d) were reported. The cycle numbers were labeled at the top of each figure, with the exception of (a) where the cycle numbers were indicated on the x-axis. Cycles with supplementation were shaded in (b), (c), and (d). Underlined cycle numbers indicate cycles that did not meet criteria for automated cycling and that were thus manually triggered. Cycle 15 and part of cycle 16 were removed

from Figure (c) and (d) due to excessive flow of nitrogen entering the fermenter as a result of nitrogen regulator failure. 77

Figure 4.4 Analysis of samples from SCF demonstration. Cycle time (a) amount of biomass (b), and concentrations of glucose (c) and ethanol (d) were plotted for the beginning and end of all cycles. Medium supplemented with ergosterol (0.02 g/L) and Tween 80 (0.8 g/L) was used for cycles 1~17; the concentrations of ergosterol and Tween 80 were tripled for the remaining cycles. Cycle 4 was disrupted by halting agitation and temperature control for ~7 h. Cycle numbers were labeled at the initial stage of each cycle, with the exception of (a) where the cycle number was indicated on the x-axis. The horizontal line in (a) represents the fermentation time for batch operated under similar conditions (Additional Table 1 in Appendix A). In (b-d) data is reported as the average from at least three replicates, with error bars representing standard deviations. 81

Figure 4.5 Online monitoring parameters from SCF demonstration. Gas flow rate (a), slope of gas flow rate (b), total volume of gas evolved per cycle (c), and pH (d) were monitored throughout SCF operation. Medium supplemented with ergosterol (0.02 g/L) and Tween 80 (0.8 g/L) was used for cycles 1-17; the concentrations of ergosterol and Tween 80 were tripled for the remaining cycles. Cycle 4 was disrupted by halting agitation and temperature control for ~7 h. Cycle numbers were labeled at the top of each figure, with the exception of (c) where the cycle numbers were indicated on the x-axis. The horizontal line in (c) represents the total volume of gas evolved in batch operation conducted under similar conditions (Additional Figure 4c in Appendix A)..... 83

Figure 4.6 Ethanol volumetric productivity during SCF. Medium supplemented with ergosterol (0.02 g/L) and Tween 80 (0.8 g/L) was used for cycles 1~17; the concentrations of ergosterol and Tween 80 were tripled for the remaining cycles. Cycle 4 was disrupted by halting agitation and temperature control for ~7 h. The horizontal line represents the volumetric productivity in batch operation conducted under similar conditions. The data reported is the average from at least three replicates, with error bars representing standard deviations..... 85

Figure 5.1 Overview of the proposed strategy for producing ethanol from wood pulp. Wood pulp was put together with one Canadian dollar for size comparison. 98

Figure 5.2 Batch fermentation of wood pulp hydrolysate-based medium. Parameters monitored included sugars and ethanol (a), pH (b), evolved gas flow rate (c), and its slope (d). Means from analytical triplicates are reported in panel (a), with error bars representing standard deviation. For panel (c), ccm represents cubic centimeter of gas evolved per minute at 25 °C and 1 atm. For panel (d), the slope of the gas flow rate was reported in cubic centimeter per minute per cycle time (ccm/h).....100

Figure 5.3 SCF operation using wood pulp hydrolysate-based medium. Dry cell weight (a), glucose content (b), xylose content (c), and ethanol titer (d) as a function of fermentation time. Cycle numbers are indicated at the beginning of each cycle. Means from analytical triplicates are reported, with error bars representing standard deviation.....101

Figure 5.4 Online monitoring parameters during SCF operation using wood pulp hydrolysate. Evolved gas flow rate (a), slope of evolved gas flow rate (b), total volume of gas produced per cycle (c), and pH (d) as a function of fermentation time. Cycle numbers are indicated at the top of the curves for each cycle, except for panel (c), where cycle numbers were indicated on the x-axis. The horizontal line in panel (c) represents the total gas evolved at the time the minimum in slope is reached during batch operation (Additional Figure 7b in Appendix B) under similar conditions. For panels (a) and (b), ccm represents cubic centimeter of gas evolved per minute.....102

Figure 5.5 Kinetic study of SCF cycle 10. Dry cell weight (a), glucose content (b), xylose content (c), and ethanol titer (d) as a function of cycle time. Means from analytical triplicates are reported, with error bars representing standard deviation.....104

Figure 5.6 Cycle time and ethanol volumetric productivity observed during SCF operation. Cycle time (a) and ethanol volumetric productivity (b) were calculated for each SCF cycle. Horizontal lines for panel (a) and (b) represent the cycle time and ethanol volumetric productivity, respectively, obtained from batch fermentation.....105

Figure 5.7 Second fermentation stage using wood pulp hydrolysate-based medium. At the end of each SCF cycle, the harvested culture was transferred into shake flasks for a second fermentation stage. This second stage was stopped when the concurrent SCF cycle ended, such that the cycle time was equal for both stages. Dry cell weight (a), xylose content (b),

and ethanol titer (c) were analyzed for each cycle of SCF at the beginning and the end of the second fermentation stage.108

List of abbreviations

GHG	greenhouse gas
HPLC	high performance liquid chromatography
GC	gas chromatography
SCF	self-cycling fermentation
FFV	flexible fuel vehicle
SSF	simultaneous saccharification and fermentation
DDGS	distiller's dried grains with solubles
NREL	National Renewable Energy Laboratory
SHF	separate hydrolysis and fermentation
HHF	hybrid hydrolysis and fermentation
CBP	consolidated bioprocessing
CNC	cellulose nanocrystal
ATP	adenosine triphosphate
NADH	nicotinamide adenine dinucleotide
TCA	tricarboxylic acid
NADPH	nicotinamide adenine dinucleotide phosphate
CER	carbon dioxide evolution rate
GOPOD	glucose oxidase/oxidase
OD ₆₀₀	optical density at 600 nm
YNB	yeast nitrogen base
YPD	yeast extract peptone dextrose
P_{batch}, P_{SCF}	annual ethanol productivity (ton/year) for batch and SCF, respectively
t_{annual}	annual fermentation operation time, h
$t_{f-batch}, t_{d-batch}$	for a single batch campaign, the residence time (h) and downtime (h), respectively
C_{batch}, C_{SCF}	ethanol titer produced per cycle (g/L) in batch and SCF, respectively
N_{batch}, N_{SCF}	the number of campaigns possible in a year for batch and

	SCF, respectively
V	working volume, L
x	for a single SCF campaign, assumed numbers of cycles that a plant can continuously run
$t_{f-cycle 1}, C_{f-cycle 1}$	for the first cycle of an SCF campaign, the residence time took (h) and the titer of ethanol produced (g/L), respectively
$t_{f-subsequent cycles}, C_{f-subsequent cycles}$	for cycles following the first one in an SCF campaign, the residence time the cycle took (h), and the titer of ethanol it produced (g/L), respectively
$t_{d-(x-1) cycles}$	down time (h) for each cycle in a single SCF campaign, except cycle x
$t_{d-cycle x}$	down time for cycle x (the last cycle) in a single SCF campaign
$t_{f-SCF}, t_{d-SCF}, E_{SCF}$	for a single SCF campaign with x cycles, the total of residence time (h) and the total downtime (h), and the total amount of ethanol produced (g), respectively
ccm	the unit of gas flow rate, cubic centimeter per minute
ccm/h	the unit for slope against cycle time, cubic centimeter per minute per cycle time
$[G]_t$	the concentration of glucose at time t (g/L)
$[G]_o$	the initial concentration of glucose (g/L)
$V_{g, Total}$	the total volume of gas evolved (L)
$V_{g,t}$	the volume of gas evolved from the onset of fermentation to time t (L)
$[EtOH]_t$	the concentration of ethanol at time t (g/L)
$[EtOH]_{Total}$	the final concentration of ethanol produced during the fermentation (g/L)

Chapter 1 Introduction

1.1 Background

Of all biofuels, ethanol is the most widely used for transportation [1,2]. Cellulosic ethanol is produced from lignocellulosic materials, the most abundant feedstock on the planet [3,4]. As a renewable source of fuel, ethanol represents a great opportunity to help meet future energy demands and reduce greenhouse gas (GHG) emissions. Consequently, the production of cellulosic ethanol has been attracting plenty of interests from all over the world [5].

Lignocellulosic feedstocks contain three types of polymers: cellulose, hemicellulose, and lignin. Cellulose and hemicellulose are mostly composed of sugars and contribute to the production of ethanol, while lignin consists of aromatic compounds that are considered as valuable by-products [5–8]. Owing to the complexity and rigidity of this feedstock, the production of cellulosic ethanol typically involves a pretreatment to open up its complex structure, so that hydrolyzing enzymes can gain access to cellulose and hemicellulose and convert them into monomer sugars. The monomer sugars are then fermented to produce ethanol, and the final ethanol product is then separated by distillation [9].

Over the past few decades, ethanol production technologies have improved tremendously, with a primary focus on improving the efficiency and reducing the costs of pretreatment and enzymatic hydrolysis [5,9–14]. However, the production of cellulosic ethanol is still faced with major technological hurdles and limited by its relatively high production costs, which hinder the rapid growth of the industry [15–17]. Compared to pretreatment and enzymatic hydrolysis, less attention has been given to improve the process of fermentation itself, even if the processing strategy used for fermentation plays a paramount role in ethanol production [10].

Current fermentation strategies for cellulosic ethanol production are primarily based on batch process. For this operation, medium and inoculum are added to the fermenter to initiate fermentation; once it is completed, the culture is subject to downstream distillation, and the fermenter is then cleaned, sterilized, and refilled with fresh medium to start a new batch [18,19]. This batch approach, despite its ease of

operation, has many limitations. For instance, the process is rarely well controlled. In general, ethanol fermentations require intensive labor to monitor the process; samples are taken at various intervals, prepared, and analyzed using expensive equipment, such as high performance liquid chromatography (HPLC) and/or a gas chromatography (GC) [19,20]. In addition, seed cultures need to be prepared for each batch fermentation, which represents a time-consuming multiple scale-up process [18,19]. Inside the batch fermenter, cells grow through lag, exponential, and stationary phases, but no significant production of ethanol occurs in either the lag or stationary phase [19]. Overall, these factors contribute to batch fermentation having relatively low productivity [10]. Work is thus required to advance fermentation systems to improve the performance of the overall ethanol production process.

In contrast to batch operation, self-cycling fermentation (SCF) strategies have been shown to improve productivity in many microbial production systems, such as the production of surfactant [21], protein [22], shikimic acid [23], etc. SCF is a semi-continuous cycling technique, which essentially builds on sequential batch fermentations; but upon the onset of stationary phase, half of the culture volume is automatically removed and replaced with fresh, sterile medium to start the next cycle [24]. This ratio of one half implies each cycle corresponds to one doubling, or one generation, of the microorganism. Theoretically, the process can be repeated for a large number of cycles [25–29]. SCF is automated using a real-time sensing parameter that is related to cellular growth and capable of indicating the onset of stationary phase. Once the onset of stationary phase is identified, the cycling process can be initiated [24]. Through SCF operation, the lag and stationary phases can be eliminated, and, as a consequence, the fermentation time is significantly reduced, also enhancing productivity. As mentioned above, such improved productivity has been achieved using SCF applied to many microbial fermentation systems, primarily under aerobic conditions [21–23,29].

Although SCF has been used for many fermentation schemes, it has not yet been successfully implemented for ethanol production. This is likely due to the complexity of the feedstocks and the requirement of anaerobic conditions. Whether the ethanol fermentation

process can be automatically monitored in real-time, and whether SCF can help improve productivity in ethanol production in industrial settings remains as important questions.

1.2 Research objective

The primary focus of this thesis is the investigation of the feasibility and performance of applying SCF to ethanol production, with the aim to automate the fermentation process and improve productivity. It is hoped that this research can help the cellulosic ethanol industry become more economically competitive.

This major objective will be achieved by addressing the following questions in succession:

1) Can a manual cycling approach simulating SCF at the scale of 500-mL shake flask and using a synthetic medium as feedstock help improve ethanol productivity?

2) Can SCF be implemented for ethanol fermentation using a synthetic medium as feedstock under anaerobic conditions? If so, can an SCF system be designed and constructed to improve ethanol productivity in a 5-L fermenter?

3) Can this newly developed SCF system be operated using a medium derived from lignocellulosic materials as feedstock and will it have the same benefits in term of ethanol productivity?

The three questions above are answered in Chapter 3: Improving ethanol productivity through self-cycling fermentation of yeast: a proof of concept, Chapter 4: Improved ethanol productivity through gas flow rate-driven self-cycling fermentation, and Chapter 5: Application of self-cycling fermentation using wood pulp hydrolysates for improved ethanol productivity, respectively.

Specifically, a five-cycle proof-of-concept study was performed at shake flask scale (Chapter 3). This mimicked SCF operation through manual cycling of the fermentation at the end of each cycle. The length of each cycle was determined based on the time required to utilize the glucose within the medium, which was determined through continual sampling. Results showed stable production patterns of ethanol and biomass (measured by optical density), as well as significant improvements with regards to ethanol productivity. Hence, the research proceeded towards building, implementing, and testing a real SCF system using a 5-L fermenter under anaerobic conditions using a synthetic medium as

feedstock (Chapter 4). The evolved gas flow rate was identified as a suitable parameter to indicate the onset of stationary phase for ethanol fermentation under anaerobic conditions and was consequently incorporated as a cycling criterion for the SCF system. As a result, the SCF system showed repeatable and robust behavior for over 20 cycles, and dramatically improved the ethanol productivity. As an interesting phenomenon, cell flocculation was observed during the operation of SCF. Hence, dry cell weight was used for biomass measurements. Finally, a real feedstock, obtained from the hydrolysis of wood pulp, was incorporated into the SCF system (Chapter 5). The wood pulp hydrolysate was fed to the SCF which was run for 10 cycles. The automated cycling strategy achieved stable operation and significant improvements in productivities.

Chapter 2 Literature review

2.1 Biofuels

Worldwide energy consumption increased to around 11 billion equivalent tons of oil in 2018 [15,30]. Based on projected population growth, the global demand for energy is predicted to increase by approximately 30% by the year 2040 [30,31], yet this demand is unlikely to be met by the oil and gas industry alone [32]. In addition to energy supply, the world needs technologies with a lower carbon intensity due to environmental concerns [30,33]. Through the Paris Agreement, a global goal was set to keep average temperature increase below 2 °C above pre-industrial levels, with a main focus on decreasing GHG emissions [34]. Promisingly, the production of renewable energy – including biofuel, wind power, solar, geothermal, and marine tidal energy – has been increasing, becoming the fastest growing energy source to help relieve carbon emission problems [30].

Of the global energy consumption, 21% comes from the transportation sector, and its demand is projected to grow strongly for the next couple of decades [30]. Biofuels are the primary renewable energy in the transportation sector. They consist of a solid, liquid, or gaseous fuel, such as ethanol, butanol, hydrogen, methane, biogas, and fatty acids, and can be obtained from the conversion of biomass including plant matter, vegetable oils, animal fats, algae, municipal solid waste, sewage, etc. [35,36]. The production of biofuels is expected to increase by 15% between 2017 and 2023 [37]. It was also estimated that by 2040, the demand for biofuels would be at least 3-fold greater than it was in 2015 [38].

2.1.1 Ethanol

Ethanol is currently the most important biofuel [39] and the most widely applied in the transportation sector [1,2]. It is a two-carbon alkane with one hydrogen substituted by a hydroxyl group: $\text{CH}_3\text{CH}_2\text{OH}$ (molecular weight: 46.07 g/mol). It has a density of 0.789 g/cm³ at 20 °C, a boiling temperature of 78.2 °C at 1 atm, and a melting point of -114.1 °C. It is colorless and miscible with water [40].

Clean and renewable, ethanol can be used as a fuel alternative or homogeneously blended with gasoline for transportation [1]. A common blend ratio between ethanol and gasoline is at or below 10% (E10), generally regarded as requiring no modification of

automobile engines [41,42]. With engine modification, the blend ratio can be higher [43]; for instance, reaching 51-83% for flex fuel vehicles (FFVs). Such high ethanol level fuels have been used for multiple vehicle brands and models, such as Chrysler 300, Chevrolet Express, Dodge Grand Caravan, Ford Escape, GMC Savana, Jeep, Toyota, etc. [44].

Ethanol can help improve engine performance. It contains 35% oxygen [5], making it a fuel additive to petroleum gasoline which has no oxygen itself [45]. As such, ethanol functions as an oxygenate, to promote a more complete combustion and a lower emission of toxic chemicals [43]. It is also recognized that, as a fuel source, ethanol has its limitations; for instance, a lower volumetric energy content compared to gasoline, which means a tank would need to be filled more frequently to drive similar distances [42,46]. In addition, since ethanol is fully miscible with water, it is not feasible to transport it with gasoline, as this would lead to phase separation inside pipes [47].

Production-wise, ethanol can be obtained from various bio-based resources, including wheat straw, which absorbs atmospheric CO₂ as the plant grows. Despite the fact that upon combustion in engines, the carbon is returned to the atmosphere, overall life-cycle analyses still show a considerable net reduction of CO₂, compared to gasoline [44]. Specifically, on a life-cycle basis, ethanol produced from renewable materials can reduce the carbon intensity by 19% to 115% when compared to gasoline, depending on the type of feedstock used for the production [48]. In addition to ethanol, high value by-products (see Section 2.2) are obtained through a full utilization of biomass and the implementation of strategic processing approaches [15,48–50].

2.1.2 Global ethanol production

The world experienced a quick increase in the production of ethanol, from around 15 billion liters per year in 1990s [51] to 120 billion liters in 2017 [52]. As indicated by Figure 2.1, the US ethanol production, for which corn grain has been used as the major feedstock, gradually increased in the 1990s but really started to boom around 2002 [53,54], and since 2005, the US has become the largest ethanol producing country in the world [55]. In 2018, it produced approximately 61 billion liters of ethanol (Figure 2.1) [54], followed by Brazil with an estimated at ~31 billion liters using a different feedstock—sugarcane [56].

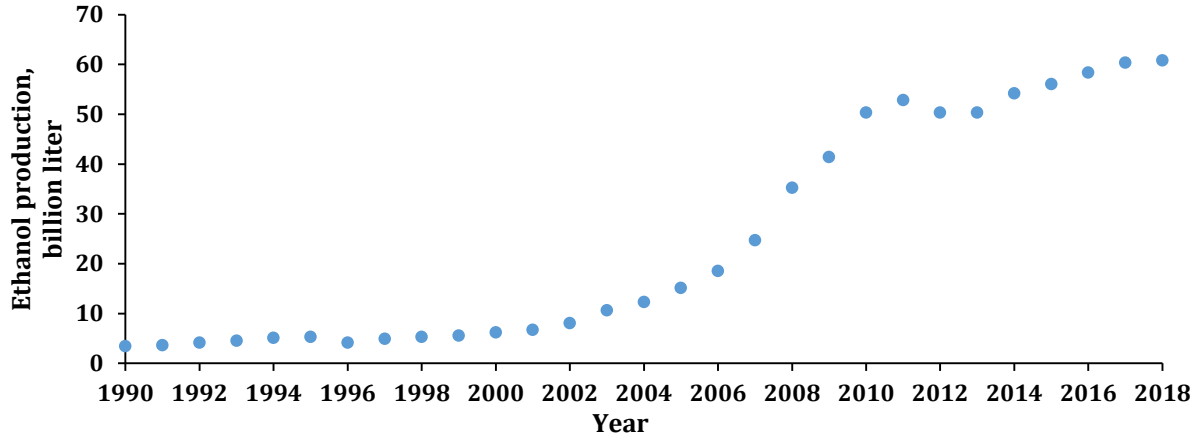


Figure 2.1 Annual production volume of ethanol in the United States. This figure was produced using data from Bai *et al.* in 2008 [53] and the Department of Energy in 2019 [54].

The United States and Brazil currently dominate the global ethanol production, and the scenario is projected to continue with 80% of the global production achieved by these two countries in 2023 [37]. By 2027, China is expected to become the third leading country for ethanol production, with around 11 billion liters ethanol; meanwhile, global annual ethanol production is estimated to be approximately 131 billion liters [52]. Assuming a price of 0.35 USD/L [57], this amount of ethanol production would represent a ~46 billion-dollar industry.

Based on a report from the Food and Agriculture Organization of the United Nations, the major feedstocks currently used for ethanol production (i.e. grains and sugarcane) are expected to dominate ethanol production in the near future [52], owing to their mature production technologies. Although ethanol production from lignocellulosic feedstock became a commercial reality in the mid-2010s [5], since then the industry has experienced several ups and downs, and limited development in production capacity was observed [56,58]. Hence, technological barriers and economic challenges need to be overcome to ensure the future success of the cellulosic ethanol industry [17].

2.2 Feedstocks for ethanol production

The feedstocks used for ethanol production mostly fall within two categories—1st generation ethanol is primarily produced from starch- and sugar-based materials, while 2nd generation ethanol mainly comes from lignocellulose. This Section talks about the processes of ethanol production from 1st and 2nd generation feedstocks from a general and global perspective. Further details on yeast metabolism and fermentation strategies are included by Sections 2.3 and 2.4.

2.2.1 1st generation feedstock

Approximately 60% of the global ethanol production comes from grain crops that are rich in starch. These feedstocks include, but are not limited to, corn, wheat, barley, rye, rice, oat, cassava, potato [55,59,60]. The remaining portion of ethanol production mostly comes from sugar-based materials, such as sugarcane, sugar beets, sweet sorghum, fruits, palm juice, etc. [19,61,62].

2.2.1.1 Starch-based feedstocks

Starches, despite their different shapes and sizes, are insoluble granules [63,64]. They are polymers composed of a large number of glucose monomers linked by α -1,4- and α -1,6-glycosidic bonds (Figure 2.2). Two forms of starch co-exist in the feedstocks. One is a linear amylose chain, which has up to 1,000 glucose units linked by α -1,4-glycosidic bonds and, for example, amylose accounts for 10-27% of the total corn starch (Figure 2.2). The remaining portion is present as amylopectin, which contains the same α -1,4-glycosidic bonds as amylose, but is also branched through α -1,6-glycosidic linkages (Figure 2.2). The number of glucose units in amylopectin is much larger than amylose, being as high as 10,000 [64,65]. *Saccharomyces cerevisiae*, the mostly commonly used yeast for ethanol fermentation [53,60], does not possess amylase or glucosidase, two enzymes that facilitate digestion of starch polymers into simple sugars which can then be fermented into ethanol [55,64].

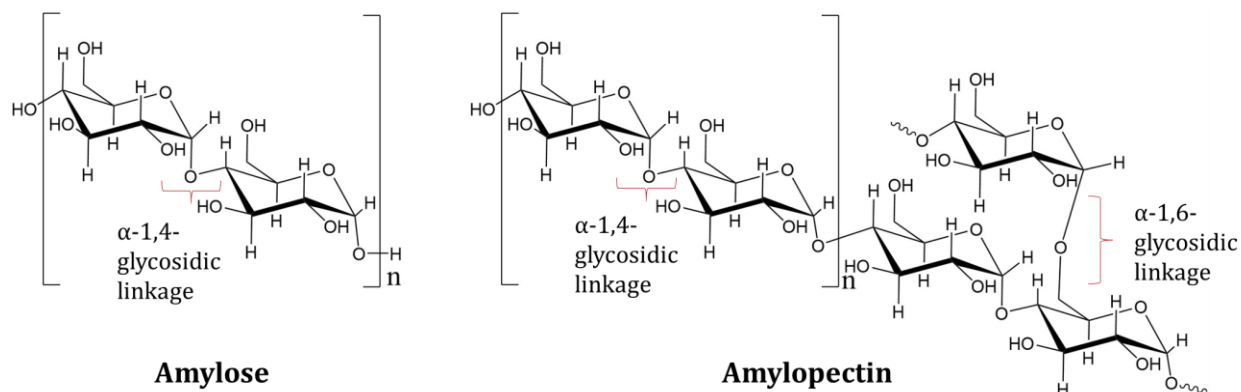


Figure 2.2 Glucose linkages within starch. The structure was drawn by adapting from Maity in 2015 [66].

Taking corn as an example to introduce the overall ethanol production process, corn kernels contain starch (61-78%), protein (6-12%), and fat (3-6%), along with a small amount of fiber, sugar, and minerals [19,67,68]. For ethanol production, kernels are ground into granules of appropriate size to promote subsequent water penetration and enzymatic digestion [65]. Depending on the initial treatment of corn grains, ethanol comes from either dry or wet milling processing. Dry-grind mill facilities account for nearly 90% of the ethanol plants in the United States [44], and the corresponding process of ethanol production from starch-rich materials is presented in Figure 2.3. After mixing with water, the milled grains absorb water and form a mash, which is then subjected to cooking and liquefaction at high temperatures (90-120 °C) for 1-2 hours [64,69]. During liquefaction, thermally stable amylase is added to the mash, to randomly hydrolyze α -1,4-glycosidic bonds and reduce the size of starch polymers into dextrans, which are more soluble in water and less viscous than the original starch polymers [60,64]. After liquefaction, the mash is cooled for saccharification. Glucoamylase enzymes are then added to cleave both α -1,4- and α -1,6-glycosidic bonds and produce mono- or disaccharides, such as glucose and maltose [19,59]. Overall, as high temperature is required for liquefaction, excess energy input is required, representing approximately 10-20% of the value of the final ethanol product [63].

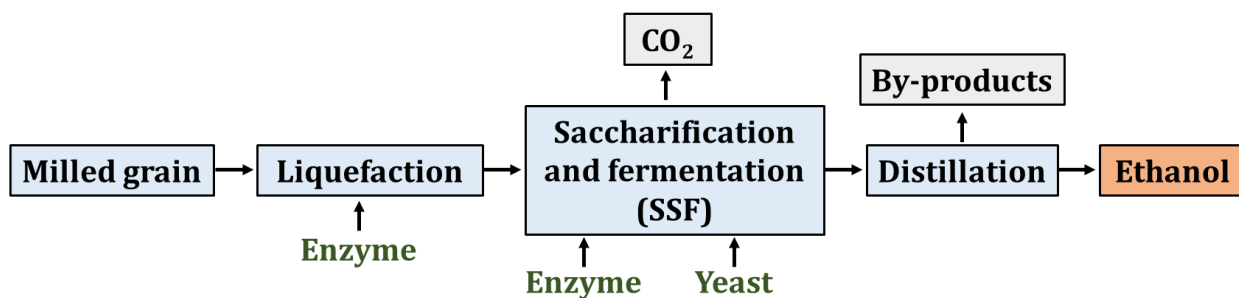
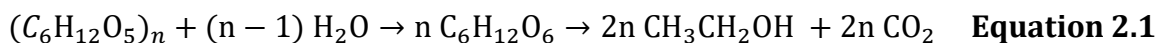


Figure 2.3 The starch to ethanol production process (dry-grind). This diagram was adapted from Naik *et al.* in 2010 [62] and Koehler *et al.* in 2019 [44].

Due to the development of improved enzyme technologies, the liquefaction temperature can now be substantially reduced. A raw starch-hydrolyzing enzyme mixture, for instance, Stargen™ 001, contains a modified cocktail of amylase and glucoamylase with high enzymatic activity. The cocktail enzymes can work synergistically to break down raw starch granules into dextrans at low temperature (≤ 48 °C) and also to hydrolyze dextrin into monomer sugars [69,70]. By performing liquefaction with raw starch-hydrolyzing enzymes at low temperature, the energy demand of the process can be substantially reduced [63].

After saccharification, sugars are ready to be consumed by yeast for ethanol production via fermentation. Urea or ammonium sulfate is supplemented to the mash as a nitrogen source for yeast growth [64,69,70]. Yeast, which is usually commercially purchased, is used to inoculate cultures up to a cell number of $\sim 10^7$ per mL of mash [60,69,71]. The yeast *S. cerevisiae* is able to efficiently produce ethanol under anaerobic condition, according to Equation 2.1 ($n > 1$) [59]. The detailed metabolic pathway for the conversion of sugar to ethanol is presented in Section 2.3.1. Theoretically, 0.9 g of starch can be hydrolyzed into 1 g of glucose, which would be converted into 0.51 g of ethanol and 0.49 g (approximately 0.25 L) of CO_2 [19,59]. However, the maximum fermentation efficiency (actual amount of ethanol produced per glucose divided by 0.51 g) is less likely to reach beyond 93%, as yeast cells also use glucose to build biomass and other molecules, including acetate and fatty acids [53,72].



The current starch-to-ethanol industry integrates saccharification and fermentation into a single reactor through a process called simultaneous saccharification and fermentation (SSF; Figure 2.3). The SSF begins with a short pre-saccharification of the mash at around 50 °C to release initial amounts of sugars, followed by a reduction in temperature to around 30 °C to facilitate yeast growth [69,73,74]. The highlight of the design is that the sugar release rate during the enzymatic hydrolysis (e.g. using Stargen™ 001) is similar to the ethanol production rate by yeast cells. By adopting this strategy, the system will not over accumulate sugars, thus minimizing feedback inhibition for enzymes and osmotic pressure for yeast – both of which are encountered in processes with discrete enzymatic hydrolysis and fermentation steps [60,64]. During this ethanol fermentation process, contamination primarily comes from bacteria that belong to *Lactobacillus* species. These bacteria grow faster than the yeast, compete for nutrients, thus, resulting in a loss of ethanol yield [19,63,65]. To reduce the chance of contamination, SSF is usually initiated with a low pH (~4) [19,69,70]. It generally takes 2-3 days to reach maximum ethanol titer for the fermentation [64,69,70].

Upon completion of fermentation, the mash is transferred into a surge tank, followed by distillation to separate ethanol, and finally the product is purified using a molecular sieve to remove the remaining water [19]. The final ethanol product can be as pure as 99%, after being denatured with gasoline [60].

Distillation is well standardized throughout the industry [73], and it accounts for 30% of the total production cost [75]. Studies have shown that cost efficient distillation requires the ethanol content to be ~5% (v/v) [16,76]. A higher ethanol titer, which requires higher solids input, would help further reduce energy input and capital costs [14,75]. Current industrial fermentations are able to produce starch-derived ethanol with a final titer higher than 15% (v/v) ethanol [77]; cases where more than 20% (v/v) have been reported in some plants in the United States [60]. This high ethanol titer can significantly benefit ethanol producers, by reducing water use, labour intensity per production, capital costs, and contamination from bacteria [75].

In addition to ethanol, some value-added by-products are generated during fermentation, mostly from the remaining solids. These help improve the profitability of an ethanol plant [45]. At the end of fermentation, the mash is transferred to the distillation column, and the remaining stillage can be further processed to produce corn distiller's oil and distiller's dried grains with solubles (DDGS) which is commonly used as animal feed [44]. Furthermore, yeast also produce CO₂, which is released through the fermenter vent line, captured by most plants, and commonly used for beverage carbonation or dry ice production [19,44,60,64]. Through production of DDGS and corn distillers oil, an average additional 26% profit can be achieved by a dry mill ethanol plant [44].

2.2.1.2 Sugar-based feedstocks

Sugarcane is well-investigated and commonly implemented as a feedstock for ethanol fermentation, primarily in Brazil. In general, sugarcane contains 68-72% (w/w) water, about 0.5% (w/w) minerals, and 12-17% (w/w) sugars, which include approximately 90% sucrose, 10% glucose and fructose [78,79].

A striking difference between sugar- and starch-based feedstocks is that the former has high quantities of readily fermentable sugars, such as sucrose, glucose, and fructose [19]. Hence, there is no need for additional enzymes to promote hydrolysis prior to yeast fermentation. Furthermore, *S. cerevisiae* produces an invertase enzyme outside of the cell membrane that breaks sucrose into glucose and fructose, which can then be transported through the cell membrane for ethanol production [55].

A brief production process is illustrated in Figure 2.4. Generally, the feedstock is washed, crushed, and intensively extracted to produce juice, with a co-generation of bagasse during the process [59]. The sugar solution is mixed with molasses, a syrup by-product from sugar production, or evaporated to achieve a concentration of 20-25% (w/w) for fermentation [59,65]. In terms of fermentation operation, fed-batch is commonly used [19,80], and more information on the fermentation processing can be found in Section 2.3. Upon the completion of fermentation, a 7-11% (v/v) ethanol titer can be reached [5]. Owing to the use of a clear juice solution [59], the solids present at the end of the fed-batch process are mainly cells, which are centrifuged and re-used for the next fermentation run [19].

The recycling of yeast provides additional benefits to the process through cost savings with regards to purchasing yeast, a reduced requirement for yeast propagation as inoculum for fermentation, and an increased initial density of yeast (10-18% w/v, wet basis) for the next run [5,65]. It also leads to faster fermentation rates and shorter production than starch-to-ethanol—6-12 hours per fed-batch fermentation at 32-33 °C [19,80]. Contamination is reduced by treating cells with sulfuric or phosphoric acid solutions (pH 2.0-2.5) for 2-3 hours [5,19,59,65]. The cells can be recycled for 400-600 times, essentially a total operation time of 200-250 days [5,19]. This yeast recycling method, however, would unlikely work in the starch-to-ethanol process as there are high concentrations of grain residues present at the end of fermentation; rather, the fermented mash, including yeast, is all incorporated in the distillation step [72].

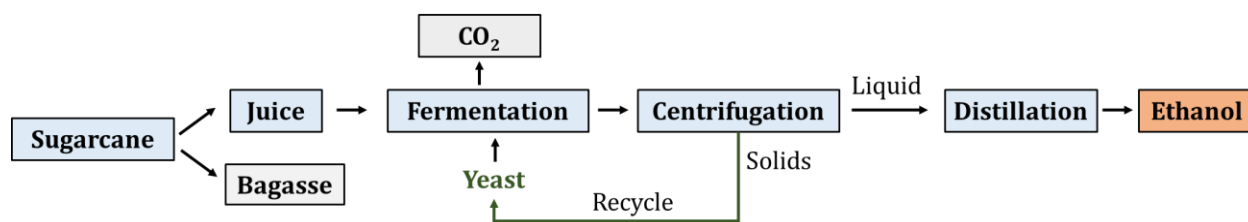


Figure 2.4 The production of ethanol from sugarcane. The process described is adapted from Dias *et al.* in 2010 [81] and Ingledew *et al.* in 2009 [19].

Flocculation at the end of fermentation is a highly desirable characteristic that can facilitate cell recovery and recycling. Yeast flocculation is an asexual and reversible aggregation of cells, which results in a quick separation of cells from the liquid culture [82,83]. It has been used in the brewing industry as an easy way to separate cells from end products [84]. Although its mechanism is not fully understood, cell flocculation has been linked to the pH of cultures, the nutrients in the growth medium, the presence of inhibitors, the strain of yeast, etc. [85,86], as well as the activation of FLO genes responsible for cell-to-cell adhesion [87]. In the context of bioethanol production, flocculation can greatly facilitate separation of cells from the liquid, improving cell recycling and reducing requirements for product recovery (for all feedstock types), thus saving capital and

operational costs for downstream processing steps such as centrifugation or filtration [18,53,65].

Unlike DDGS from the starch-to-ethanol process, the sugar juice that is recovered after fermentation and centrifugation in the sugar-to-ethanol industry has a low nutrient content and thus, it is usually used as an irrigation source for sugarcane fields [19]. Furthermore, the sugarcane bagasse that is generated as a by-product is primarily composed of lignocellulose and is usually burned to produce steam or electricity to drive the ethanol plant [81,88]. Similarly, the processing of 1st generation ethanol from other feedstocks, such as wheat straw and corn stover, also generates lignocellulosic by-products.

Over the past 40 years, technological advances have contributed to the acceleration of the 1st generation ethanol industry and helped reduce production costs by around 60% in the United States and Brazil. This has resulted in a mature ethanol industry with cost-efficient production processes [89,90]. However, in recent years, ethanol producers have focused on utilizing lignocellulosic feedstocks and residues for ethanol production in an attempt to reduce carbon intensity and reliance on food-based crops [17].

2.2.2 2nd generation feedstocks

2nd generation feedstocks for ethanol production refers to lignocellulosic materials, such as agricultural waste (corn cob, corn stover, wheat straw, rice straw, soybean straw, rice hull, sugarcane bagasse), forestry materials (willow, poplar, pine, saw dust, wood chips, bark), energy crops (miscanthus, switchgrass, reed canarygrass), etc. [7,8,91,92]. As the most abundant polymer on the planet, lignocellulosic biomass is produced at approximately 1×10^{11} tons each year [3,4]. Ethanol produced from lignocellulosic biomass, on a life-cycle basis, can contribute to a greater reduction in GHG emission than 1st generation ethanol [48], and it has great potential to replace 30% of the petroleum-based fuel consumption in the United States [93].

Lignocellulosic materials vary in composition among feedstocks but are generally composed of cellulose (40-50% of total dry weight), hemicellulose (20-40%), lignin (15-30%), and small portions of extractives, free sugars, and minerals [5,94]. Cellulose is an unbranched polysaccharide that links glucose monomers through β -1,4-glycosidic bond (Figure 2.5a) [5]. The cellulose chains are then gathered together to form microfibril

bundles [8]. Cellulose contains highly ordered crystalline regions, which are interrupted by amorphous regions (Figure 2.5b) [7,95]. Hemicellulose, a shorter and highly branched polysaccharide, is mostly composed of monomer sugars with five carbons (i.e. xylose, arabinose) and six carbons (i.e. glucose, galactose, mannose), and/or uronic acids [6,7]. Overall, cellulose microfibrils are wrapped by hemicellulose through hydrogen bonds and both cellulose and hemicellulose can be depolymerized into sugars. Conversely, lignin is an amorphous, hydrophobic polymer consisting of aromatics [7,8], and it acts as a glue to seal the whole structure (Figure 2.5b). The three macromolecules together form a complex and rigid structure (Figure 2.5b), protecting the plant against degradation, thus explaining why it can be difficult to retrieve sugar units from polysaccharides for ethanol production [5,7,16].

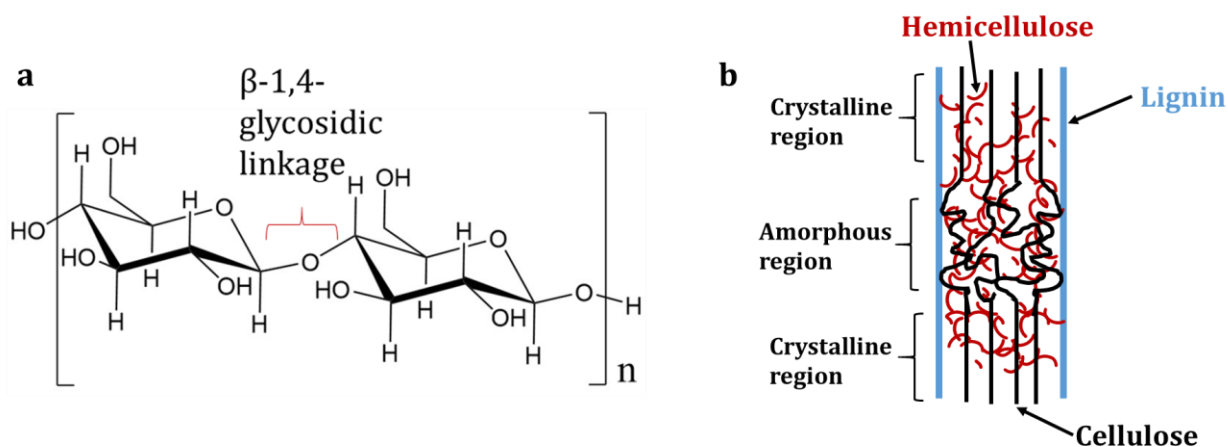


Figure 2.5 Chemical structure of cellulose (a) and a sketch of lignocellulosic material (b). For figure (b), black, red, and blue lines represent cellulose, hemicellulose, and lignin, respectively. Cellulose structure is drawn with crystalline and amorphous regions. Figure (b) was adapted from Mosier *et al.* in 2005 [96].

As shown in Figure 2.6, to produce ethanol from lignocellulosic materials, the feedstock goes through pretreatment and enzymatic hydrolysis to release sugars that are fermented into ethanol, which is then recovered by distillation [8,18]. Pretreatment opens up the complex structure of the polymer matrix, breaks lignin, and disrupts the crystalline regions of cellulose, thus, giving enzymes access to polysaccharides for ensuing hydrolysis

[97]. As a result, hemicellulose is partially broken down into sugar oligomers and monomers, and a small portion of cellulose is converted to glucose. Depending on the method of pretreatment applied, chemicals such as furfural, 5-hydroxymethyl furfural, acetic acid, and phenolic compounds could be formed, which can inhibit subsequent enzymatic hydrolysis and fermentation [5]. Since the pretreatment employed strongly impacts the efficiency of the downstream process and represents 40% of the total processing cost [98], an approach that enables high digestibility at a low cost is vital for the overall process economics [96]. Various methods have been investigated, two of which are widely used and relatively cost effective: 1) steam explosion, an approach through which biomass is heated under high pressure steam (0.7-4.8 MPa), and the reaction is terminated by an abrupt release of pressure; and 2) a dilute acid pretreatment where acid (e.g. sulfuric acid) is added to the biomass-water mixture at a high temperature (120-190 °C), whereas no abrupt pressure release is involved [5,9-11,18,96,99-101].

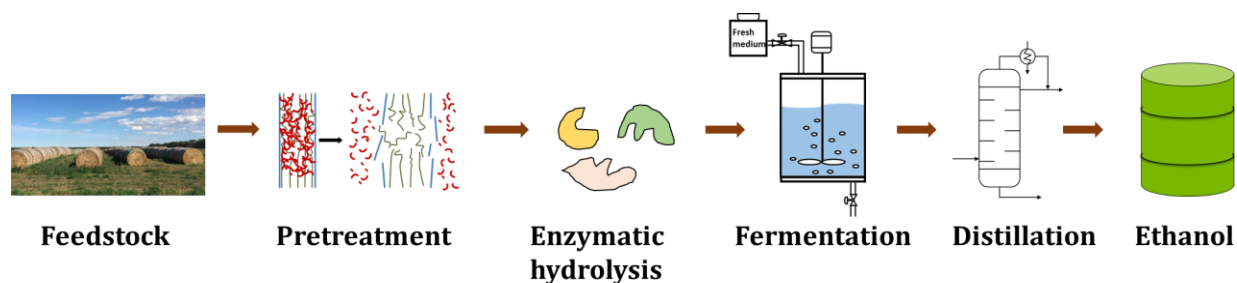


Figure 2.6 The steps to produce cellulosic ethanol.

Following pretreatment, the solids are exposed to enzymatic treatment, where cellulose and hemicellulose are hydrolyzed into monomer sugars—a process also known as saccharification. The main enzymes (cellulases) used for cellulose hydrolysis contain endoglucanase, exoglucanase, and β -glycosidase, and the three work together to cleave glycosidic bonds. Specifically, endoglucanase randomly breaks down the glycosidic bonds within the amorphous regions of the cellulose matrix, resulting in reducing and non-reducing ends. These ends are then hydrolyzed by exoglucanase to release cellobiose, a disaccharide, which can be further broken down into glucose monomer by β -glycosidase

[102]. Optimal performance for hydrolysis requires conditions such as a pH of 4.5-5.5 and a temperature of 50-55 °C [5]. To further facilitate cellulose hydrolysis, accessory enzymes can be added. For instance, xylanase promotes the access of cellulases to cellulose by breaking down hemicellulose into C5 and C6 sugar monomers, which can also be fermented to ethanol. As a result, glucose and xylose become the first and second most abundant sugars among enzymatic hydrolysates, respectively [5]. At the end of hydrolysis, monomer sugars are released into the liquid solution; the insoluble solids are primarily composed of lignin, which can be separated from the liquid and removed from the reactor [5,103].

The enzymes involved in hydrolysis are commonly sourced from the filamentous fungi *Trichoderma reesei* at large scale [5,102]. For a cellulosic ethanol plant, the enzymes can be either produced on site, or purchased from other plants, with the former being considered more cost effective [18]. Attributed to technological improvements, enzyme costs have been substantially reduced over the last decade [14].

After enzymatic hydrolysis, the mash can be supplemented with corn steep liquor (0.25-1% (w/w)) which contains nitrogen, vitamins, and trace minerals for microbial growth and ethanol production [18,103]. Anaerobic conditions favor ethanol production during fermentation, which is performed at 30-35 °C [5,18]. More details regarding microorganisms, fermentation, and its associated seed culture preparation are discussed in Section 2.3.

An ideal process scenario requires low enzyme loading, fermentation of both C5 and C6 sugars into ethanol at high yield, and high ethanol productivity [5,14]. Similar to 1st generation ethanol (Section 2.2.1.1), ethanol titers greater than 5% (v/v) help improve the overall process economics, especially with regards to distillation [76]. According to Larsen *et al.* in 2008 [104] and Santos *et al.* in 2016 [5], this would require a solids loading of 20-25% (w/w), although cellulosic slurries become increasingly viscous when solids are loaded above 15% (w/w), which results in limitations in mixing, temperature control, sampling efficiency, etc. [14]. However, considering a hydrolysis yield of 70-80% and a fermentation efficiency of 90%, the solids loading could be reduced slightly. For instance, the National Renewable Energy Laboratory (NREL) demonstrated the production of

ethanol at titers over 70 g/L (~8.7% v/v) with 20% (w/w) solids loading of corn stover [9]. Further improvement of the system in 2016 resulted in higher solids loading (20-28%, w/w) and an ethanol titer of ~86 g/L (over 10 % (v/v)) [105]. Nevertheless, high ethanol titer is always desired for ethanol production as the primary strategy to reduce distillation costs.

Depending on the process, hydrolysis and fermentation can be performed as SSF, separate hydrolysis and fermentation (SHF), hybrid hydrolysis and fermentation (HHF), or consolidated bioprocessing (CBP). SSF is similar to that described for the starch-to-ethanol process (Section 2.2.1.1), with the main advantages being minimized feedback inhibition to enzymes and reduced osmotic stress to the microorganism. Nevertheless, the two processes require a compromise in operating conditions, as ideal conditions for each step are different (hydrolysis: temperature of 50-55 °C and pH 4.5-5.5; fermentation: temperature of 30-35 °C and pH 5.5-7) [106]. This results in a reduced performance for both processes. Conversely, in SHF, hydrolysis and fermentation are conducted sequentially and separately in different reactors. This provides flexible and optimal operation conditions for both, yet has limitations with regards to a reduced hydrolysis rate in the latter stages of hydrolysis as the released monomer and oligomeric sugars result in feedback inhibition of the enzymes [5,106]. As a modified version of SSF and SHF, HHF initiates hydrolysis in one reactor, and when the sugar release rate drops, the mash is transferred to a second reactor. At this point, the temperature is reduced and the pH is increased to facilitate SSF. This gives HHF the advantage of reduced feedback enzyme inhibition, but the success of this configuration relies on multiple factors, for instance, the timing of the switch from hydrolysis to the fermentation reactor [106]. In CBP, hydrolysis and fermentation are integrated with pretreatment in a single reactor. This strategy, which uses one microorganism to hydrolyze lignocellulose and ferment sugars, greatly reduces capital costs by negating the need for constructing multiple reactors. However, CBP is still far from application, primarily due to the barriers on developing strains that are well-suited for the strategy [103]. Current technological development of enzymes and microorganisms, which have different optimal operating conditions, favors the use of SHF and HHF for cellulosic ethanol production [5,107].

Overall, the majority of research and progress regarding 2nd generation ethanol fermentation has focused on improving the processing configurations between fermentation and hydrolysis (i.e. SSF, SHF, HHF, CBP, etc.) [5], genetically modifying microorganisms to consume both C5 and C6 sugars (discussed in Section 2.3.1), and improving strain tolerance to inhibitors [108,109].

Because of the complexity and rigidity of the feedstock and difficulties in sugar conversion [94], 2nd generation ethanol still has a higher production cost than 1st generation ethanol [15]. 2nd generation ethanol facilities have capital costs 5-10 fold greater and production costs 2-5 times higher than those of corn ethanol plants [61]. For a cellulosic ethanol plant, 34% and 33% of the total cost comes from capital costs and operational costs, respectively, with the remainder arising from feedstock costs [16,17].

In recent years, promising breakthroughs have been achieved regarding longstanding technical barriers. For instance, Poet-DSM, an important ethanol producer in the US, resolved its pretreatment bottleneck in enzymatic digestibility for cellulosic ethanol production [12]. In addition to achieving high ethanol titers (over 8% v/v) [9,105], NREL has identified a cellulase enzyme that aggressively attacks cellulose with a high degree of crystallinity, which would greatly facilitate the hydrolysis process [13]. With major challenges successfully being overcome, ethanol fermentation itself starts to become a limiting factor in achieving high ethanol productivity.

Similar to 1st generation ethanol, the cellulosic ethanol industry can also generate valuable by-products. For instance, inhibitors (e.g. furfural) generated from pretreatment can be separated from solids and recovered from the solution as valuable chemicals [110]. Lignin can be removed after pretreatment or after hydrolysis for the production of high value materials or chemicals [111]. An attractive by-product from the lignocellulosic world is cellulose nanocrystals (CNCs). CNCs are nano-sized particles (width: 3-20 nm, length: 50-2000 nm) in a crystalline form generated from cellulose materials [112]. They have unique properties, such as a large surface area, a low density, and a high strength – comparable to steel [112,113]. In addition to being renewable and biodegradable materials, CNCs can reinforce various polymer materials [112]. Recently, a controlled enzymatic treatment of wood pulp followed by acid hydrolysis showed great promise for co-production of

cellulosic ethanol and CNCs [114]. The enzymatic hydrolysis released a sugar stream that could potentially be used for ethanol fermentation; acid hydrolysis of the remaining solids generated a high yield of CNCs. This technical development has great potential in valorizing the product stream and reducing the production cost of cellulosic ethanol.

2.3 Ethanol fermentation

2.3.1 Microorganism and metabolic pathways

Various types of microorganisms can produce ethanol from glucose, but the yeast *S. cerevisiae* stands out for industrial ethanol production. This is because *S. cerevisiae* is not only one of the most well-studied microorganism, resistant to low pH, and insensitive to bacteriophage [115], but it is also able to tolerate high ethanol concentration and grow fast under anaerobic conditions [5,19,53,55,60].

S. cerevisiae is a unicellular fungus varying in size from 5-10 μm in length and 5-7 μm in width [116]. It can adopt various shapes, such as ovoid, spherical, and ellipsoidal [55]. When grown in fermentation cultures, yeasts can also present themselves as isolated cells, pairs, chains, or clusters and reproduce by budding [19,55].

As an essential element of ethanol plants, yeasts produce ethanol through a series of metabolic pathways. Wild type *S. cerevisiae* can consume sucrose (hydrolyzed into glucose and fructose outside the plasma membrane), glucose, fructose, galactose, and mannose, which are transported into the cell by diffusion for ensuing metabolic conversions [117]. Taking glucose as an example for metabolic conversion to ethanol, the first primary pathway of the process is glycolysis, which is also termed the Embden-Meyerhof-Parnas pathway (Figure 2.7). After being transported into the cytoplasm, glucose is phosphorylated and isomerized into fructose-6-phosphate, which is then phosphorylated into fructose-1,6-biphosphate. The fructose-1,6-biphosphate is cleaved into dihydroxyacetone phosphate and glyceraldehyde-3-phosphate, the latter of which is eventually converted into pyruvate. During glycolysis, 2 units of adenosine triphosphate (ATP) are consumed due to phosphorylation of glucose and fructose-6-phosphate, and 4 units of ATP are produced, which results in a net gain of 2 ATP units. In addition, nicotinamide adenine dinucleotide (NAD⁺), an important cofactor (shaded in grey, Figure

2.7), is reduced to NADH when glyceraldehyde-3-phosphate is metabolized to 1,3-bisphosphateglycerate [65].

Under aerobic conditions, NADH is able to donate electrons to the electron transport chain to facilitate oxidative phosphorylation in which oxygen is the terminal electron acceptor. However, under anaerobic conditions, NAD⁺ cannot be replenished in the same manner. Thus, in the absence of oxygen, pyruvate enters the ethanol fermentation pathway (Figure 2.7). Pyruvate is initially reduced first to acetaldehyde – with CO₂ being released – and then to ethanol. By doing so, the yeast is able to recycle the NAD⁺ required for glycolysis to continue. Furthermore, during anaerobic cell growth, pyruvate can be used for synthesis of other useful molecules (e.g. proteins) related to biomass production, which could also lead to a build-up of NADH (Figure 2.7). To prevent an imbalance of redox potential, the yeast reduces dihydroxyacetone phosphate into glycerol-3-phosphate, which is dephosphorylated into glycerol (Figure 2.7). As a result, NAD⁺ is formed from the surplus NADH, achieving a balance of redox potential and making glycerol a common product during alcohol fermentation [19,65]. In theory, 1 mole of glucose is converted into 2 moles of pyruvate, which is reduced to 2 moles of ethanol, 2 moles of CO₂ (Equation 2.1), and 2 moles of ATP. Ethanol and CO₂ then leave the cells by diffusion [19].

In the presence of oxygen, the yeast oxidizes pyruvate into a series of organic acids through the tricarboxylic acid (TCA) cycle, which releases CO₂ and H₂O. Compared to the anaerobic pathway, 1 mole of glucose is converted into 6 moles of CO₂ and 36-38 moles of ATP via the TCA cycle and the electron transport chain. In this case, ~0.5 g of biomass are generated from 1.0 g of glucose, which is ~10-fold higher than the biomass produced during anaerobic cultivation [5,60].

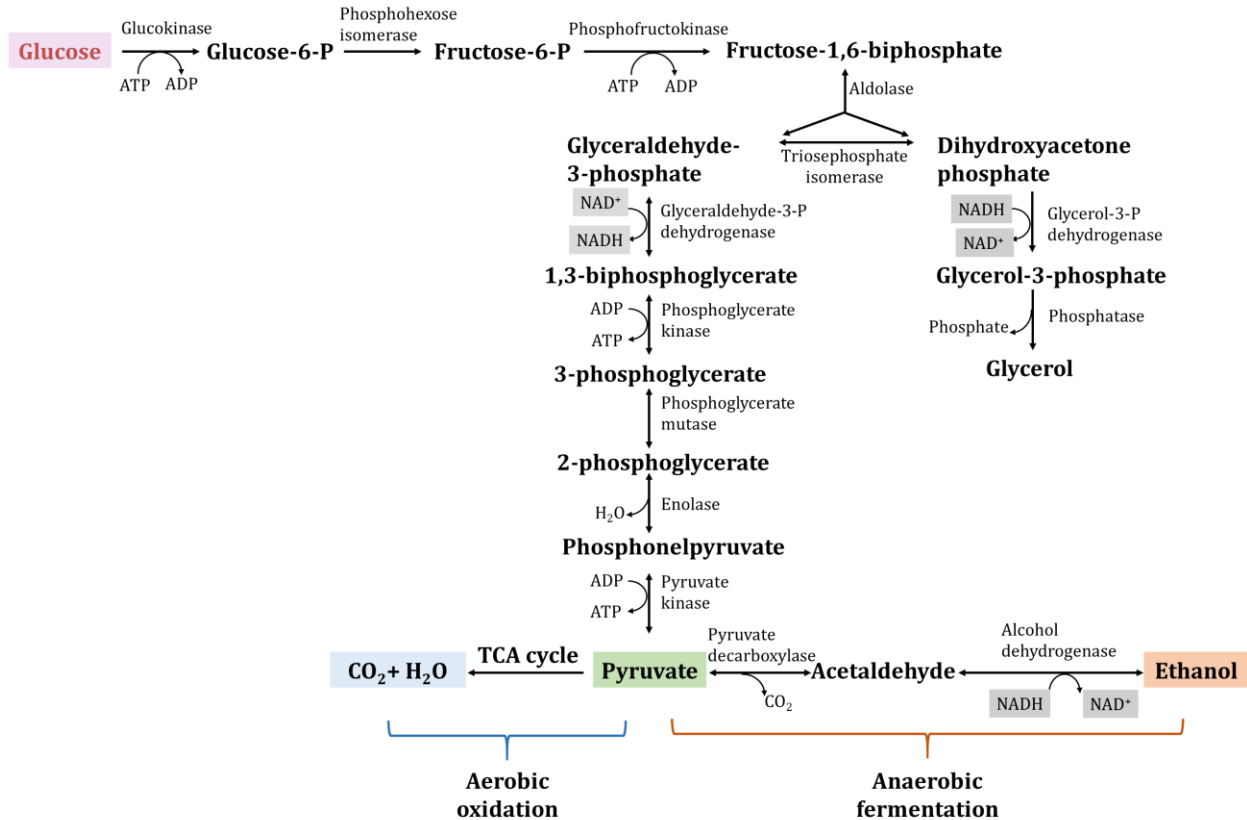


Figure 2.7 The metabolic pathway for ethanol production using glucose as the carbon source for *S. cerevisiae* (figure adapted from Jacques *et al.* in 2003 [65] and Ingledew and Lin in 2011 [60]). “P” represents phosphate, and TCA represents tricarboxylic acid.

As yeast divides, its plasma membrane needs to be extended. Although yeast can grow under anaerobic conditions, it still requires molecular oxygen for sustained synthesis of sterols and unsaturated fatty acids, which are crucial for maintaining the integrity, permeability, and rigidity of the cell plasma membrane [116]. Figure 2.8 shows the production of sterols in yeast. The key enzyme, squalene monooxygenase, catalyzes the conversion of squalene to squalene 2,3-epoxide; molecular oxygen is consumed in the course of this conversion. Then, lanosterol is formed, which is used for the production of ergosterol, the main sterol in *S. cerevisiae* [118]. For the synthesis of fatty acids (Figure 2.9), palmitic acid (a 16-carbon saturated fatty acid) is initially produced and can be used to produce other fatty acids. However, for the production of unsaturated fatty acids, the enzyme catalyzing the reaction, desaturase OLE1, is activated by oxygen and low

temperatures [118]. If oxygen is absent, ergosterol and unsaturated fatty acids cannot be produced. Upon division, the mother cells need to distribute these molecules to their daughter cells, which eventually results in a diminished level of sterols and unsaturated fatty acids, thus, limiting the number of possible cell divisions to about five [119].

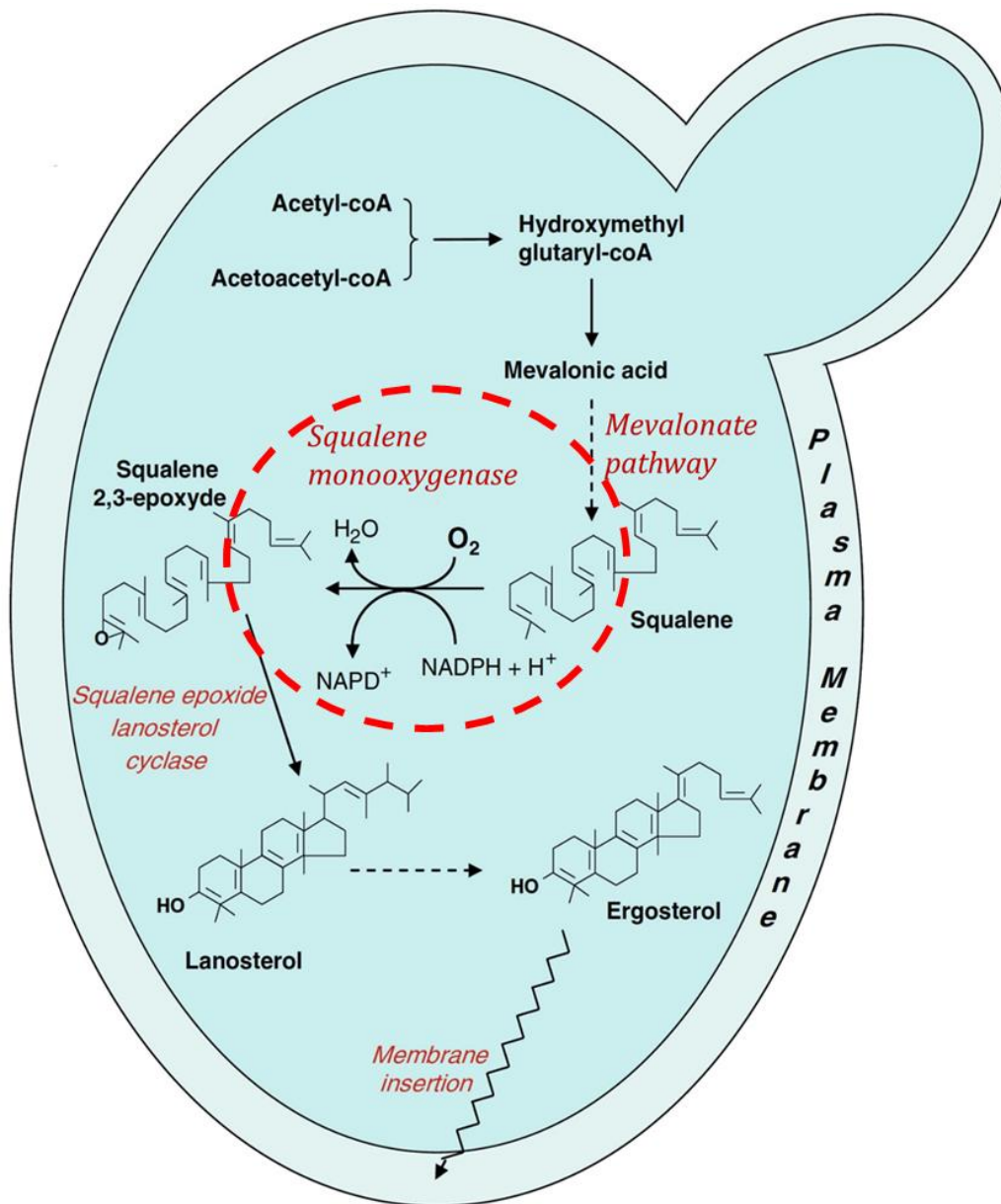


Figure 2.8 The synthesis of ergosterol in yeast cells. Wine chemistry and biochemistry by Moreno-Arribas, M. Victoria, Polo, M. Carmen [118]. Reproduced with permission of Springer in the format Thesis/Dissertation via Copyright Clearance Center. Minor modification was made for the figure.

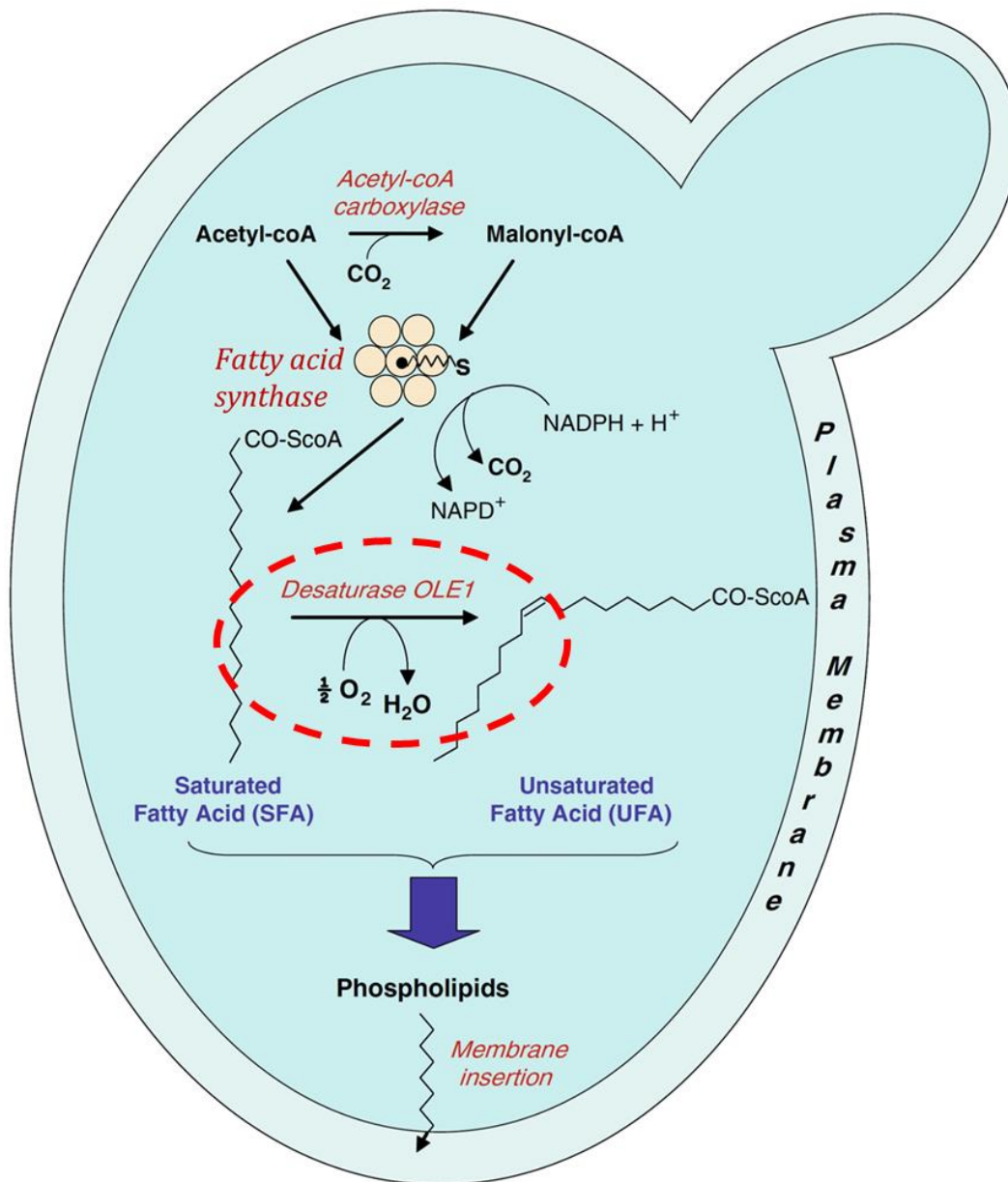
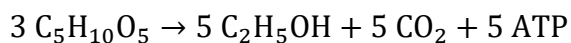


Figure 2.9 The synthesis of unsaturated fatty acids in yeast cells. Wine chemistry and biochemistry by Moreno-Arribas, M. Victoria, Polo, M. Carmen [118]. Reproduced with permission of Springer in the format Thesis/Dissertation via Copyright Clearance Center. Minor modification was made for the figure.

As mentioned previously (Section 2.2.2), xylose is abundantly present in the enzymatic hydrolysate of lignocellulosic feedstock, and the conversion of xylose to ethanol will help improve the final concentration of ethanol. However, despite its capability of

fermenting xylulose (an intermediate of xylose catabolism), wild type *S. cerevisiae* does not typically produce ethanol from xylose [5,120]. Hence, a genetic modification for the conversion of xylose to xylulose is necessary. This can be facilitated by learning from wild-type organisms that are capable of performing this conversion, for instance, *Scheffersomyces stipitis* [121], *Candida shehatae* [122], and *Spathaspora passalidarum* [123].

As shown in Figure 2.10, there are two major microbial pathways for transforming xylose into xylulose that can be introduced. The first one is the xylose reductase/xylitol dehydrogenase pathway that uses a two-step reduction and oxidation. Xylose reductase, with nicotinamide adenine dinucleotide phosphate (NADPH) or nicotinamide adenine dinucleotide (NADH) as a co-factor, reduces xylose into xylitol, which is then oxidized into xylulose by xylitol dehydrogenase using NAD(P)⁺ as the co-factor. The second is the xylose isomerase pathway, which employs xylose isomerase to reduce xylose directly into xylulose, without any co-factors [5]. After the production of xylulose, as shown in Figure 2.11, the molecule is phosphorylated to xylulose-5-phosphate before entering the pentose phosphate pathway. Xylulose-5-phosphate is then transformed into glyceraldehyde-3-phosphate and fructose-6-phosphate, which are channelled into glycolysis and converted into pyruvate. Under anaerobic conditions, pyruvate is reduced to ethanol [5]. Overall, 3 moles of xylose (or 1 g) can be converted into 5 moles of ethanol (or 0.51 g), with a net gain of 5 moles of ATP (Equation 2.2) [124].



Equation 2.2

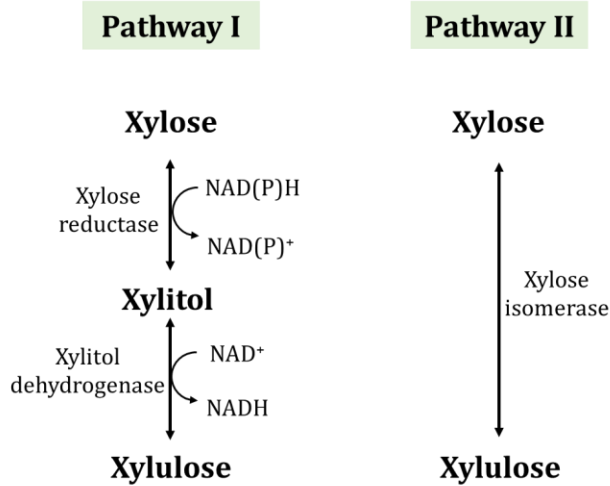


Figure 2.10 Major microbial pathways for converting xylose into xylulose. Adapted from Santos *et al.* in 2016 [5] and McMillan in 1993 [124].

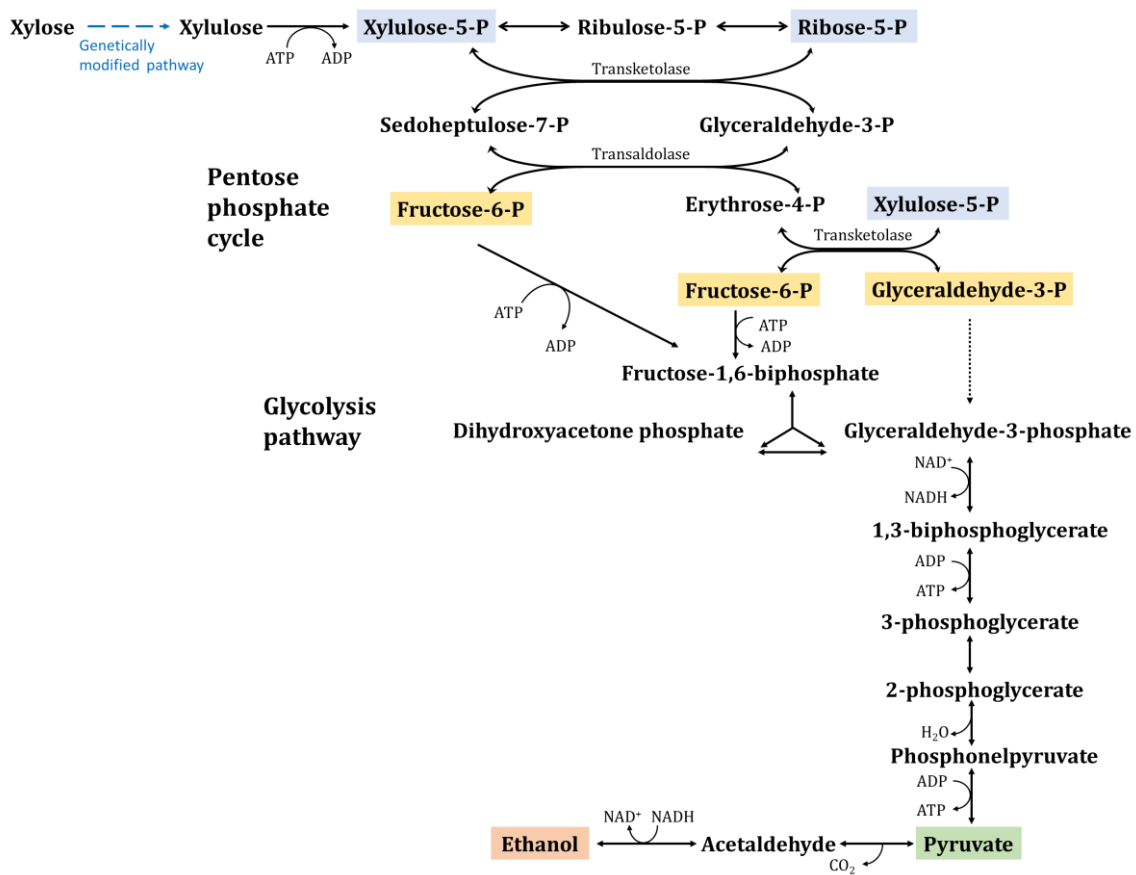


Figure 2.11 Common pathway for xylose fermentation to ethanol. Adapted from Santos *et al.* in 2016 [125] and McMillan in 1993 [124]. Note that the enzymes for glycolysis and ethanol production pathways are not shown here (can be seen on Figure 2.7).

Although genetic engineering and evolutionary strategies have enabled *S. cerevisiae* to consume both C5 and C6 sugars, fermenting both sugars in an efficient and simultaneous way remains as a challenge for the industry [5]. For instance, a diauxic growth pattern, where one sugar is consumed preferentially before consumption of the second sugar, is frequently reported for genetically modified microorganism. In addition, the consumption rate of glucose is generally faster than that of xylose [115,126–129].

2.3.2 Batch fermentation

Conventional strategies for industrial fermentation include batch (the most common approach), fed-batch, and continuous operations.

Batch fermentation is initiated by adding substrate and inoculum, and the working volume is fixed throughout the process, except for small amount of samples being withdrawn to monitor fermentation status. At the end of batch fermentation, the entire culture is harvested to extract or purify the target product, and, often, the fermenter is then cleaned up, sterilized, filled with new substrate, and inoculated to start a new batch campaign [19]. For this thesis, a campaign is defined to consist of the fermentation period from inoculation until the end of fermentation, right before the cleaning process is initiated.

During batch fermentation, the cell population inside the fermenter typically experiences lag, exponential, stationary, and sometimes death phases (Figure 2.12). The lag phase starts after inoculation, and during this period, the cell population barely increases. During this period, yeast cells are metabolically active but are sensing and adapting to their new environment, with synthesis of necessary components for substrate assimilation. Following lag phase, the cell population grows exponentially, as cell division constantly occurs until the limiting nutrient approaches depletion or inhibitor levels become too high for the cells to grow. This is the time at which cells enter stationary phase, characterized by having the highest cell population, without much cellular activities; if stationary phase is long enough, cells start to die and enter the death phase [19].

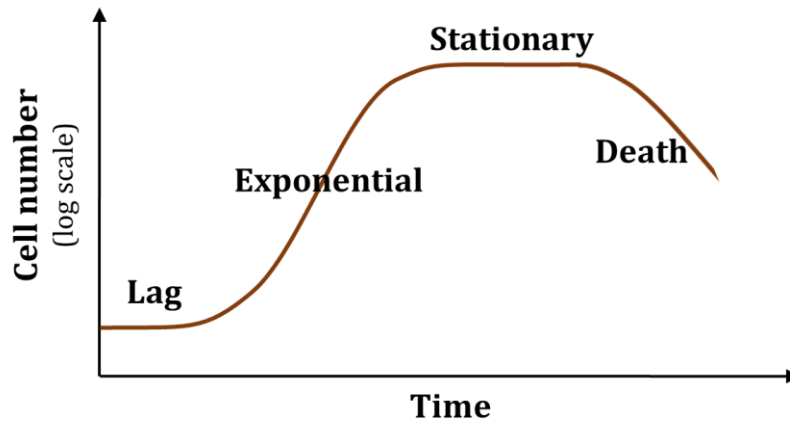


Figure 2.12 Cell growth during batch fermentation. Adapted from Ingledew *et al.* in 2009 [19].

If the product of fermentation is not biomass itself, it is usually a primary (growth-associated) or secondary (produced after the onset of stationary phase) metabolite of the microorganism. In the case of ethanol, production is tightly linked to microbial growth and its production becomes insignificant during stationary phase, thus making ethanol a typical primary metabolite [53].

For batch ethanol fermentation, it is desirable to minimize the length of the lag, stationary and death phases, and optimize the cell growth rate in the exponential phase, during which ethanol is mainly produced. By doing so, the overall fermentation time can be reduced, thus enhancing ethanol productivity [19]. The lag phase can be reduced by increasing the size of the inoculum, using exponential growing cells for inoculation, or using inocula that have a history of growing under similar environments [5,19]. Stationary phase can be minimized by constantly monitoring the fermentation status and stopping the process as soon as the cell population and ethanol concentration reach a plateau, or a limiting nutrient is exhausted [19].

The monitoring of fermentation status can benefit the overall process. It can help minimize fermentation time in stationary phase, improve productivity, and help an operator make instant decisions upon identification of incidents or disturbances during fermentation [19]. Fermenters are commonly equipped with online sensors to monitor or

control variables including pH, dissolved oxygen, temperature, mixing rate, etc., and the sensors can be cleaned in place or sterilized *in situ*. Nevertheless, these sensors cannot provide sufficient information on the fermentation status, which confers important parameters such as substrate consumption, ethanol content, and growth phase of the cells [19]. Conventional ways to monitor the fermentation process include periodic sampling from the reactor, followed by sample preparation and analysis of sugars, ethanol, and acids concentrations by offline instruments such as HPLC and GC. These approaches, however, have certain limitations. For instance, constant labor is needed to take and prepare samples, then run them on HPLC or GC, which is also time consuming and requires expensive instrumentation [19,20].

In recent years, attempts to monitor ethanol and/or residual sugar concentrations in real-time using automated approaches have received more attention. Near-infrared, Fourier transformed infrared, and Raman spectroscopies have been proposed as quicker and cheaper alternatives to current approaches [130–133]. Specifically, the spectroscopic parts are installed inside or outside the fermenter, and the information obtained is correlated with HPLC and GC data to establish chemical concentrations. Spectroscopic data would then indicate the progress of substrate consumption and ethanol production. Yet, solids present in the fermentation culture may block the spectroscopic instrument or interfere with the signal, and overlapping signals from different molecules can reduce the accuracy of the measurement. Also, a spectral library needs to be built through calibration of a number of samples collected under various fermentation conditions. Therefore, those approaches are a long way from being applied to monitor and automatically control fermentation, which is considered essential for cellulosic ethanol production [19].

Overall, for batch fermentation, it is easy to operate and separate different campaigns by performing clean-up and sterilization, thus, minimizing contamination between campaigns. It also allows for complete substrate utilization, which gives high a ethanol yield [10,19]. Currently, more than 84% of the alcohol plants in North America operate fermentation in a batch mode [60]. However, although commercially purchased yeast (e.g. dry active yeast) and recycled yeast are directly used as inoculum for starch-to-ethanol and sugarcane-to-ethanol processes, respectively, current 2nd generation ethanol

fermentation requires a seed culture to start. As seen in Figure 2.13, yeast propagation is needed for cellulosic ethanol production in every batch, for which a series of seed trains are prepared where the size is progressively scaled up in multiple reactors of increasing volumes [5,18,19]. During batch fermentation, the lag and exponential phases (Figure 2.12) are almost unavoidable, which makes the overall fermentation time long and lowers productivity [10,19]. Also, at the end of each batch campaign, the clean-up and sterilization steps (Figure 2.13) take time and are necessary for every single run, contributing to a reduction of available fermentation time in a given period [19,134]. Furthermore, fermentations are commonly observed to be variable between batches, as a result of changes in operation conditions [19].

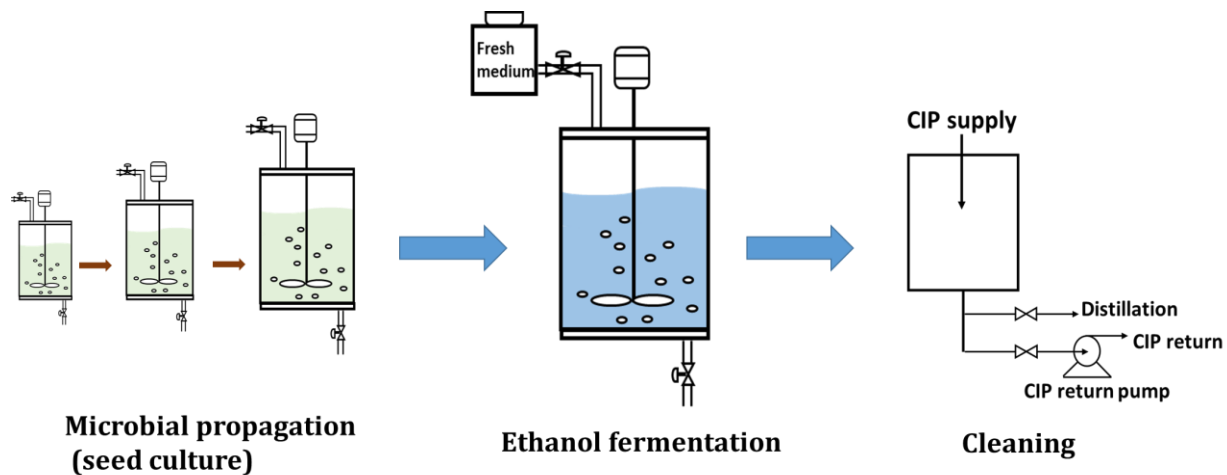


Figure 2.13 Fermentation process for cellulosic ethanol in a batch mode.

2.3.3 Fed-batch fermentation

For ethanol fermentation operated in fed-batch mode (Figure 2.14), the process starts similarly to batch operation, yet with a smaller working volume. Fresh medium is continuously or intermittently added into the reactor until the maximum volume limitation of the fermenter is reached. At this point, the entire culture can be subjected to downstream processing to stop the fed-batch campaign. Then, the fermenter is cleaned and sterilized for the next fed-batch campaign [19,134].

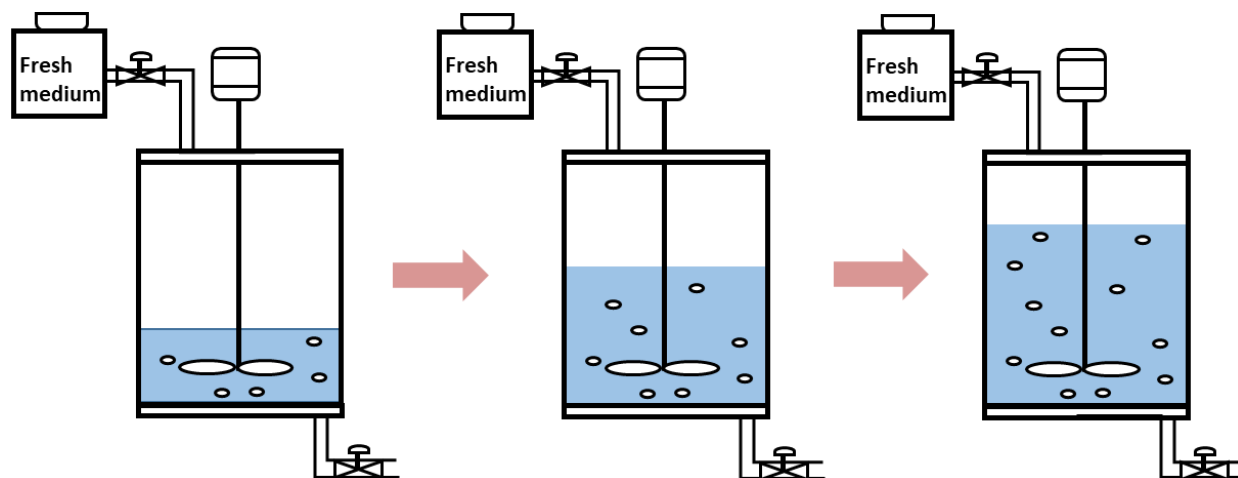


Figure 2.14 Fermentation process in fed-batch mode. Fresh medium is constantly added and the fermentation volume in the reactor increases throughout the run.

Fed-batch operation is widely used for the production of ethanol using a sugar-based feedstock (discussed in Section 2.2.1.2); about 83% of the plants in Brazil use fed-batch, with the rest using continuous operation [135]. As a modified version of batch operation, fed-batch fermentation provides many benefits. For instance, osmotic pressure from sugars in fed-batch can become negligible, as the nutrients are added at a slow rate, which maintains the substrate(s) concentration at low levels; under some conditions, the feeding speed is manipulated to be similar to the sugar consumption rate by yeast [19,78]. The feeding rate and concentration of limiting substrate(s) need to be well determined for this operation strategy. In addition, since the culture is not removed until the end of a fed-batch campaign, washout of limiting nutrient is minimized for the process, as is the case with batch fermentation [19]. However, the feeding volume is limited to the fixed volume of a reactor, and the down time requirement is similar to batch [19]. Furthermore, the indication of the end of a fed-batch campaign and the subsequent filling process is usually not automated [24].

2.3.4 Continuous fermentation

Continuous fermentation, also called chemostat, runs in a continuous manner. It starts similarly to a batch process but keeps cell concentration stable by supplying a continuous flow of fresh medium [19]. As illustrated by Figure 2.15, fresh medium is

continuously added to the fermenter at a certain speed, while the fermentation culture is simultaneously removed at the same rate, making the internal volume of the culture constant [19,65].

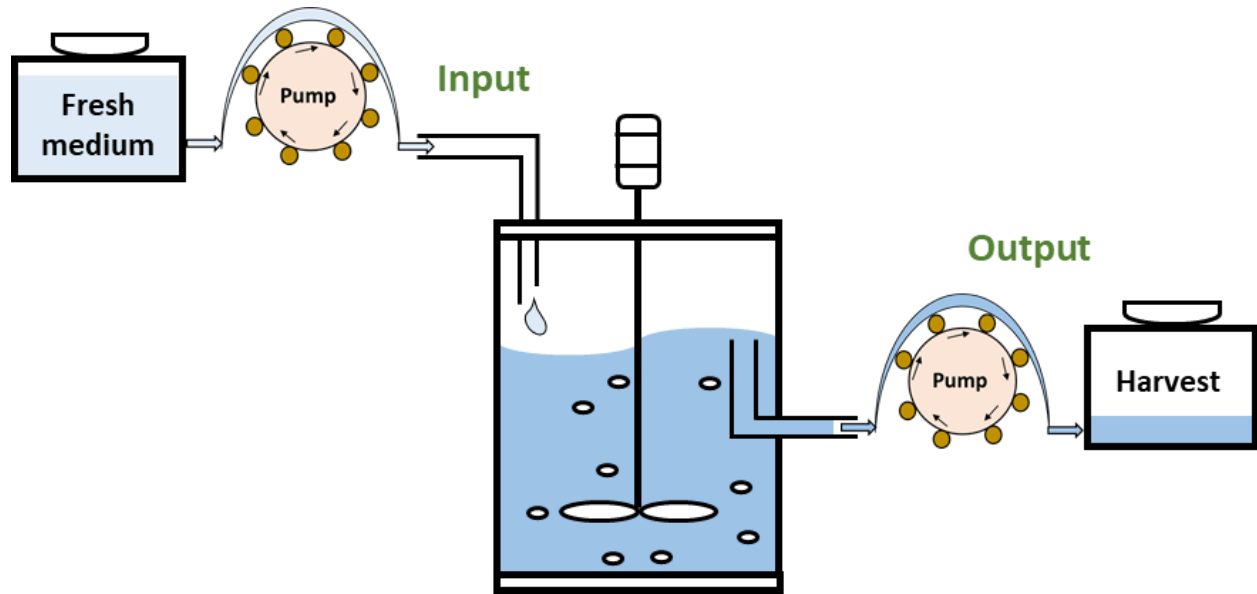


Figure 2.15 A schematic diagram of continuous fermentation. The flow rate of the input medium and output culture are well controlled to be the same rate. Adapted from Jacques *et al.* in 2003 [65].

A dilution rate represents the flow rate of feed/harvest divided by the working volume of the fermentation. For continuous ethanol fermentation at steady state, the dilution rate equals the maximum specific growth rate of the cell population at given conditions. If the dilution rate exceeds the maximum specific growth rate for the yeast under the conditions applied, a high ethanol volumetric productivity (the amount of ethanol produced per working volume within a certain time) can be reached due to the reduced time. However, a washout of the cells will take place, resulting in lower biomass density inside the fermenter, which would translate into a lower utilization of sugars and reduced ethanol titer in the output stream [19,136,137]. Conversely, a lower dilution rate causes accumulation of the biomass, more utilization of the substrate and higher

concentration of ethanol, but would likely result in a longer fermentation time and lower productivity [19].

The operation of continuous fermentation, after reaching steady state, eliminates the lag phase, and thus the yeast maintains a high growth rate, making the ethanol volumetric productivity higher than batch or fed-batch. This higher ethanol volumetric productivity can be translated into smaller bioreactor volumes, and therefore, less capital investments. In addition, the use of a chemostat increases the efficiency of equipment for long-term sustained fermentations. Theoretically, the process can be operated indefinitely, which can substantially reduce the contribution of down time for cleaning, sterilization, and filling, and reduce labor costs [10,19,60,138].

Nevertheless, due to constant feeding and removing of medium, nutrients (i.e. sugars) are being washed out throughout the process [139]. The loss of sugars can increase production costs for cellulosic ethanol, as they are converted from lignocellulosic hydrolysates after important processes such as pretreatment and enzymatic hydrolysis (discussed in Section 2.2.2). Multi-stage train reactors can follow the initial fermenter and maintain the continuous flow to help utilize more of nutrients for ethanol production [65]. However, research has shown that significant amounts of sugar can still remain after three sequential chemostat fermentations [139,140], and this arrangement requires more capital investments. Furthermore, due to long-term operation of the system without a turnover, bacteria can adapt to the conditions and disturb the balanced chemostat status for yeasts, leading to reduced ethanol production [19,59,65]. In this case, the process needs to be shut down, cleaned, sterilized, and it would take time to establish a new a steady state for the subsequent continuous fermentation campaign [65].

For cellulosic ethanol, the current practice primarily employs batch for fermentation [9]. However, little research has been conducted to improve the processing outcome [19,76,141]. Hence, there is a need to improve ethanol productivity and reduce the associated labor for cellulosic ethanol using advanced fermentation strategies.

2.4 Self-cycling fermentation (SCF)

SCF is a semi-continuous fermentation technique developed in the 1970s. As indicated in Figure 2.16, SCF is a cycling strategy which starts as a batch fermentation; but

upon the onset of stationary phase, half of the culture volume is automatically removed for downstream processing, and replaced by the same volume of fresh medium to start the next cycle [24]. SCF is an automated repetition of this process, with robust and repeatable performance patterns observed for many successive cycles. This approach has been used for protein surfactant production by the bacteria *Bacillus subtilis* (over 80 cycles) [25,26], aromatics degradation by the bacteria *Pseudomonas putida* (over 100 cycles) [27], phenol degradation by the bacteria *Pseudomonas putida* (over 120 cycles) [28], and citric acid by the yeast *Candida lipolytica* (over 130 cycles) [29].

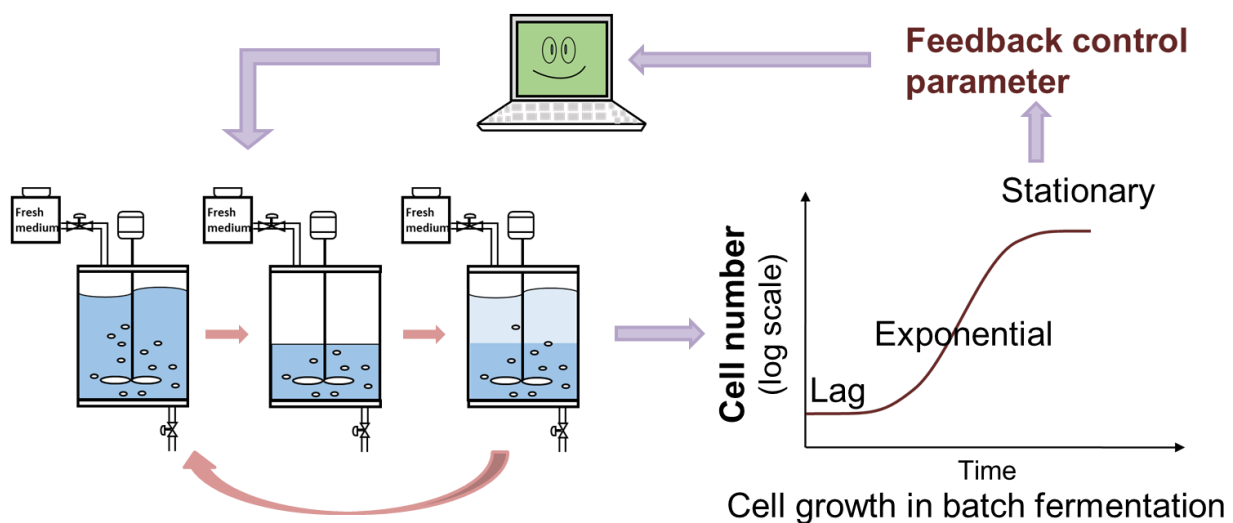


Figure 2.16 A schematic presentation of SCF operation. The system uses one fermenter monitored by a feedback control parameter, which automatically triggers the removal and replacement of half of the culture inside the fermenter.

2.4.1 Feedback control of SCF

The key challenge to automating the SCF process is to incorporate a feedback control scheme to monitor the fermentation in real-time and identify the onset of stationary phase (Figure 2.16). At this point, the cycle is recognized as being complete and the cycling process is automatically triggered, with half of the culture being harvested and replaced with fresh medium [24]. A feedback control scheme uses a real-time sensing parameter, which is related to the metabolic state of the microbial population under given

conditions [24]; for stationary phase, it could be the depletion of a limiting nutrient [28,142].

Taking dissolved oxygen as an example, for aerobic fermentations, oxygen demand increases during growth but decreases when growth ceases. As reported by Brown and Cooper in 1991, due to quick microbial growth, the dissolved oxygen content in the culture is sharply reduced. Upon the onset of stationary phase, the oxygen level inside the culture reaches a minimum level, followed by a rapid rise [21]. This makes the transient change of dissolved oxygen a widely used feedback control parameter in SCF [24,26–29,142]. In this case, since industrial fermenters are commonly equipped with a dissolved oxygen probe [19], it is easy for conventional fermenters to be adapted into an SCF mode.

As cells grow, CO₂ is usually released from the fermenter as a by-product. This makes carbon dioxide evolution rate (CER) another feedback control parameter for SCFs that are run under aerobic conditions. CER is calculated using Equation 2.3.

$$\text{CER} = \frac{P}{RTV} Q(\text{CO}_2 \text{ gas out} - \text{CO}_2 \text{ air input}) \quad \text{Equation 2.3}$$

In this equation, P is the pressure (atm), R is the ideal gas constant (atm·L/(mol·K)), T is the temperature of the venting gas mixture (K), V is the working volume of the liquid inside the fermenter (L), Q is the volumetric gas flow rate for the existing gas stream (L/h), CO_{2 gas out} is the gaseous CO₂ concentration read by a near-infrared sensor in the venting line of a fermenter, and CO_{2 air input} is the gaseous CO₂ concentration obtained from the constant air flow into the fermenter. CER has a unit of mol/(L·h) [143].

CER shows transitional changes that coincide with the beginning of stationary phase [23,143]. A carbon dioxide sensor is installed outside the SCF fermenter, avoiding the need for direct contact with the culture. Hence, using CER as a feedback control greatly reduces the possibility of probe fouling by the liquid culture [143], thus minimizing the chance of interrupting the culture by replacing the sensor during fermentation and making this approach more robust than using a dissolved oxygen probe.

Until now, SCF has been successfully applied to many microbial fermentations that are performed under aerobic conditions. Conversely, SCFs operated under anaerobic conditions did not achieve the desired processing goals [24]. For instance, redox potential, despite being a difficult signal to interpret [24], was proposed as a feedback control parameter for microbial degradation of aromatics in the absence of oxygen [144]. However, the redox potential did not show a transitional change or a repeatable pattern upon the arrival of stationary phase, which, unless manually interrupted, could easily result in indefinite running of a cycle.

It is worth noting that CER would not be a suitable feedback control candidate for SCF for ethanol production under anaerobic conditions. This is because under anaerobic conditions, the gaseous CO₂ exiting the fermenter is not mixed with other gases, and thus it can easily saturate the infrared sensor throughout the fermentation process. Another way to address the saturation problem is by supplying a constant flow of make-up gas (excluding O₂ and CO₂) to the fermenter, so that the existing gas stream is not fully dominated by CO₂. However, this constant gas purge would likely bring additional costs to the process and promote the evaporation of ethanol. Overall, identifying an appropriate feedback control strategy for SCF under anaerobic conditions remains a paramount challenge.

2.4.2 Productivity improvement

Due to the real-time feedback control and automated cycling process, completion of an SCF cycle is immediately followed by the next cycle; the strategy allows the cycle time to be determined by the microorganism undergoing fermentation under the specific growing conditions [24,143]. This is distinct from a manual interruption, which would cut off or prolong the cycle, resulting in either a washout of substrate or longer fermentation time [24,28,142].

Since 50% of the volume is exchanged in an SCF fermenter, the cell number, starting from the second cycle, is doubled during each cycle, and thus the cycle time was found to equal doubling time under given SCF conditions. This also makes the cycles (except cycle 1) identical, stable, and reproducible [21,28,143]. As a result of SCF operation, the limiting nutrient is fully used, and no stationary phase is observed; after the initial cycle, lag phase

is eliminated, hence, cells are always growing under exponential phase, maximizing the growth rate for each fermentation cycle [21,24,29].

The operation of SCF can bring many advantages for microbial productions. For instance, a considerable improvement in productivity has been observed for many microbial fermentation systems using SCF, compared to conventional techniques [21–23,29]. This is usually due to the large size of inoculum left at the end of each cycle, a higher substrate consumption rate, and reduced fermentation time for each cycle [24,28,29]. Improved product yield was also reported in some cases [23], though the underlying mechanism was not established. In addition, SCF operations achieved reliable and stable patterns among cycles and runs, and it was robust enough to quickly recover after disturbances [28,143]. Since down time is significantly reduced during SCF operation, the total production under a given period of time (e.g. a year) can also be improved. Alternatively, the total operation time for a plant can be reduced for a given production target.

Standard SCF mainly targets microbial growth or primary metabolite production, but two-stage SCFs were also reported for the production of non-growth related products [145]. At the onset of stationary phase for each cycle, the harvested culture was transferred into a secondary reactor to continue fermentation instead of being dumped for downstream processing; meanwhile the main fermenter starts the next cycle by replacing the volume of harvest with fresh medium [24]. This two-stage SCF operation decouples microbial growth and metabolic production, which provides convenience and flexibility for the process. For instance, Storms *et al.* in 2012 used a two-stage SCF to produce β -glycosidase from a lysogenic bacterial strain [22]. The strain is lysogenic at a low temperature but the prophage can be induced for lysis and β -glycosidase production at a higher temperature. The SCF was started by cultivating the strain at its growth temperature, and upon the detection of stationary phase, the culture was automatically transferred to a second reactor. During the second stage, a higher temperature was used, and lysis was induced to produce β -glycosidase. Compared to batch fermentation performed under similar conditions, this two-stage SCF operation strategy increased the

integrated specific productivity (the amount of product per working volume per time used per cell population) by 50%.

2.4.3 Cell synchrony

A very interesting outcome from SCF operation, after the repetition of several cycles, is the synchronization of the cell population inside the fermenter [22,24,29,143]. Synchrony means that all the live cells inside the fermenter are at the same stage of the cell cycle, and they are dividing at the same time. The degree of synchrony can be calculated according to Equation 2.4.

$$F = \frac{N_t}{N_0} - 2^{t/g} \quad \text{Equation 2.4}$$

For this equation, N_t is the amount of cells at time t , N_0 is the initial amount of cells, t is a time interval, and g is the doubling time of a culture growing under normal conditions. Under SCF operation (cycle number ≥ 2), N_t/N_0 is equal to 2, t is the time required for cell division, and g is the cycle time. A value of 0 for the synchrony index (F) indicates no synchrony in the population, while $F = 1$ indicates a perfectly synchronized population. A significant synchrony is achieved when F is greater than 0.6 [143,146].

The underlying mechanism on how synchrony is achieved on a molecular level and whether synchrony contributes to an improvement of productivity, a common observation with SCF, remains an unsolved questions [24].

2.4.4 Existing cycling approaches for ethanol production

In the literature, there have been a few attempts to use cycling operation strategies for ethanol production, where repeated batch was the common term used. Some of these strategies used monitoring parameters to determine fermentation time and also compared productivity with conventional techniques. These are discussed further below.

Kida *et al.* in 1991 and 1992 used a flocculating *S. cerevisiae* strain for ethanol production in molasses medium. The gas evolution rate was used to monitor fermentation, and when it reached a level lower than 10% of the maximum rate, the mash was allowed to settle for 30 min before the clear liquid was removed and replaced (likely 75% volume

exchange). The rationale for using such a feedback control was not mentioned. In addition, when a slightly different fermentation environment (slightly higher temperature or mash loading) was used, the same feedback control for cycling fermentation resulted in decreased cell viability, lower ethanol titer, and/or longer fermentation time [147,148]. Hence, a better feedback control needs to be used for such systems.

Feng *et al.* in 2012 attempted to use *S. cerevisiae* for ethanol fermentation of a synthetic medium containing a high glucose content (200-250 g/L). The redox potential was proposed to monitor the process, and 50% replacement of the culture was used for cycling [149]. However, the feedback control pattern was not stable between cycles, as air was sparged into the culture to increase the value of redox potential when it fell below a certain level. This artificially disrupted the yeast metabolic pathways along with the redox readings of the culture. As a result, high concentration of glucose residues remained at the end of cycles, and a lower ethanol volumetric productivity was observed compared to the first batch, primarily attributed to a long fermentation time (more than half of the value of batch). The improvement in annual ethanol productivity (the amount of ethanol that can be produced over a year at large scale) claimed by the authors was solely attributed to a reduction in down time, as any other repeated batch fermentation would have.

Ma *et al.* in 2007 and 2009 mentioned using CER to control ethanol production from kitchen refuse, a complex medium to which glucose was added. At the end of a batch, 60% or 75% exchange of the culture was made, resulting in improvements in ethanol volumetric productivity averaging 46% and 36% compared to first batch, respectively [150,151]. However, air was constantly supplied to the culture for CER readings, and there was no established relationship between CER and the end of a cycle. In addition, an extra standing period (20 min) was used to settle solids before harvesting. Thus, the ethanol production could be improved by anaerobic conditions, and the cycle time could be further reduced by using an appropriate feedback control parameter.

As of yet, there has been no successful report of applying SCF for ethanol production with improved productivity. Based on the literature, it is clear that: 1) identifying a suitable monitoring parameter and cycling criteria that can give repeatable feedback control is crucial; 2) the feedback control parameter should align well with the metabolism of the

microorganism used in the fermentation system; and 3) it is necessary to clearly define and tightly control the amount of variables within one experiment.

Chapter 3 Improving ethanol productivity through self-cycling fermentation of yeast: a proof of concept*

3.1 Abstract

The cellulosic ethanol industry has developed efficient strategies for converting sugars obtained from various cellulosic feedstocks to bioethanol. However, any further major improvements in ethanol productivity will require development of novel and innovative fermentation strategies that enhance incumbent technologies in a cost-effective manner. The present study investigates the feasibility of applying self-cycling fermentation (SCF) to cellulosic ethanol production to elevate productivity. SCF is a semi-continuous cycling process that employs the following strategy: once the onset of stationary phase is detected, half of the broth volume is automatically harvested and replaced with fresh medium to initiate the next cycle. SCF has been shown to increase product yield and/or productivity in many types of microbial cultivation. To test whether this cycling process could increase productivity during ethanol fermentations, we mimicked the process by manually cycling the fermentation for five cycles in shake flasks, and then compared the results to batch operation. Mimicking SCF for five cycles resulted in regular patterns with regards to glucose consumption, ethanol titer, pH, and biomass production. Compared to batch fermentation, our cycling strategy displayed improved ethanol volumetric productivity (the titer of ethanol produced in a given cycle per corresponding cycle time) and specific productivity (the amount of ethanol produced per cellular biomass) by $43.1 \pm 11.6\%$ and $42.7 \pm 9.8\%$, respectively. Five successive cycles contributed to an improvement of overall productivity (the aggregate amount of ethanol produced at the end of a given cycle per total processing time) and the estimated annual ethanol productivity (the amount of ethanol produced per year) by $64.4 \pm 3.3\%$ and $33.1 \pm 7.2\%$, respectively. Collectively, this study provides proof-of-concept that applying SCF to ethanol production could

* A version of this chapter was published as Wang, J., Chae, M., Sauvageau, D., & Bressler, D. C. (2017). Improving ethanol productivity through self-cycling fermentation of yeast: a proof of concept. *Biotechnology for biofuels*, 10, 193.

significantly increase productivities, which will help strengthen the cellulosic ethanol industry.

Keywords: Cellulosic ethanol, Batch, Self-cycling fermentation, Manual cycling fermentation, Ethanol volumetric productivity, Specific productivity, Overall productivity, Annual ethanol productivity, Production cost, Capital cost.

3.2 Introduction

The global interest in cellulosic ethanol has surged due to the abundance of feedstock [4], increasing concerns for environmental sustainability and security of energy supplies [152], and the reduction of greenhouse gas emissions compared to 1st generation ethanol [153]. Production of cellulosic ethanol requires a pretreatment to open the complex structure of lignocellulosic materials, enzymatic hydrolysis to digest polymers into monomer sugars, microbial propagation to generate inoculum, fermentation of monomer sugars to produce ethanol, and distillation to acquire ethanol. However, according to Chen *et al.* [17], the cellulosic ethanol industry, as compared to mature 1st generation ethanol, is still faced with economic challenges such as high production costs. Therefore, technologies for the production of cellulosic ethanol still need extensive development. Various approaches have been attempted to offset costs, which have been primarily focused on development of effective pretreatment methods to facilitate hydrolysis and fermentation (*i.e.* efficient sugar digestion and inhibitors reduction, respectively) [154], reduction of enzyme costs/usage [155], and modification/improvement of strains that are efficient in co-fermentation of pentose and hexose sugars under inhibition conditions [108]. Researchers are also working on processing configurations, which are mainly focused on the relationship between hydrolysis and batch fermentation, such as separate hydrolysis and fermentation (SHF), simultaneous saccharification and fermentation (SSF), hybrid hydrolysis and fermentation (HHF), and consolidated bioprocessing (CBP); with SHF and HHF currently being more applicable [5]. Yet much less effort has been spent on the development of bioprocessing strategies that increase productivity through fermentation methodologies.

Batch operation is a widely used and preferred method for ethanol fermentation [18,135]. However, batch fermentation incorporates lag and stationary phases, during

which ethanol is not being produced at substantial levels. Furthermore, significant downtime is necessary after each fermentation to clean up the reactor and prepare for the next campaign. Thus, one approach to improving productivity of batch fermentation would be to reduce fermentation time and downtime. In addition, to achieve the desired levels of ethanol production, industrial ethanol facilities require a number of large batch bioreactors that operate intermittently to ensure a continuous supply of fermentation product for distillation [55]. Correspondingly, microbial propagation, a lengthy and multi-stage scale-up process that provides fermenters with seed culture, is needed for every batch fermentation cycle [18]. Therefore, batch fermentation and its associated seed cultivation contribute to high capital and operating costs. Altogether, capital and operating costs account for 34% and 33% of the total production costs of cellulosic biofuel, respectively [16]. One approach to address these cost issues is to develop a novel fermentation strategy that will improve productivity.

Self-cycling fermentation (SCF) is a semi-continuous cycling process where an online monitoring parameter is used to identify the onset of stationary phase. This identification automatically triggers the removal of half of the fermenter contents, which is immediately replaced with fresh, sterile medium to start a subsequent cycle of growth [24]. Through the operation of SCF, cells are synchronized, which means that all or almost all the cells are dividing at the same time. The actual growth rate of cells will vary depending on growth conditions, which will impact the time required to reach stationary phase, linked to the depletion of a limiting nutrient. Nevertheless, regardless of the time it takes for cells to enter stationary phase, an indicative real-time parameter can be used to trigger the removal and replacement of fermentation broth. Therefore, compared to batch operation, SCF (starting from cycle 2) avoids lag and stationary phases, which means that cells are always in exponential growth, and cycle time equals to generation time [24]. Dissolved oxygen, redox potential, and carbon dioxide evolution rate are commonly monitored parameters in batch reactors, and have all been used as real-time parameters to indicate cell growth and trigger the automation process of SCF [29,143,144]. Theoretically, SCF can continue indefinitely, with a successful demonstration by Wentworth *et al.* of more than 100 consecutive cycles for the production of citric acid [29]. Compared to batch

fermentation, SCF has also demonstrated increased product yield and/or productivity for many microbial production systems, such as citric acid [29], bioemulsifier [21], shikimic acid [23], and recombinant protein β -galactosidase [22]. Despite these achievements, SCF has not yet been successfully employed for ethanol production.

This study was designed as a proof-of-concept for SCF process to test if productivity can be elevated for cellulosic ethanol production. Shake flask was used for ethanol fermentation, and the cycling process was manually performed to mimic automated SCF. It suggests that applying SCF to ethanol fermentation can greatly improve productivity.

3.3 Methods

3.3.1 Yeast, medium, and inoculum

Superstart™ active distillers dry yeast, *Saccharomyces cerevisiae*, was purchased from Lallemand Ethanol Technology (Milwaukee, WI, USA). The yeast powder was hydrated, and after dilution, cell suspensions were spread on yeast extract peptone dextrose (YPD) agar plates (10 g/L yeast extract (Sigma-Aldrich, St. Louis, MO, USA); 20 g/L peptone, (Sigma-Aldrich, St. Louis, MO, USA); 20 g/L D-glucose (Sigma-Aldrich, St. Louis, MO, USA); 14 g/L agar (Thermo Fisher Scientific, Waltham, MA, USA)) and cultivated for two days at 30 °C. Individual colonies were transferred to YPD liquid medium (no agar) in glass tubes for overnight cultivation at 30.0 °C and 230 rpm. Some of the overnight culture was transferred to fresh YPD medium to obtain an optical density at 600 nm (OD_{600}) of roughly 0.3, and was then allowed to grow under the same conditions until the OD_{600} reached 1.0. The broth was then mixed with 50% (v/v) glycerol at a ratio of 1:1, and stored in vials at -80 °C to produce glycerol stock strains. When required, the stock strain was streaked on a YPD agar plate and allowed to cultivate for two days at 30.0 °C, and then stored in a 4 °C fridge. Colonies were transferred to a fresh YPD agar plate monthly.

For all seed cultures and fermentations performed in this work, chemically defined medium was used: 50 g/L D-glucose (Sigma-Aldrich, Oakville, ON, Canada), 6.7 g/L yeast nitrogen base (YNB) with amino acids (Sigma-Aldrich, St. Louis, MO, USA), and 0.1 M sodium phosphate buffer ($NaH_2PO_4 \cdot 2H_2O/Na_2HPO_4 \cdot 2H_2O$, Thermo Fisher Scientific,

Waltham, MA, USA) at pH 6.0. The medium was filter sterilized (Sartolab™ P20 Plus Filter Systems: 0.2 µm, Thermo Fisher Scientific, Waltham, MA, USA) prior to being used.

To prepare the inoculum, isolated colonies on YPD plates were transferred to 10 mL of chemically defined medium in glass tubes and incubated overnight at 30.0 °C with shaking at 200-250 rpm. A portion of this starter culture was transferred to a 1-L shake flask containing 180 or 600 mL fresh medium to obtain an OD₆₀₀ of ~0.2 for further incubation under the same condition. When an OD₆₀₀ of ~0.5 was achieved in the shake flask, the culture was used to inoculate the fermentation experiments described below (Sections 3.3.2 and 3.3.3). The inoculum volume for all experiments in the report was ~8% (v/v) of the fermentation medium.

3.3.2 Dynamic study of yeast fermentation

To baseline the dynamic changes that occur during batch ethanol fermentation using our fermentation system, a total of 24 shake flasks (500 mL) with 270 mL of chemically defined medium (described in Section 3.3.1) were inoculated with yeast (8%, v/v). The shake flasks were incubated at 30.0 °C with shaking at 200 rpm. Each flask was attached to an S-lock filled with distilled water to minimize air from flowing in the flask and to release gas out of the flask. At eight specific time points, three flasks were taken out of the incubator and sacrificed for analysis, allowing for analyses to be carried out in triplicate.

3.3.3 Cycling fermentation

This experiment, in which cycling was performed manually, was designed to mimic the process of SCF, and test whether our fermentation system could result in a stable process of reproducible cycles. The initial cycle had a working volume of 280 mL in a 500-mL shake flask. Additional shake flasks were incubated in parallel to allow for analysis of glucose levels at a given time point. Within fermentation cycles, the additional flasks were taken out from the incubator and monitored to determine the time at which glucose was virtually depleted (less than 1 g/L; analytical method described below). At this point, experimental flasks were taken out of the incubator and half of the broth volume (140 mL) was manually removed, and immediately replaced with an equal volume of sterile medium to start the next cycle. Immediately after the sterile media was added, the flask was gently

mixed and a 10-mL sample was removed for analysis. This process was repeated until the end of 5th cycle. It should be noted that for each successive cycle, a smaller amount of broth was removed/replaced due to the drop in fermentation broth volume resulting from withdrawal of 10 mL of samples taken for analysis. For example, at the end of cycle 2, there was a total working volume of 270 mL and thus only 135 mL were removed/replaced. All shake flasks were capped with an S-lock filled with distilled water. This experiment was performed in triplicate.

3.3.4 Analytical methods

Optical density (OD₆₀₀) was measured using a spectrophotometer (Ultrospec 4300 pro, Biochrom, England, UK). High OD₆₀₀ values of fermentation broth were diluted with medium to fall within the range of 0.2 ~ 0.9, and cell concentration was calculated according to the appropriate dilution factor. The broth pH was measured using a pH meter (Accumet® AB 15, Fisher Scientific, Thermo Fisher Scientific, Waltham, MA, USA). After filtration (0.22 µm) of samples, the concentrations of glucose, lactic acid, glycerol, and acetic acid were measured by high performance liquid chromatography (HPLC, 1200 series, Agilent Technologies, Mississauga, ON, Canada) coupled with a refractive index detector (1100 series, Agilent Technologies, Mississauga, ON, Canada) and Aminex HPX-87H column (Bio-Rad, Hercules, CA, USA). The analysis was performed using 5 mM sulfuric acid for 30 min at a flow rate of 0.5 mL/min and at a temperature of 60 °C [71]. For samples with glucose content less than 1 g/L or for quick confirmation of glucose depletion during manual cycling fermentation experiments, a Megazyme D-Glucose (glucose oxidase/peroxidase; GOPOD) assay kit (Bray, Ireland) was used, and the whole procedure took no more than 20 minutes. In this method, glucose concentration was determined through an absorbance reading at 510 nm, which quantified the amount of a quinoneimine dye derived through enzymatic processing of glucose. Samples were filtered (0.22 µm), mixed with GOPOD reagent, incubated at 50.0 °C, and the absorbance reading was compared against both blank and standard samples.

Ethanol content was determined by gas chromatography (GC, 7890A, Agilent Technologies, Mississauga, ON, Canada) coupled with a flame ionization detector (Arian Inc., Palo Alto, CA, USA), Resteck Stabilwax-DA column (0.5 µm × 30 m × 0.53 mm), and an

autosampler (7693, Agilent Technologies, Mississauga, ON, Canada). Helium was used as the carrier gas under a constant pressure control of 7.5 psig. A split ratio of 20:1 was used for a sample injection volume of 1 μ L. The temperatures used for injection and FID are 170 and 190 $^{\circ}$ C, respectively. During GC analysis, the oven started at a temperature of 35 $^{\circ}$ C with a 3-min hold, then the temperature increased to 190 $^{\circ}$ C by 20 $^{\circ}$ C/min, followed by a final hold for 1 min [69]. To account for ethanol evaporation during sample preparation, 1-butanol was added to sample as the internal standard, and samples were vigorously mixed and filtered (0.22 μ m) before GC analysis [71]. Fermentation efficiency was calculated by using the following equation:

$$\text{Fermentation efficiency} = \left(\frac{\text{amount of ethanol produced}}{\text{amount of glucose consumed}} \div 0.511 \right) \times 100 \quad \text{Equation 3.1}$$

Theoretically, 0.511 gram of ethanol is produced per gram of glucose. Fermentation samples were examined under a microscope to confirm the lack of bacterial contamination.

3.3.5 Statistical analysis

Analysis of variance (ANOVA) was conducted with Tukey test set at 95% confidence level by GraphPad Prism 5.04 software (La Jolla, CA, USA). Suspected outliers were evaluated by Q-Test (95% confidence) within triplicate results. The OD₆₀₀ measurement for one of the three flasks examined at the end of cycle 4 of the manual cycling experiment was confirmed as an outlier, and was therefore excluded from our data analyses; the other parameters assessed passed the test and were kept.

3.4 Results

3.4.1 Dynamic study of batch fermentation

The primary goal of the present work was to explore whether a self-cycling fermentation strategy can be incorporated into ethanol production to improve productivity and/or increase product yield. As a baseline comparison for our system, batch fermentation was performed, with several parameters (OD₆₀₀, pH, glucose, and ethanol concentrations) being monitored at various time points (Figure 3.1). During fermentation, glucose, the main carbon source, was consumed by yeast for growth and ethanol

production. Glucose was depleted at ~20.5 h, when cell concentration (measured by OD₆₀₀) and ethanol yield reached maximum values. The pH of the fermentation broth dropped while the yeasts were growing and stabilized before the onset of stationary phase. The fermentation efficiency at 20.5 h was 86.1 ± 0.4%. Based on the growth curve generated through OD₆₀₀ readings, we estimated the generation time to be approximately 6 hours. Inspection of cells under a microscope confirmed that there was no bacterial contamination.

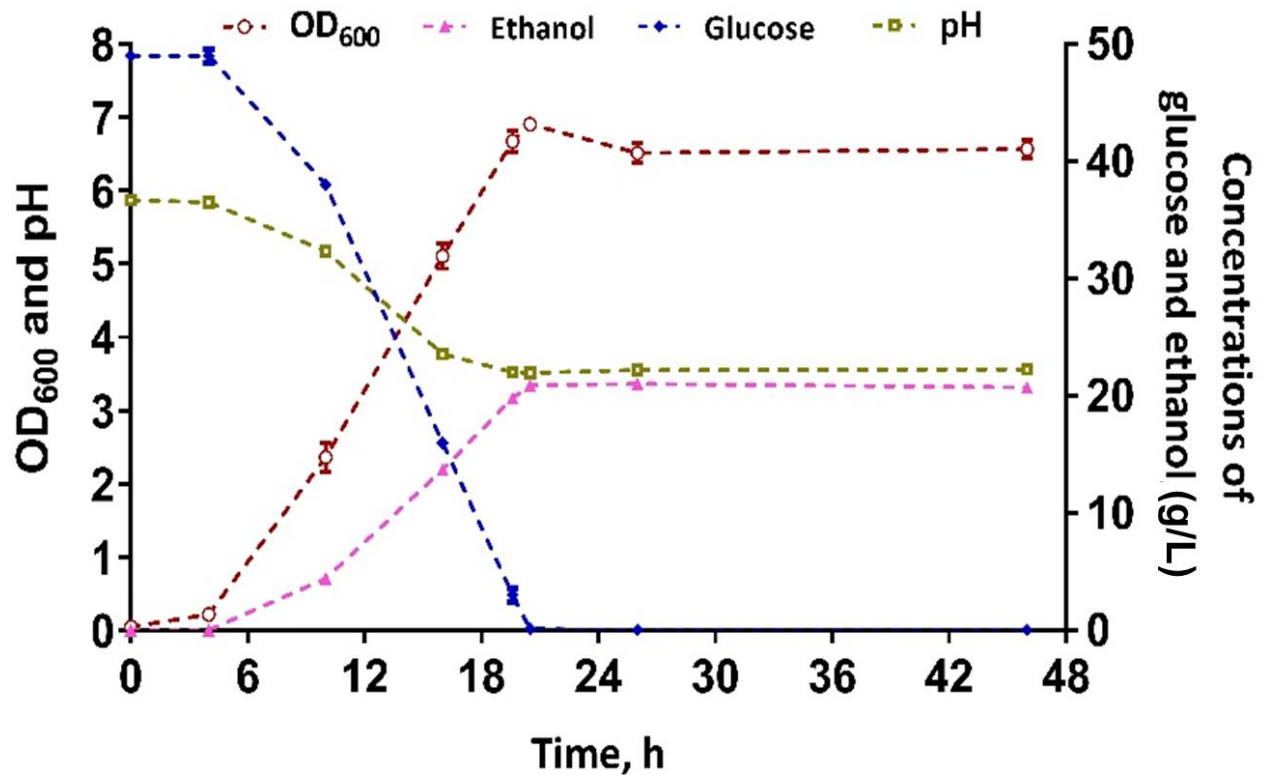


Figure 3.1 Dynamic study of batch fermentation in shake flasks. Optical density (OD₆₀₀), pH, glucose consumption, and ethanol production were monitored over a 46 h period. Error bars represent standard deviation of triplicate experiments.

3.4.2 Cycling study

Following the batch fermentation experiments, we performed cycling fermentations to determine the impact of incorporating this methodology into an ethanol production system. In this work, cycle time is defined as the time used only for fermentation, excluding

the harvest and replacement steps. Once the depletion of glucose had been confirmed, half the fermentation broth was removed and replaced with an equal amount of fresh growth medium, initiating the next fermentation cycle. This was repeated for a total of 5 fermentation cycles. Based on this strategy, in cycle 1, the input content of glucose, as well as the produced amount of ethanol, was roughly twice as much as corresponding values from cycles 2 to 5 (Figure 3.2 and Table 3.1). As shown in Figure 3.2b, glucose was completely consumed at the end of all cycles. For cycles 2 to 5, although a smaller amount of ethanol was generated in each cycle compared to cycle 1 (Table 3.1), the final concentration of ethanol (g/L) was statistically equal in all cycles (Figure 3.2c). Additionally, when compared on a per glucose input basis, the yield of ethanol produced was statistically similar in all cycles (Table 3.1). Thus, the key significance of these experiments is the dramatic decrease in fermentation time required to produce ethanol when the SCF approach was employed. For example, cycle 1 produced 5.6 ± 0.0 g of ethanol in 21.9 ± 0.1 h, while cycles 2, 3, and 4 together produced 7.2 ± 0.2 g of ethanol in 18.8 ± 0.0 h. Thus, cycles 2, 3, and 4 produced $129.2 \pm 2.3\%$ of the ethanol generated in cycle 1, but in only $86.0 \pm 0.5\%$ of the time.

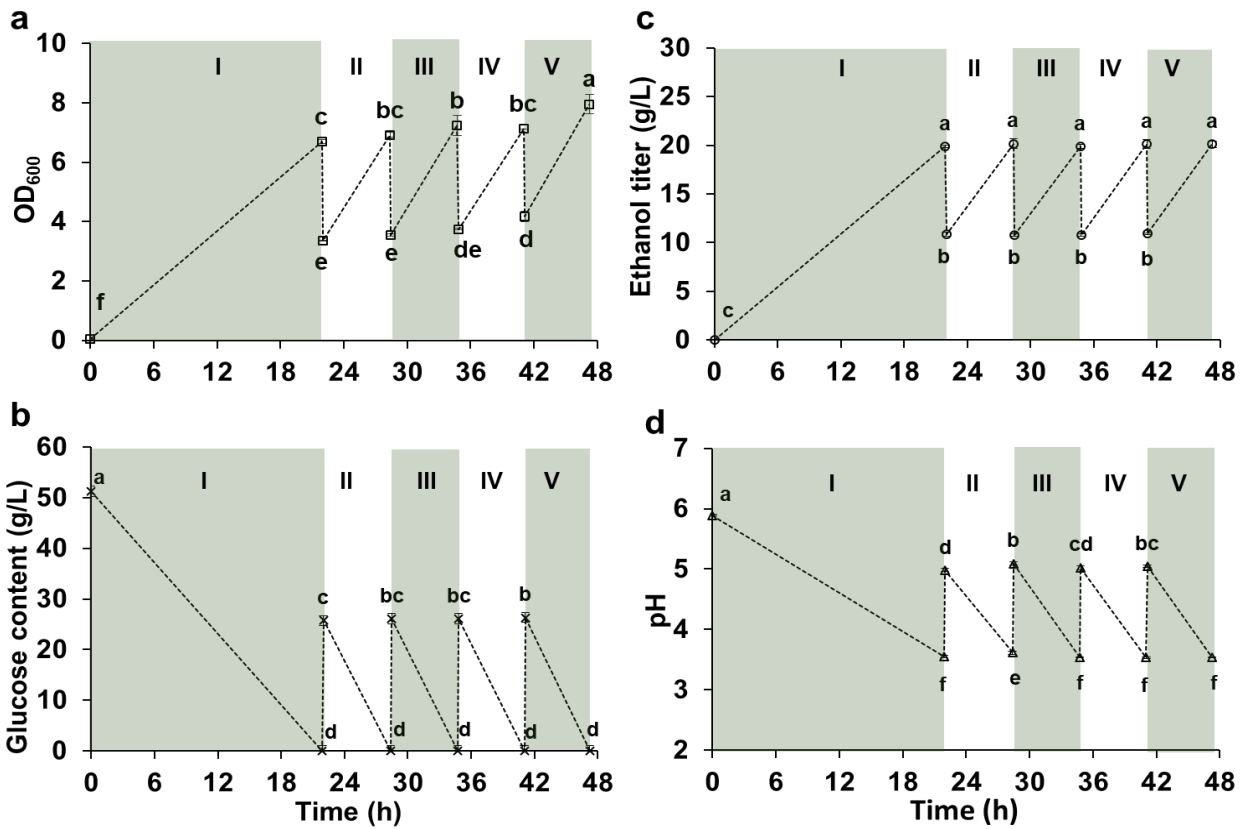


Figure 3.2 Cycling fermentation experiments in shake flasks. OD₆₀₀ (a), glucose concentration (b), ethanol content (c), and pH (d) of the culture were monitored through 5 cycles over a 47 h period. The cycle numbers are indicated with roman numerals. Error bars represent standard deviation of triplicate experiments, except for the OD₆₀₀ value at 40.9 h in Figure 3.2a (the end of cycle 4), which shows the result of duplicate samples (see Materials and methods). Means that do not share the same letter are statistically different (95% confidence level, Tukey).

Table 3.1 Cycling fermentations and overall productivity improvement.

Cycle Number	Cycle time (h)	Glucose available at onset of cycle (g)	Amount of ethanol produced in a given cycle (g)	Yield of ethanol produced in a given cycle per glucose fed (g/g)	Overall productivity improvement compared to batch
1	21.9 ± 0.1 ^a	14.3 ± 0.0 ^a	5.6 ± 0.0 ^a	0.4 ± 0.0 ^a	-9.7 ± 0.6% ^a
2	6.4 ± 0.0 ^b	6.9 ± 0.1 ^b	2.5 ± 0.2 ^b	0.4 ± 0.0 ^a	15.6 ± 3.4% ^b
3	6.3 ± 0.0 ^{bc}	6.8 ± 0.0 ^c	2.4 ± 0.1 ^{bc}	0.3 ± 0.0 ^a	34.9 ± 2.0% ^c
4	6.2 ± 0.0 ^{cd}	6.5 ± 0.0 ^d	2.3 ± 0.1 ^{bc}	0.4 ± 0.0 ^a	51.1 ± 2.7% ^d
5	6.1 ± 0.0 ^d	6.3 ± 0.1 ^e	2.2 ± 0.1 ^c	0.3 ± 0.0 ^a	64.4 ± 3.3% ^e

Numbers indicate the mean ± standard deviation of triplicate experiments. Within the same column, values with different superscript letters are statistically different.

Figure 3.2d shows that the first cycle started with a pH of 5.9 ± 0.0 and dropped to 3.5 ± 0.1 by the end of the cycle. After the first manual removal and broth replacement, the buffer capacity of the added medium was not strong enough to bring the pH back to the original value, stabilizing at around pH 5.0. For successive cycles, the pH fluctuated roughly from pH 5.0 at the beginning of the cycles to pH 3.5 at their ends. In terms of yeast growth (Figure 3.2a), cultures from all cycles ended with a statistically similar optical density, except for cycle 5, which generated a statistically higher value than the other cycles. However, the starting OD_{600} values of cycles generally increased as a function of cycle number, with cycle 5 being the highest among all cycles. Furthermore, when the change in OD_{600} was compared amongst cycles 2 to 5, there was no significant difference.

Ethanol volumetric productivity (Figure 3.3a) represents the ethanol produced (g/L) each cycle per corresponding cycle time (h). Compared to the 1st cycle, which is essentially a normal batch fermentation, successive manual cycling significantly improved ethanol volumetric productivity (Figure 3.3a). For example, cycle 2 displayed an ethanol volumetric productivity increase of $60.4 \pm 12.1\%$ and $43.1 \pm 11.6\%$, compared to cycle 1 and batch

fermentation (Figure 3.1), respectively. Specific productivity (Figure 3.3b) – representing the ethanol volumetric productivity per biomass content (based on OD₆₀₀ readings) – was $55.1 \pm 9.7\%$ and $42.7 \pm 9.8\%$ greater in cycle 2 than in the first cycle and batch fermentation, respectively. These values did not differ significantly in cycles 2 to 5. To obtain an approximation of the influence of self-cycling fermentation on overall production efficiency, we calculated the overall productivity based on the laboratory conditions used (Figure 3.3c). Overall productivity for a cycle considers the ethanol (g/L) accumulated at the end of the cycle per total process time – which includes medium preparation, the cumulative fermentation cycle time, as well as the time required for the harvesting and refilling steps (3 min each in lab conditions). For a single batch fermentation, medium preparation, sterilization of media and equipment, and seed cultivation took a total of 21.8 h, while slightly longer was spent for manual cycling fermentation runs (22.7 h); this increase was due to longer time necessary for filter sterilization of a larger volume of medium and a longer period of seed culture cultivation. The length of batch fermentation (20.5 h) was adapted from our dynamic study as similar laboratory procedures, reagents, and glassware were used for both. For the total process, 42.2 ± 0.0 h and 69.9 ± 0.1 h were spent for batch and manual cycling fermentation (5 cycles), respectively, which means that manual cycling for 5 fermentation cycles took $65.4 \pm 0.2\%$ longer than batch. Compared to batch, an increase of cycle number in manual cycling fermentation significantly improved overall productivity (Figure 3.3c), and a $64.4 \pm 3.3\%$ improvement was observed when 5 cycles were involved (Table 3.1).

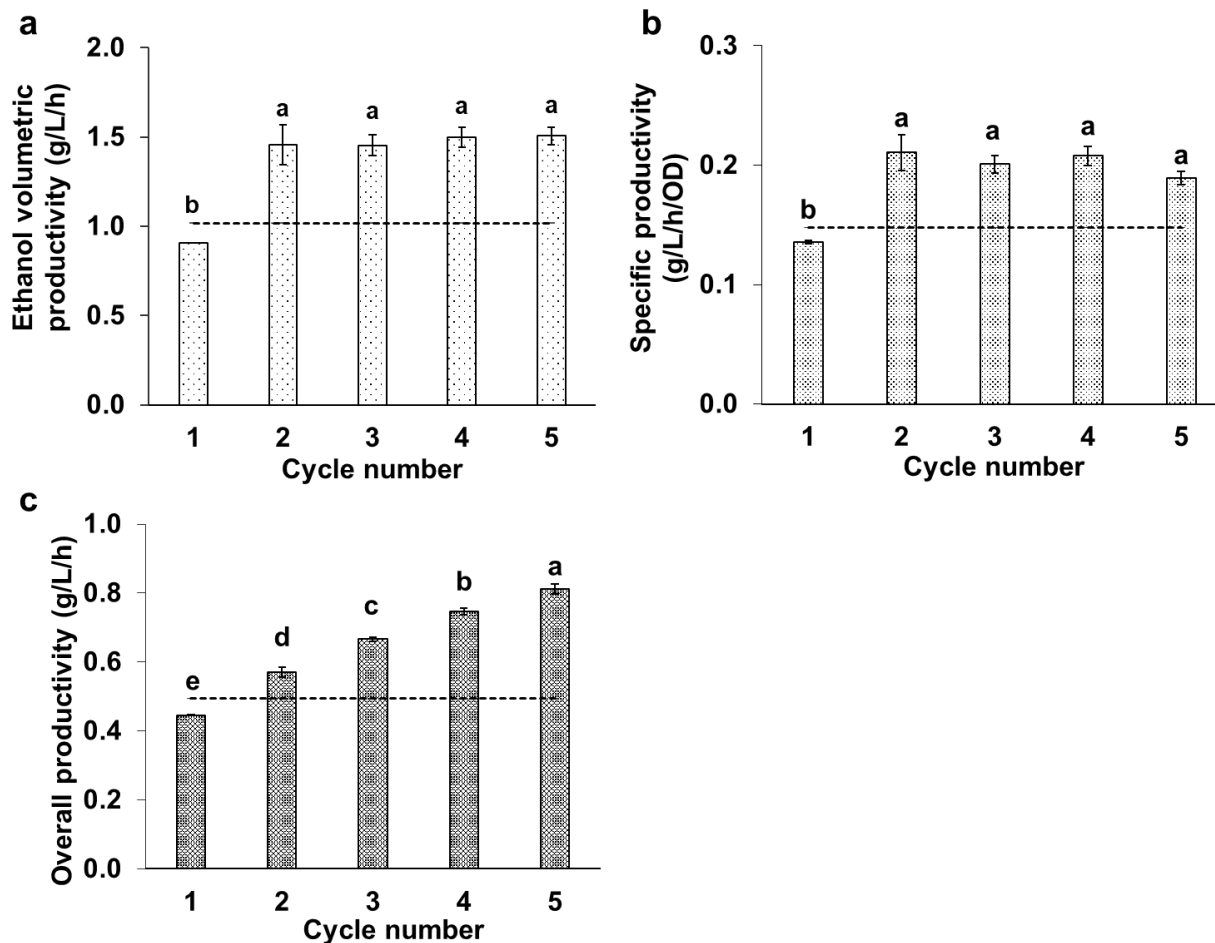


Figure 3.3 Productivities of cycling fermentation experiments conducted in shake flasks. Ethanol volumetric productivity (a), specific productivity (b), and overall productivity (c) were determined for manual cycling experiments. The horizontal solid line represents the mean values obtained through a dynamic batch study (Figure 3.1), where ethanol production reached a plateau at ~20.5 h. Error bars represent standard deviation of triplicate experiments, except for cycle 4 in Figure 3.3b, which represents duplicate samples (see materials and methods). Means that do not share the same letter are statistically different (95% confidence level, Tukey).

3.4.3 Annual ethanol productivity for potential scale-up

To appreciate how implementation of a self-cycling strategy could potentially impact annual ethanol production goals at large-scale, we compared SCF with batch in

terms of annual ethanol productivity, which represents the ethanol produced per year (P , ton/year). Feng *et al.* determined the annual fermentation operation time (t_{annual}) for an ethanol plant to be 7920 h (330 days) [149]. For a reactor with a working volume (V) of 10^5 L, downtime between cycles was estimated at 6.0 h ($t_{d-batch}$) and 0.25 h for batch and SCF methodology, respectively [149]. Residence time ($t_{f-batch}$, t_{f-SCF}) and ethanol produced (C_{batch} , C_{SCF}) per campaign for batch and SCF were adapted from our dynamic batch and manual cycling studies (cycle 1 and 2), respectively. For demonstration of the calculations below, mean values of triplicate experimental results were used.

For batch fermentation, the number of campaigns (N_{batch}) possible in a year would be:

$$N_{batch} = \frac{t_{annual}}{t_{f-batch} + t_{d-batch}} = \frac{7920 \text{ h/year}}{20.5 \text{ h/campaign} + 6.0 \text{ h/campaign}} = 299 \text{ campaign/year}$$

Thus, the annual ethanol productivity for batch fermentation (P_{batch}) would be:

$$\begin{aligned} P_{batch} &= N_{batch} \times C_{batch} \times V = 299 \text{ campaign/year} \times 20.9 \text{ g/L/campaign} \times 10^5 \text{ L} \\ &= 6.25 \times 10^8 \text{ g/year} = 625 \text{ ton/year} \end{aligned} \quad \text{Equation 3.2}$$

We assume that a plant can continuously run SCF for x ($x \geq 1$) cycle numbers (with 0.25 h downtime between cycles) each campaign, after which point, the reactor will need to be cleaned and set up for a new campaign (6 h downtime following the last SCF cycle; assumed to be the same as batch).

For a single SCF campaign, the total of residence time (t_{f-SCF}) would be the sum of all x cycles:

$$\begin{aligned} t_{f-SCF} &= t_{f-cycle 1} + (t_{f-subsequent cycles})(x - 1) \text{ cycles} = 21.9 \text{ h} + (6.4 \text{ h/cycle})(x - 1) \text{ cycles} \\ &= 15.5 \text{ h} + 6.4x \text{ h} \end{aligned}$$

Similarly, the total downtime (t_{d-SCF}) for a single SCF campaign can be summarized as follows:

$$\begin{aligned} t_{d-SCF} &= (t_{d-(x-1) cycles})(x - 1) \text{ cycles} + t_{d-cycle x} = (0.25 \text{ h/cycle})(x - 1) \text{ cycles} + 6.0 \text{ h} \\ &= 5.75 \text{ h} + 0.25x \text{ h} \end{aligned}$$

Therefore, the total number of SCF campaigns that can be run each year (N_{SCF}) can then be determined as such:

$$N_{SCF} = \frac{t_{annual}}{t_{f-SCF} + t_{d-SCF}} = \frac{7920 \text{ h/year}}{[(15.5 \text{ h} + 6.4x \text{ h}) + (5.75 \text{ h} + 0.25x \text{ h})]/\text{campaign}} = \frac{7920 \text{ h/year}}{[21.25 \text{ h} + 6.65x \text{ h}]/\text{campaign}}$$

Using the SCF strategy, the total amount of ethanol produced per campaign with x cycles (E_{SCF}) can be calculated as shown below:

$$\begin{aligned} E_{SCF} &= (C_{f-cycle 1})(V) + (C_{f-subsequent cycles})(V)(x - 1) \text{ cycles} \\ &= V \times [(C_{f-cycle 1}) + (C_{f-subsequent cycles})(x - 1) \text{ cycles}]/\text{campaign} \\ &= 10^5 \text{ L} \times [19.9 \text{ g/L} + (9.3 \text{ g/L/cycle})(x - 1) \text{ cycles}]/\text{campaign} \\ &= 10^5 \text{ L} \times [10.6 \text{ g/L} + 9.3x \text{ g/L}]/\text{campaign} \end{aligned}$$

Therefore, the annual ethanol productivity (P_{SCF}) would be:

$$\begin{aligned} P_{SCF} &= N_{SCF} \times E_{SCF} = \frac{7920 \text{ h/year}}{[21.25 \text{ h} + 6.65x \text{ h}]/\text{campaign}} \times 10^5 \text{ L} \times [10.6 \text{ g/L} + 9.3x \text{ g/L}]/\text{campaign} \\ &= \frac{792 \times (10.6 + 9.3x)}{21.25 + 6.65x} \text{ ton/year} \end{aligned} \quad \text{Equation 3.3}$$

If cycling fermentation is operated for 5 consecutive cycles ($x = 5$), as was the case in our manual cycling study, P_{SCF} would be 830 ± 41 ton/year, representing a $33.1 \pm 7.2\%$ improvement in annual ethanol productivity compared to batch (P_{batch} , 624 ± 3 ton/year). As implied by Figure 3.4, as the number of consecutive cycles (x) in each SCF campaign increases, the annual ethanol productivity (P_{SCF}) initially increases sharply before the increase becomes almost negligible (as the fraction of downtime to production time becomes negligible). Moreover, annual ethanol productivity in SCF (P_{SCF}) is expected to be significantly greater than that of batch fermentation (P_{batch}), even when only 2 cycles ($x \geq 2$) are operated for each SCF campaign.

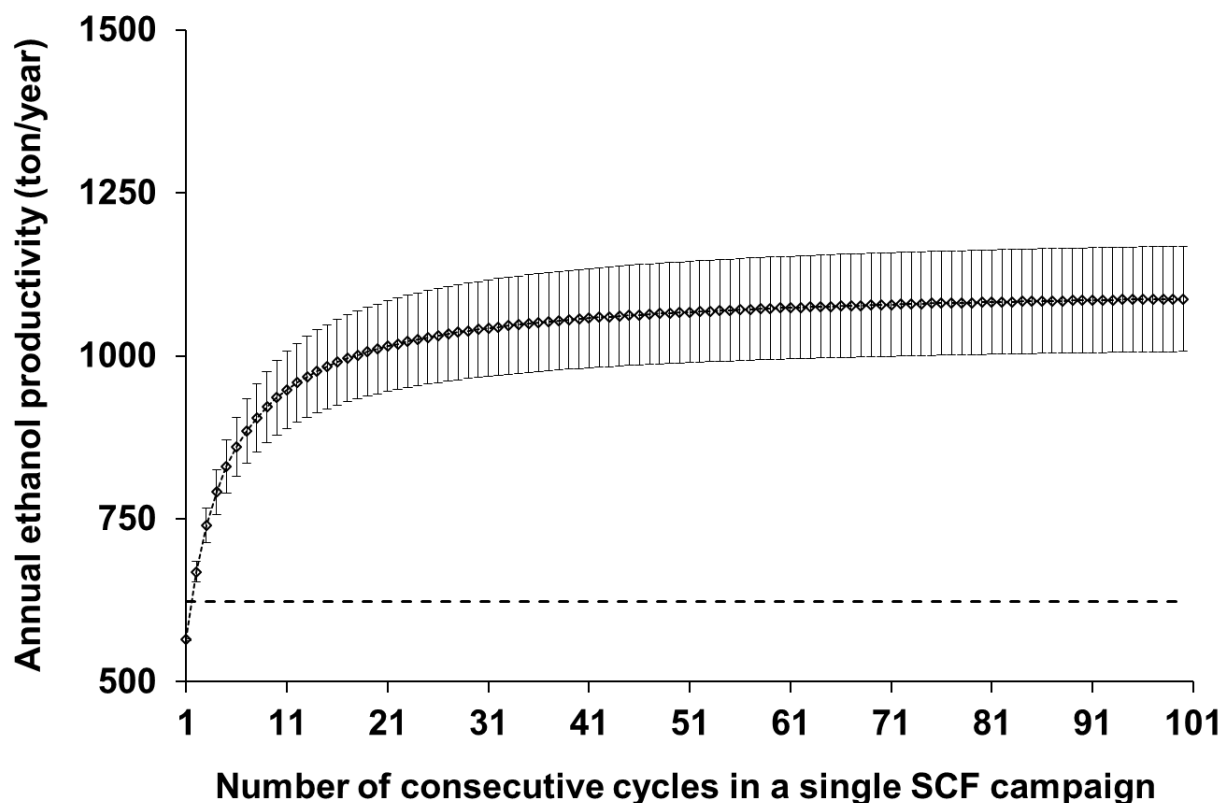


Figure 3.4 Annual ethanol productivity derived from experiments using shake flasks. Annual ethanol productivity was calculated assuming the number of consecutive cycles operated for each SCF campaign could range from 1 to 100. The horizontal solid line represents the mean values obtained through a dynamic batch study (Figure 3.1), where ethanol production reached a plateau at ~ 20.5 h. Error bars were calculated from the errors in ethanol yield and cycle time of SCF cycles and represent standard deviation of triplicate experiments.

Examined from a different perspective, the goal of SCF application may be to achieve the same annual ethanol productivity as batch fermentation (based on 625 ton/year), but in a shorter amount of time (*i.e.* fewer campaigns). Using the equation above, if SCF operation is based on 5 consecutive cycles ($x = 5$), each SCF campaign will produce 5.7 tons of ethanol (E_{SCF}). Therefore, the number of SCF campaigns required to produce 625 tons of ethanol through SCF is roughly 110 per year (P_{batch}/E_{SCF}). Given that each SCF campaign

would require a total of 54.5 h ($t_{f-SCF} + t_{d-SCF}$), the total time required for 110 campaigns is roughly 6000 h. This is approximately 1900 h (~80 days) shorter than the annual fermentation time required for batch fermentation to produce the same amount of ethanol.

3.5 Discussion

3.5.1 Dynamic study

Ethanol production is tightly associated with cell growth. As such, when the limiting nutrient is depleted under anaerobic conditions, yeast stops growing and producing ethanol, entering into stationary phase. In the present study, the ethanol titer was lower than what has been achieved in industry [10]; this is because a defined medium (6.7 g/L YNB with amino acids, 0.1 mol/L phosphate buffer, and 50 g/L glucose), where glucose was the main carbon source, was used at a low concentration, instead of directly using a typical hydrolysate of lignocellulosic material that contains a mixture of pentose and hexose sugars, corn steep liquor, and inhibitors [18]. This was done in order to simplify the implementation of SCF operation for the study at hand.

Nevertheless, given the data on glucose consumption and ethanol production in batch fermentation (Figure 3.1), the medium system was adequately buffered and was able to achieve relatively high fermentation efficiency and biomass yield. The drop of pH may also help reduce the risk of bacterial. As is typical during ethanol fermentation, the pH of our batch system decreased, likely because the uptake of buffering materials such as amino nitrogen compounds, the excretion of organic acids [156], the utilization of ammonium – which releases hydrogen ions outside of the cell [157] – and the production of carbonic acid due to the reaction of carbon dioxide (released by yeast) with water. contamination for ethanol production at industrial settings [19]. It should be noted that the fermentation efficiency observed in the batch fermentation is lower than those typically observed in fermentations using wheat grain as feedstock (roughly 90-93%) [71,158]. One explanation for this may be the presence of oxygen in the headspace of shake flasks, which would enable yeast to momentarily grow aerobically to produce biomass, rather than ethanol. Furthermore, the medium used was not optimized for ethanol production, as is the case with ethanol fermentations using grains. Despite the suboptimal conditions, the

fermentation efficiency still reached $86.1 \pm 0.4\%$. Furthermore, we are exploring the use of other media that could be employed in SCF operation to further improve fermentation efficiency.

3.5.2 Cycling study

Since Figure 3.1 revealed that the onset of stationary phase was tightly linked to the depletion of glucose, identification of the specific time point where glucose is depleted is important for SCF systems as this may allow for harvest and fresh medium addition right as cells would enter stationary phase, where ethanol production ends and cell metabolism begins to change. As suggested in the manual cycling study, sugar was depleted by the end of each cycle (Figure 3.2b), which would help bioethanol producers avoid unnecessary sugar losses and improve process economics. This also gives SCF an advantage over chemostat operation, where some of the nutrients are washed out throughout the process.

It should be noted that, for cycles 2 to 5, there was a slight gradual increase in starting cell concentration (Figure 3.2a), yet no significant difference in OD_{600} change was found among the four cycles. This is possibly due to the settling of cells during manual broth removal, which made the cell concentration of removed sample slightly lower than that of the broth left inside of shake flasks. The settling might be the reason why one of the three samples at the end of cycle 4 was rejected as an outlier (Q-Test) of its parallel samples in cell concentration (as measured by OD_{600}). Whereas the measurements of the other parameters (pH, glucose and ethanol concentrations) used techniques that are not related to cell concentration and the values were retained by Q-test, we still incorporated that sample for the results of parameters not based on OD_{600} . All in all, this settling phenomenon will likely not be an issue in scale-up due to continual stirring during broth removal.

It should also be noted that due to the sampling required for analysis, the fermentation broth volume decreased by 10 mL in each cycle, which led to a reduction in total glucose input (g) and also the total amount of ethanol produced (g) from cycles 1 to 5 (Table 3.1). While such sampling may have slightly decreased total ethanol production in our shake flask studies, this would not be significant in bioreactor operation, as sampling volumes are negligible in larger vessels. Nevertheless, our data clearly provide proof-of-

concept that our SCF approach to ethanol production can retain ethanol yield and increase ethanol yield per fermentation time.

As shown in the cycling experiments, which mimicked SCF, at the end of each cycle, half of the cell population was harvested with the other half serving as the “inoculum” (50% (v/v) of the working volume) for the next cycle. SCF can contribute several benefits to the ethanol production process.

Firstly, in current cellulosic ethanol plants, a few steps are typically required to gradually scale up a seed culture for inoculation, which is a common practice for batch fermentation [18]. Whereas for SCF operation, once inoculated for the first cycle, the yeast propagation process in multiple seed tanks is no longer required for subsequent cycles, and is only necessary when a new SCF campaign is initiated. Thus, the more cycles incorporated into an SCF campaign, the fewer microbial propagation steps would be required. This will save nutrients, energy, and work hours spent on the propagation stage. Furthermore, the cycling strategy of SCF is easily compatible with current processing infrastructure, since the removed volume of broth can be fed continuously into a distillation column, and fresh medium could be pumped from the hydrolysis section (SHF) of an integrated process.

Secondly, as shown in the cycling experiments (Table 3.1), compared to batch operation, fermentation time is dramatically reduced in SCF, without compromising the ethanol yield. This is likely because the lag and stationary phases are removed from SCF operation [24], and, therefore, cells are always in exponential growth. It should be noted that only two data points are shown for each cycle (Figure 3.2), so there is a possibility that the substrate was depleted earlier than reported, which could make the fermentation cycle times shorter and productivity higher. Also, cycle times varied among cycles 2-5 (Table 3.1). These cycle times are based on the confirmation of glucose disappearance (using the GOPOD method) from additional shake flasks incubated in parallel to minimize volume change of the main experimental flasks and avoid exposure to air during fermentation. Thus, this analytical procedure may have introduced a slight delay, and the cycling times reported may not be absolutely reflective of what happened in the main experimental flasks. Furthermore, although some of the cycling times were statistically different, they were only different by a few minutes. In the implementation of a fully automated SCF

system, the overestimation of cycle time is unlikely, since the fermentation will be monitored by a real-time parameter, which will automatically trigger the cycling process once cells enter stationary phase.

Finally, for cellulosic ethanol production, the pretreatment of feedstocks can form or release inhibitors, such as furfural, phenolic compounds, and weak acids, that can inhibit cell growth and ethanol production [5]. It has been reported that inhibition can be biochemically mitigated through exposing microbe seed cultures to inhibitors during propagation [159]. Therefore, for SCF, it may be worthwhile in the future to test whether the “inoculum” (*i.e.* half of the fermentation broth from the previous cycle), which has been grown in the presence of any potential inhibitors, will help the following cycle achieve better inhibitor-tolerance and therefore better ethanol production.

According to Table 3.1, the yield of ethanol produced per glucose fed was statistically similar for all cycles. Thus, the $43.1 \pm 11.6\%$ improvement in ethanol volumetric productivity (g/L/h) observed in the cycling fermentation study was due to the reduced fermentation time. This result, even though performed in shake flasks - which may lead to higher variability than controlled bioreactors, is still consistent with those of reported SCF systems - where bioreactors were used and improvements in productivity were achieved primarily due to shorter fermentation time than batch [17,19]. It should be noted that cell synchrony was not assessed in this study as synchrony has been shown to be established after 5 to 10 SCF cycles. Therefore, the reduction of fermentation time in the present study is unlikely to be due to cell synchrony. Whichever is the case, significant improvements in productivities are observed and optimization of cell synchronies could possibly further enhance these results. This supports the argument that application of SCF in industrial ethanol production may reduce the fermentation time necessary to reach current production goals, without changing existing infrastructures. The reduction of fermentation time leads to lower operation costs, which currently make up 33% of total production costs [16]. Alternatively, this improvement also suggests that current production levels could be met by employing smaller bioreactors in an SCF strategy. In this way, new cellulosic ethanol plants may be able to reduce their capital costs, which typically account for 34% of the total production cost [16]. Given the similar biomass yields of all

cycles (Figure 3.2a), the specific productivity of all cycles is clearly most impacted by the ethanol volumetric productivity. Again, this strongly suggests that the improvement in specific productivity is mainly due to the reduced cycle time. Overall productivity in a laboratory setting indicates how the cycling strategy could impact the overall process. Examining the cycling process in a single shake flask, results support that when more cycles are incorporated in a campaign, higher overall productivity is achieved (Figure 3.3c). Note that there was a $9.7 \pm 0.6\%$ reduction in overall productivity compared to batch when cycle 1 (essentially a batch cycle) was performed. This probably results from the extra time required to confirm the disappearance of glucose in parallel flasks prior to performing the manual cycling, which results in a slight overestimation of cycling times in the manual cycling study. In dynamic batch study, flasks were directly taken out from the incubator and sacrificed for dynamic analysis throughout the fermentation process. In addition, this difference could result from batch to batch variations as batch operation is known to be variable [21].

3.5.3 Annual ethanol productivity for potential scale-up

Currently, cost reductions of cellulosic ethanol production primarily come from improvements in pretreatment [154], hydrolysis [155], and strain improvement [108]. However, much less effort has been spent on improving productivity and reducing costs by directly changing processing strategies of fermentation. To get an idea whether applying cycling strategies to ethanol fermentation could increase the total amount of ethanol that could be produced per year (annual ethanol productivity) at large scale, we assumed that, with the exception of the length of downtime, SCF would operate under the same conditions as batch. According to Feng *et al.*, downtime between cycles is approximately 6 h for batch fermentation [149], which includes the time used to harvest broth, clean, sterilize, and refill the reactor. However, only 0.25 h will be needed to exchange volumes between SCF cycles [149], since only half the volume of the broth will be harvested, and no cleaning or sterilization steps are necessary between cycles. Furthermore, the time required to add fresh medium to the reactor will actually be part of the cycle time because cells continue to grow as soon as the nutrients are added to the reactor. These calculations indicate that, compared to batch operation, if a 5-cycle SCF strategy were implemented for each

campaign performed at a plant, either the amount of ethanol produced annually would be greatly increased or annual fermentation time would be dramatically reduced for the same production level. These improvements, which would help reduce production cost, are mainly attributable to the reduced fermentation time, as well as the reduced fraction of downtime.

While theoretically SCF can run indefinitely, there is a concern that in long-term continuous operation of SCF, a non-beneficial mutation or severe bacterial contamination may occur and affect ethanol productivity. This can be averted by implementing SCF operation with number of cycles (x) that is low enough to minimize the probability of mutations or contamination affecting productivity, but large enough to significantly increase annual ethanol productivity. Figure 3.4 provides a basis for the determination of an optimal number of cycles. Based on these results, we found that, with regard to annual ethanol productivity, operation of SCF for approximately 20 sequential cycles (essentially 19 generations after cycle 1) would provide a good balance between improved productivity and reduced risks of mutation/contamination.

To the best of our knowledge, the present study is the first to provide proof-of-concept that SCF could be employed for ethanol production towards elevated productivities. Feng *et al.* attempted to implement SCF operation by using redox potential as a feedback control parameter for ethanol fermentation [149]. Air was purged in the reactor when the redox potential of the broth fell below a certain level, so that redox potential could generate a transient response. However, this switch between anaerobic and aerobic conditions during fermentation likely disrupted cell metabolism, and thus affected ethanol production. Therefore, this artificial manipulation of redox potential during SCF for ethanol production led to longer fermentation time and reduced ethanol volumetric productivity compared to batch operation.

3.6 Conclusions

By mimicking the SCF process in manual cycling experiments at the shake flask-scale, the required fermentation time was greatly reduced, while maintaining statistically equivalent glucose to ethanol conversion. With respect to batch operation, our cycling strategy improved ethanol volumetric productivity by $43.1 \pm 11.6\%$, overall productivity by

64.4 ± 3.3%, and estimated annual ethanol productivity by 33.1 ± 7.2%. These elevated productivities may lead to reduced capital costs (*i.e.* the number and/or size of fermenters required) or operation costs (*i.e.* the fermentation time required), increased amounts of ethanol production per year, and could eventually lower production costs, relative to batch fermentation. This work, even though performed under sub-optimal conditions, has successfully provided proof-of-concept that adoption of an SCF strategy for cellulosic ethanol could increase productivities, thereby opening up a great possibility for applying novel cycling fermentation strategies to strengthen the cellulosic ethanol industry.

3.7 Funding

The project is funded by BioFuelNet Canada and the Natural Sciences and Engineering Research Council of Canada (NSERC).

Chapter 4 Improved bioethanol productivity through gas flow rate-driven self-cycling fermentation*

4.1 Abstract

The growth of the cellulosic ethanol industry is currently impeded by high production costs. One possible solution is to improve the performance of fermentation itself, which has great potential to improve the economics of the entire production process. Here, we demonstrated significantly improved productivity through application of an advanced fermentation approach, named self-cycling fermentation (SCF), for cellulosic ethanol production. The flow rate of outlet gas from the fermenter was used as a real-time monitoring parameter to drive the cycling of the ethanol fermentation process. Then, long-term operation of SCF under anaerobic conditions was improved by the addition of ergosterol and fatty acids, which stabilized operation and reduced fermentation time. Finally, an automated SCF system was successfully operated for 21 cycles, with robust behavior and stable ethanol production. SCF maintained similar ethanol titers to batch operation while significantly reducing fermentation and down times. This led to significant improvements in ethanol volumetric productivity (the amount of ethanol produced by a cycle per working volume per cycle time) – ranging from 37.5-75.3%, depending on the cycle number, and in annual ethanol productivity (the amount of ethanol that can be produced each year at large scale) – reaching $75.8 \pm 2.9\%$. Improved flocculation, with potential advantages for biomass removal and reduction in downstream costs, was also observed. In conclusion, our successful demonstration of SCF could help reduce production costs for the cellulosic ethanol industry through improved productivity and automated operation.

Keywords: cellulosic ethanol; batch fermentation; self-cycling fermentation; online monitoring parameter; gas flow rate; ergosterol and Tween 80; anaerobic fermentation; ethanol volumetric productivity; annual ethanol productivity; flocculation.

* A version of this chapter was accepted as Wang, J., Chae, M., Bressler, D.C., & Sauvageau, D. (2020). Improved bioethanol productivity through gas flow rate-driven self-cycling fermentation. *Biotechnology for Biofuels* 13, 14. <https://doi.org/10.1186/s13068-020-1658-6>.

4.2 Background

The US Energy Independence and Security Act of 2007 established a mandatory goal of producing 16 billion gallons of biofuel from lignocellulosic materials by 2022 [160], with cellulosic ethanol being the primary commodity. As a result, big breakthroughs in biomass conversion have been made. For example, POET-DSM claimed that a bottleneck in their pretreatment technology was resolved by enhanced enzymatic digestion of feedstocks [12], the National Renewable Energy Laboratory found that CelA cellulase from *Caldicellulosiruptor bescii* could efficiently hydrolyze cellulose with a high degree of crystallinity [13], and Nguyen *et al.* demonstrated a great improvement of ethanol titer (86 g/L) and low enzyme dosage (~ 6.5 filter paper unit \cdot g glucan⁻¹) by combining a cosolvent-enhanced lignocellulosic fractionation pretreatment strategy with simultaneous saccharification and fermentation [161]. As such, while well-recognized technical barriers to viable commercialization of cellulosic ethanol are overcome, the fermentation process itself is now identified as a limiting factor; with current techniques limited by relatively low productivity and intensive labor. Therefore, it is strategically important to develop advanced processes and pursue improvements in productivity for fermentation itself.

Chapter 3 showed how a manual cycling fermentation approach used for *Saccharomyces cerevisiae* significantly improved ethanol volumetric productivity and annual ethanol productivity – by $43.1 \pm 11.6\%$ and $33.1 \pm 7.2\%$, respectively – compared to batch operation [162]. Self-cycling fermentation (SCF) is an automated semi-continuous fermentation technique in which the onset of stationary phase, identified in real-time by a monitoring parameter, such as dissolved oxygen or carbon dioxide evolution rate (CER) in aerobic systems [21,22,29,143], triggers a cycling process. At this point, half the volume of the culture is harvested and immediately replaced by fresh medium to start the next cycle. The repetition can proceed for a number of cycles, e.g. 137 cycles for the production of citric acid [29], without contamination. During SCF operation an elevated degree of cell synchrony, where a large number of cells inside the reactor are at the same phase in their life cycle, has often been achieved with various microbial populations [23,29,143]. More details and principles regarding the concept of SCF have been described elsewhere [22,24,143]. The proof-of-concept study was carried out in 500-mL shake flasks where SCF

was manually mimicked for a total of 5 cycles [162]. On top of that, the present study is focused on how to implement real SCF into ethanol production under anaerobic conditions, how to automate the process in a 5-L fermenter, and finally, whether the real SCF process can help improve productivity.

To adapt SCF to ethanol fermentation, it is necessary to select a monitoring parameter that clearly identifies the onset of stationary phase in real-time to initiate the automated cycling process. Despite the fact that SCF has been applied to many microbial fermentation systems, the majority of them were operated under aerobic conditions [22,24,29,143]. In fact, only two research groups examined the operation of SCF under anaerobic conditions [144,149,163] – investigating microbial degradation of nitrate species in the former and ethanol production by yeast in the latter. In both cases, the researchers attempted to use oxidation-reduction potential as a monitoring parameter. Unfortunately, their work demonstrated that this parameter was not appropriate to establish reliable cycling processes.

Ethanol fermentations operated in batch mode have also been studied using online monitoring approaches, as a way to reduce the intensive labor necessary for offline chemical analysis [20]. For instance, near-infrared [130], Fourier transform infrared [131], and Raman spectroscopies [132] have all been used and mathematically correlated with concentrations of sugars and ethanol or microbial biomass to indicate the status of fermentations. These strategies are promising and could be adapted as monitoring parameters in SCF. However, the possibility of spectroscopic signals being masked or interfered by the presence of solids in the bioreactor [130,132] could be of concern, as is the need to build spectral libraries by calibrating with a large number of samples from various conditions [130,131]. Alternatively, as a co-product of ethanol generation and a proxy for metabolic activity, the CO₂ produced during fermentation could provide a strategy for operation of SCF with *S. cerevisiae* under anaerobic conditions. Sablayrolles *et al.* [164] measured the weight loss of a bioreactor, which was presumed to result primarily from the release of CO₂, as an indicator for fermentation speed in batch mode. However, weighing reactors introduces potentially insurmountable logistical challenges at larger scales.

In this study, we initially performed batch fermentation of *S. cerevisiae* to monitor patterns in flow rate of outlet gas released – measured using a mass flow meter – as a reliable monitoring parameter to be used for the feedback control of SCF operation. We then incorporated this strategy into an automated SCF system operated under anaerobic conditions. The necessity of adding ergosterol and Tween 80 to reduce fermentation time and improve stability of SCF was also assessed under anaerobic conditions. Finally, an automated SCF system was successfully operated for 21 cycles, demonstrating stable and robust patterns for sugar consumption and ethanol production, significantly improved productivities, and improved flocculation of yeast cells that could potentially facilitate downstream processing.

4.3 Methods

4.3.1 Media and yeast

Two types of medium were used for fermentations. Yeast nitrogen base (YNB) medium (50 g/L glucose and 6.7 g/L yeast nitrogen base with amino acids in 0.1 M sodium phosphate buffer (pH 6.0)) was filter-sterilized into a 10-L carboy (Nalgene™, Thermo Fisher Scientific, Waltham, MA, USA). The second medium consisted of YNB medium supplemented with 0.02 g/L ergosterol (Sigma-Aldrich, St. Louis, MO, USA) and 0.8 g/L Tween 80 (Sigma-Aldrich, St. Louis, MO, USA) [165]. The protocol for adding ergosterol and Tween 80 was adapted from Andreasen and Stier [166]. Briefly, ethanol was mixed with ergosterol and Tween 80, and the mixture was boiled until the solution was clear. This was then mixed with YNB medium (filter-sterilized) for a homogenous emulsion. Note that the resulting concentration of ethanol in the second medium was below 0.5 g/L.

The industrial yeast strain *Saccharomyces cerevisiae* Superstart™, purchased from Lallemand Ethanol Technology (Milwaukee, WI, USA), was used for this study. Yeast cells were cultivated and aliquoted into multiple glycerol stock vials and stored at -80 °C until use. Prior to each fermentation run, a new vial was thawed, streaked on solid agar (14 g/L, Thermo Fisher Scientific, Waltham, MA, USA) plates containing yeast extract peptone dextrose (50 g/L, Thermo Fisher Scientific, Waltham, MA, USA), incubated at 30 °C for 2 days, and then stored at 4 °C for 1-2 days prior to fermentation. Seed cultures were

prepared according to [162], and inoculation was made by transferring seed cultures from 500-mL shake flask into the fermenter at 8% (v/v) of the fermentation medium.

4.3.2 Fermentation system

A 5-L fermenter (Infors-HT, Bottmingen, Switzerland) equipped with a heating jacket, condenser, high and low conductivity level sensors, antifoam pump (III), temperature control, gas sparger, rotameter II and impellers was used for all fermentation experiments in this study (Figure 4.1). An EasyFerm pH probe (Hamilton Company, Reno, NV, USA) was also attached to the fermenter. All gas inlets and outlets were coupled with 0.2- μ m filters (PTFE; Sigma-Aldrich, St. Louis, MO, USA). The fermenter (Figure 4.1) was connected with hardware for feeding (a), harvesting (d), sampling (e), and gas purging to headspace (f). Two stainless steel rods, placed at the 1-L and 2-L levels (with error < 1.5%) when the mixing rate was kept at 200 rpm, were used as conductivity level sensors in the fermenter. The whole system, as shown in Figure 4.1, was controlled by a scheme developed in the Labview[®] environment (National Instrument, Austin, Texas, USA).

Feeding line (a): A 10-L carboy containing fresh sterile medium was constantly mixed to supply fresh medium to the fermenter. N₂ (99.998% purity; Praxair Canada Inc, Mississauga, ON, Canada) was used to purge the carboy prior to and during feeding of fresh medium to the fermenter to minimize the possibility of O₂ entering the system. Fresh medium was transferred at a flow rate of 300 mL/min using a peristaltic pump (I; MasterFlex[®] L/S[®] drive, Head model: 77200-60; Cole-Parmer, Montreal, QC, Canada).

Antifoam line (b): Antifoam Y-30 emulsion (Sigma-Aldrich, St. Louis, MO, USA) was sent to the fermenter through a peristaltic pump (III; Infors-HT; Bottmingen, Switzerland) to a final concentration of ~100 μ L/L culture.

Venting line (c): During fermentation, N₂ and/or CO₂ gas leaving the fermenter were vented through a condenser kept at 15 °C, followed by a gas flow meter (Whisper series, MW-200SCCM-D/5M; Alicat Scientific, Inc., Tucson, AZ, USA), which measured the temperature, pressure, flow rate, and integrated flow rate of the gas, before being released to the atmosphere. The flow meter was calibrated with pure CO₂ by the manufacturer. A gas trap with distilled water was placed between the condenser and the gas flow meter to

ensure that air would not flow back into the fermenter. Note that all values of gas flow rate are reported at 25 °C and 1 atm.

Harvesting/sampling line (d/e): The same port, divided by a Y-shape tube (e), was used for both functions. Harvesting was performed using a digital peristaltic pump (II; MasterFlex® L/S® drive, Head model: 77201-60; Cole-Parmer, Montreal, QC, Canada) at a set flow rate of 300 mL/min, with the sampling line clamped. Sampling was achieved by creating a vacuum using a syringe attached to the filter (e). After sampling, samples were transferred to sterile 15-mL centrifugation tubes, and immediately stored at -80 °C until offline analysis was performed.

Headspace purging (f): During cycling of SCF (see cycling process), N₂ was sent to the headspace of the fermenter. This balanced the pressure during harvest, minimized entry of O₂ during feeding, and minimized losses of ethanol, the volatile product.

Batch fermentation: Sterile medium was added to the fermenter through the feeding line (a), heated to 30 °C, and flushed with N₂ through the gas sparger for 30 min. After adding antifoam (b), the fermentation was initiated by inoculation and the fermenter was flushed with N₂ again for 10 min. The fermenter was incubated at 30.0 ± 0.2 °C, with an impellor mixing rate of 600 ± 2 rpm. For all fermentations performed in this study, a 2-L working volume was used.

SCF operation: The fermenter was controlled at the same conditions as for batch operation, except that at the onset of stationary phase, the cycling process was automatically performed.

Cycling criteria: The criteria to initiate cycling were set in the Labview® program as follows: cycle time > 3 h, pH < 4.0, and slope of the outlet gas flow rate reached a value lower than -20 ccm/h, which then continuously increases for 2 min. The rationale for these criteria can be found in the Results Section 4.4.1.

Cycling process (harvest and feed): When the cycling criteria were met, the impellor mixing rate dropped to 200 rpm to ensure accurate signal from level sensors, after which half the culture was withdrawn through the harvest line (d), while N₂ was automatically purged through line (f) to balance the pressure of the fermenter's headspace. When the 1-L level was reached, harvesting was stopped and fresh medium was fed

through the feeding line (a) to start a subsequent cycle. Once feeding was complete (2-L level was reached), agitation returned to 600 rpm, antifoam was added, and the N₂ purge continued for another 5 min. Finally, data logging started. Despite the fact the program was designed to automatically run the cycling process, it was possible to manually initiate cycling even if the criteria were not met (for example, if the operator saw the pH plateau at ~4, the slope of outlet gas flow rate reached a minimum (yet not as low as -20 ccm/h) and staggered with a continuous increase for over 2 min). Samples were taken during harvesting and after antifoam addition to represent the cultures at the end and beginning of cycles.

Cycle time: For batch, cycle time was defined as the time from inoculation to the point when the minimum in the slope of gas flow rate occurred. For cycle 1 of SCF, the cycle time covered from inoculation to the end of harvest; whereas for all the other SCF cycles, it was the period from start of feeding to the end of harvest.

Data logging: During fermentation, time, temperature, pH of the culture, flow rate of the outlet gas, slope of the gas flow rate, and integrated gas flow rate were calculated and recorded every 10 s. Flow rate in this report was exported as the average value over a 15-min time span. Slope of gas flow rate was calculated from a linear regression of the data over the same time span. Finally, integrated gas flow rate was calculated every 1 s as the cumulative flow rate.

Sampling: Sampling was performed as described above. For the batch fermentation, since no obvious flocculation was observed, samples were analyzed for OD₆₀₀ using a UV-Vis spectrometer (Ultrospec 4300 Pro; Amersham Biosciences, Mississauga, ON, Canada). The measurement can be referred to Section 3.3.4. For samples from SCF demonstration (21 cycles), due to flocculation, dry cell weight was performed by centrifuging the cells at 10,016 × g (accuSpin™ 400; Thermo Fisher Scientific, Waltham, MA, USA) for 10 min, replacing the supernatant – which was kept for liquid and gas chromatography analyses – with ~10 mL 0.01 mol/L sterile sodium phosphate buffer (pH 6.0), and centrifuging the cells a second time. The supernatant was then discarded and the pellet was re-suspended in deionized water, placed in a pre-weighed dish, left to dry in an oven at 60 °C until the mass stabilized. Dry cell weight was calculated using equation 4.3:

$$\text{Dry cell weight} = \frac{\text{dry weight of the dish containing sample} - \text{dry weight of empty dish}}{\text{weight of centrifuge tube with culture sample} - \text{weight of empty centrifuge tube}}$$

Equation 4.3

The supernatants of thawed centrifuged samples were analyzed by HPLC and GC, according to the procedures mentioned in Section 3.3.4. For glucose content below 1 g/L, a D-glucose kit was used (Section 3.3.4). Samples were also analyzed by microscopy throughout the study to check contamination.

4.4 Results

4.4.1 Identification of a monitoring parameter for SCF

Anaerobic batch fermentation was carried out using a specialized fermenter system (Figure 4.1) to identify a monitoring parameter indicative of the onset of stationary phase to trigger cycling for ensuing SCF operation. As implied by Figure 4.2a, typical growth patterns, characterized by lag, exponential and stationary phases, were observed for batch operation, and pH decreased below 4.0 before plateauing. During exponential growth (~4 to 22 h), concentrations of sugar and ethanol displayed a rapid and relatively linear change, while little or no changes were observed during the lag (~0 h to 4 h) and stationary (~24 h to 27 h) phases (Figure 4.2a and b). Overall, considering the time at which glucose (sole carbon source) was depleted and the maxima in OD₆₀₀ (optical density at 600 nm) and ethanol titer were reached, we can conclude that the stationary phase was reached between 22 and 24 h.

To determine whether gas released from the fermenter – essentially CO₂ generated from the active conversion of glucose to ethanol – could be used to identify the onset of stationary phase under anaerobic conditions, a flow meter was installed at the only outlet of the fermenter (Figure 4.1).

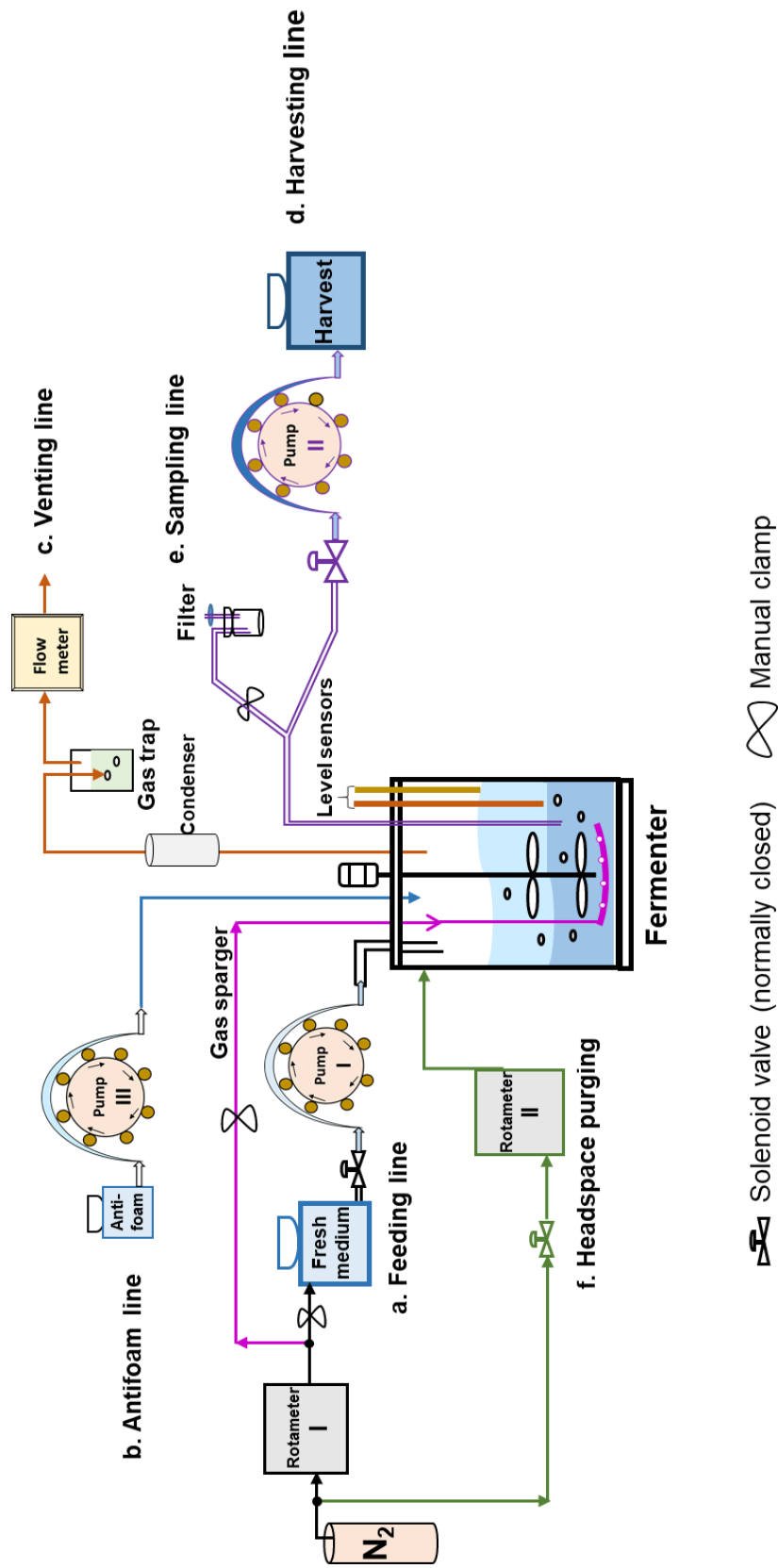


Figure 4.1 Bioreactor set up for Self-Cycling Fermentation (SCF). The temperature control and the pH probe are not shown. The control gauge for N_2 pressure from the gas cylinder was set to 4 psig during fermentation. The various components displayed in this schematic are not necessarily represented in their actual locations.

The gas flow rate and its first derivative (slope) were reported (Figure 4.2c and d, respectively). It should be noted that each sampling point seen in Figure 4.2a and b corresponds to a small downward spike in gas flow rate (Figure 4.2c) and slope (Figure 4.2d), which was caused by a small reduction in overhead gas pressure during sampling. Despite this, the flow rate of the gas venting out of the fermenter during fermentation increased to a maximum at 14-18 h and then quickly decreased (Figure 4.2c). The slope of the gas flow rate (Figure 4.2d) shows a sharp valley at 23.6 h (highlighted by the dotted vertical line), with a minimum lower than -20 ccm/h. Based on the timing of this minimum and the magnitude of the slope, we identified this parameter as a potential marker of the onset of stationary phase. Therefore, the conditions for cycling in ensuing SCF operation were considered met when 1) the slope of gas flow rate fell below -20 ccm/h and then the value continuously increased for more than 2 min; 2) the cycle time was greater than 3 h; and 3) the pH dropped below 4.0. The value of -20 ccm/h for slope value (criterion 1) was not the minimum value observed during fermentation, but served as a transitional response to identify the onset of stationary phase. The inclusion of cycle time and pH was merely to reduce the influence of fluctuations in the slope signal (Figure 4.2d).

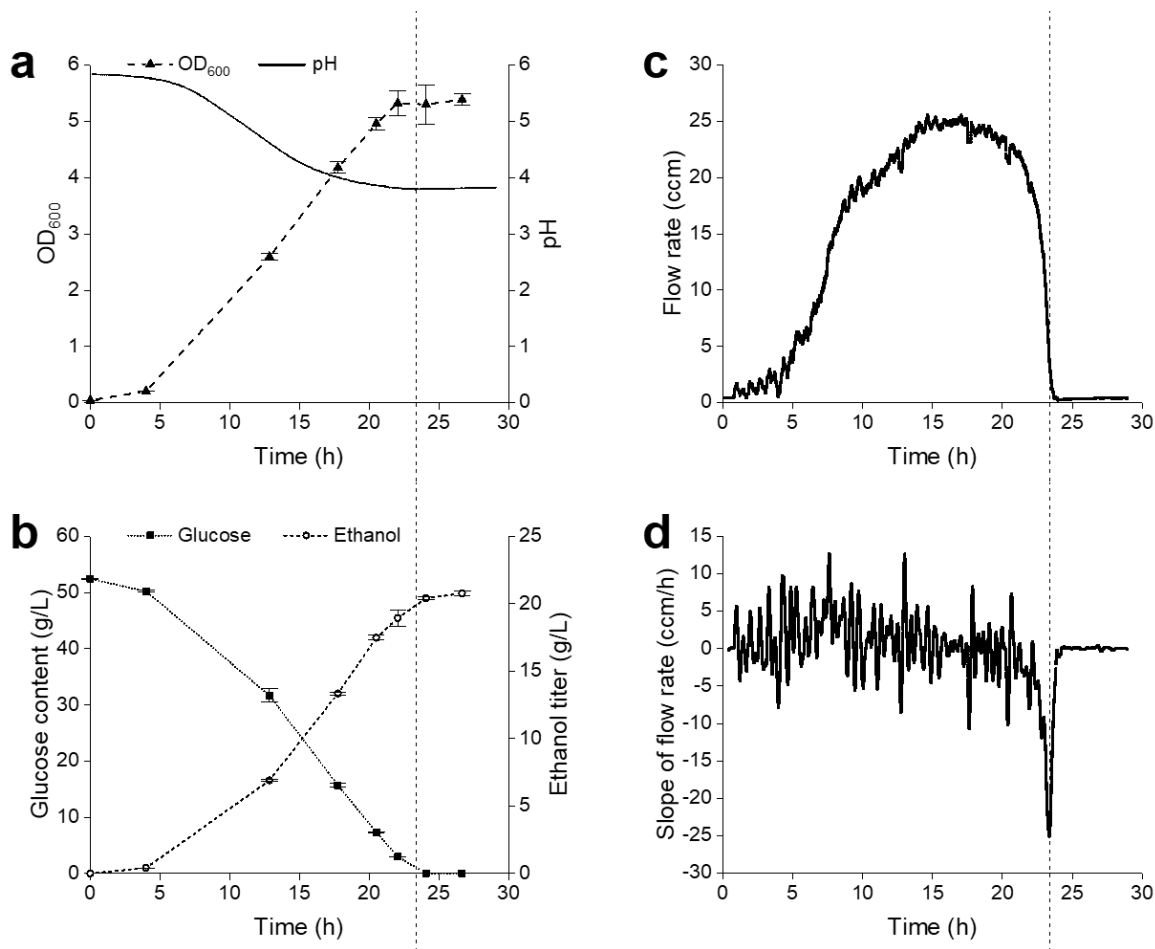


Figure 4.2 Batch fermentation. Samples were taken at different intervals during fermentation to analyze biomass contents (a), as well as glucose and ethanol concentrations (b). The data reported is the average from triplicates, with error bars representing standard deviations. The pH (a) and flow rate of the gas released during fermentation (c) were monitored in real-time, and the slope of the flow rate (d) was automatically calculated. A vertical line was added to all graphs at 23.6 h, corresponding to the sharp minimum in slope of gas flow rate (d). The gas flow rate was reported in cubic centimeter per minute (ccm) at 25 °C and 1 atm, and the slope of the gas flow rate was measured in cubic centimeter per minute per cycle time (ccm/h).

The cumulative volume of gas evolved throughout fermentation (Additional Figure 1a in Appendix A) was calculated by adding the gas flow rate at a frequency of 1s – this was similar to, yet more accurate than, the integrated area of the gas flow rate over time (Figure

4.2c). Ideally, the cumulative volume of gas evolved would be proportional to the amount of sugar consumed and ethanol produced. To confirm if this was the case, we calculated the expected sugar content and ethanol titer in the fermenter based on the cumulative gas evolved for various time points, as shown in equation 4.1 and 4.2, respectively.

$$[G]_t = [G]_o - \left(\frac{V_{g,t}}{V_{g,Total}} \times [G]_o \right) \quad \text{Equation 4.1}$$

where $[G]_t$ is the expected concentration of glucose at time t (g/L), $[G]_o$ is the initial concentration of glucose (g/L), $V_{g,Total}$ is the total volume of gas evolved (L), and $V_{g,t}$ is the volume of gas evolved from the beginning of fermentation to time t (L).

$$[EtOH]_t = \frac{V_{g,t}}{V_{g,Total}} \times [EtOH]_{Total} \quad \text{Equation 4.2}$$

where $[EtOH]_t$ is the expected concentration of ethanol at time t (g/L), and $[EtOH]_{Total}$ is the final concentration of ethanol produced during the fermentation (g/L).

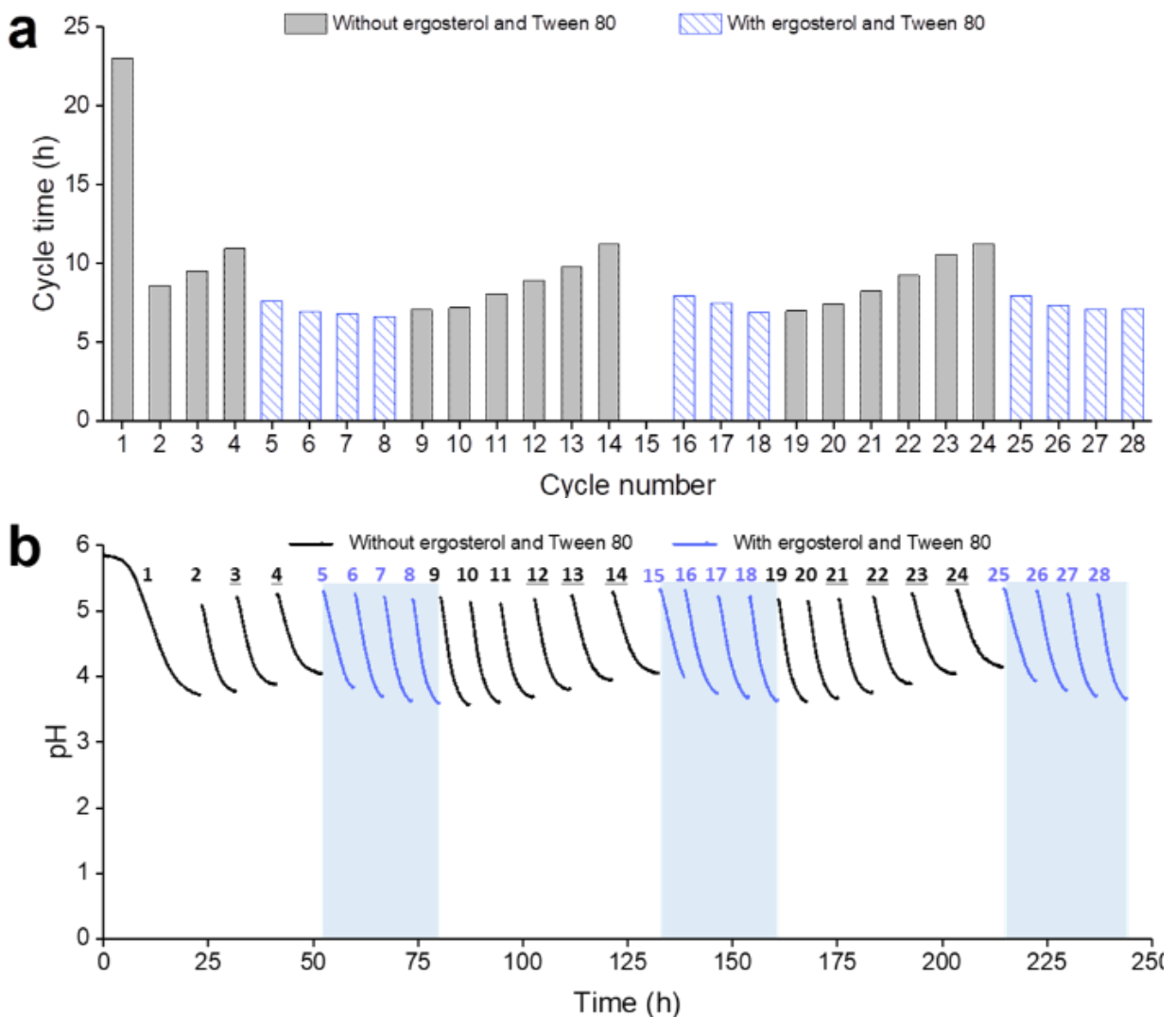
As shown in Additional Figure 1b and c (Appendix A), the predicted values obtained from equation 4.1 and 4.2 showed strong correlations with the actual values determined using a high performance liquid chromatograph (HPLC) for glucose and gas chromatograph (GC) for ethanol.

4.4.2 Assessing the requirements for ergosterol and Tween 80 in anaerobic SCF

The cycling conditions established in the batch experiments were used to operate SCF under the same fermenter system (Figure 4.1). It has been reported in batch fermentations that sterols and unsaturated fatty acids need to be added to long-term *S. cerevisiae* cultures growing under anaerobic conditions [166,167], as these important components of plasma membrane cannot be synthesized by yeast in the absence of oxygen [168]. In order to assess if this would apply to SCF operation, yeasts were grown in yeast nitrogen base medium (which does not contain sterols or fatty acids) for the first 4 SCF cycles, followed by 4 more cycles (cycles 5-8) in which the same medium was supplemented with ergosterol and Tween 80 (a source of unsaturated fatty acids). These

were repeated for cycles 9-14 (no supplementation) and 15-18 (supplementation), as well as cycles 19-24 (no supplementation) and 25-28 (supplementation).

As expected, cycle 1 behaved as a batch fermentation (Figure 4.2) in terms of cycle time, pH, gas flow rate, and slope of gas flow rate (Figure 4.3). However, cycle time progressively increased from cycles 2 to 4 (Figure 4.3a). Supplementation with ergosterol and Tween 80 in the following cycles (5-8) resulted in a significant reduction and stabilization of cycle time. These observations were consistent in the following cycles, where exclusion of ergosterol and Tween 80 (cycles 9 to 14 and 19 to 24) progressively led to longer cycle times (Figure 4.3a), higher final pH values (Figure 4.3b), lower gas flow rates (Figure 4.3c), and higher final slope values (Figure 4.3d).



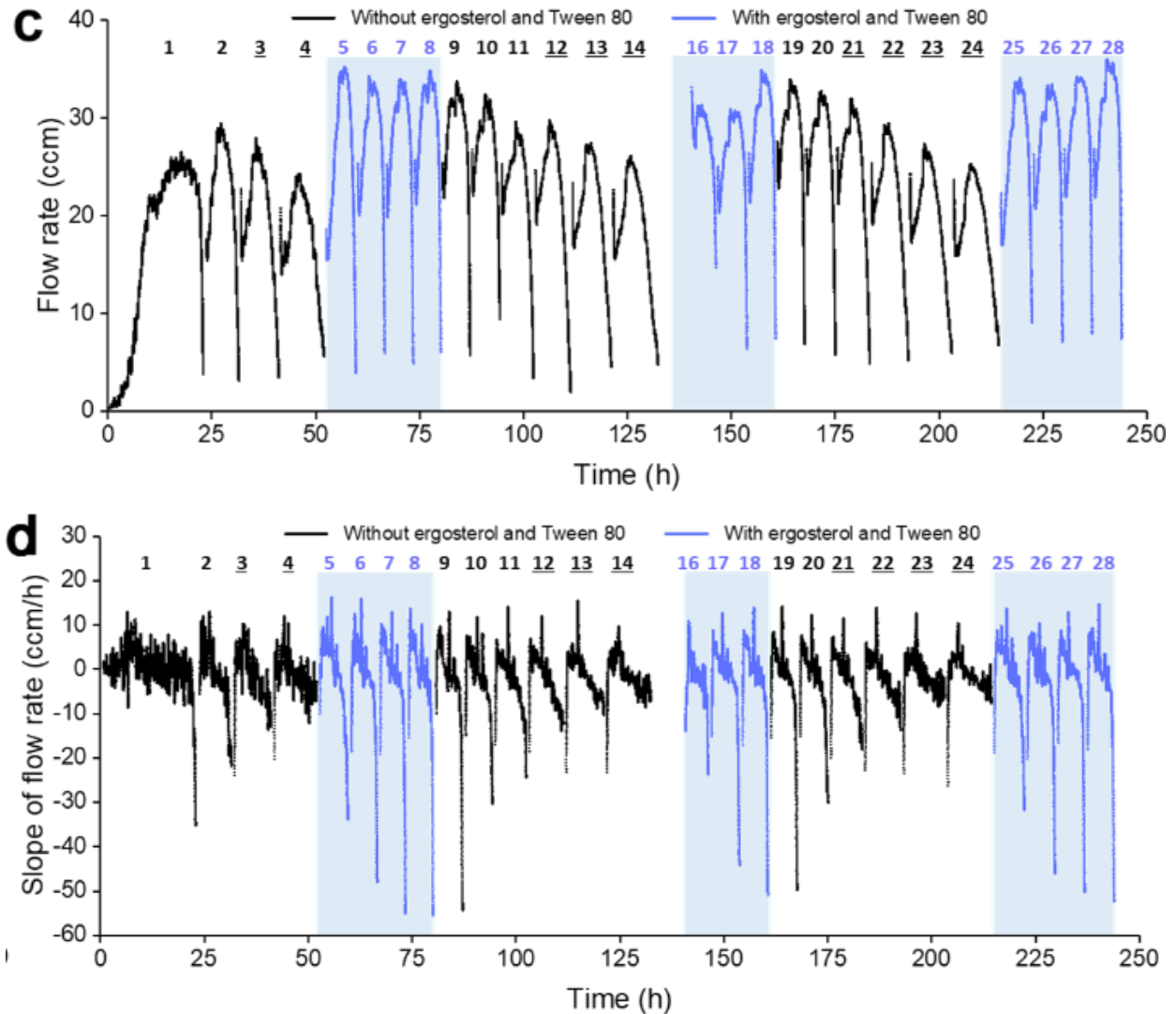


Figure 4.3 Ergosterol and Tween 80 supplementation. SCF was performed using medium without (cycles 1-4, 9-14, and 19-24) or with (cycles 5-8, 15-18, and 25-28) the supplementation of ergosterol (0.02 g/L) and Tween 80 (0.8 g/L). The cycle time (a), pH of the culture (b), as well as gas flow rate (c) and its slope (d) were reported. The cycle numbers were labeled at the top of each figure, with the exception of (a) where the cycle numbers were indicated on the x-axis. Cycles with supplementation were shaded in (b), (c), and (d). Underlined cycle numbers indicate cycles that did not meet criteria for automated cycling and that were thus manually triggered. Cycle 15 and part of cycle 16 were removed from Figure (c) and (d) due to excessive flow of nitrogen entering the fermenter as a result of nitrogen regulator failure.

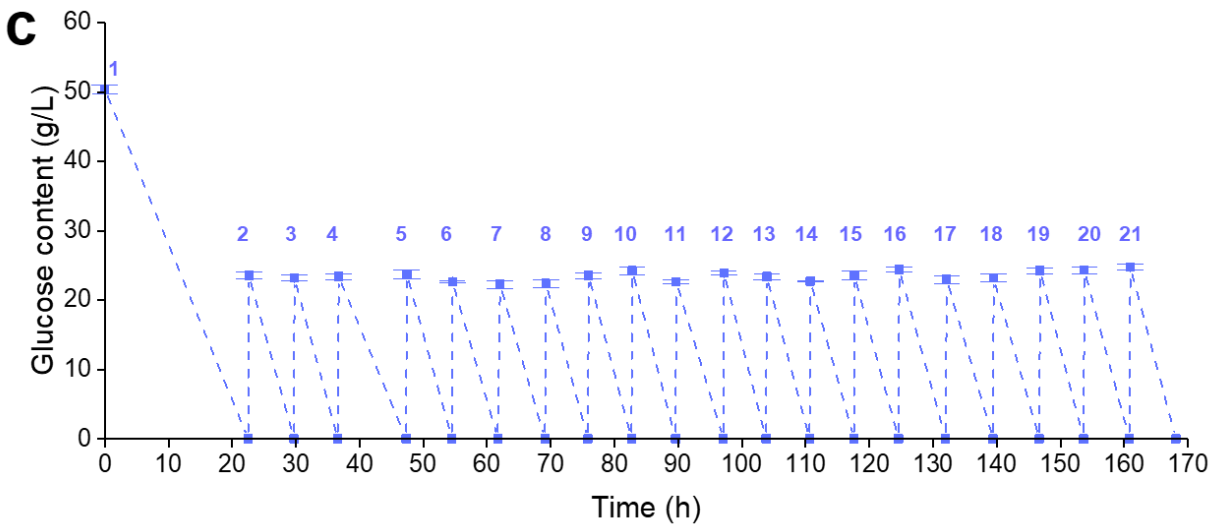
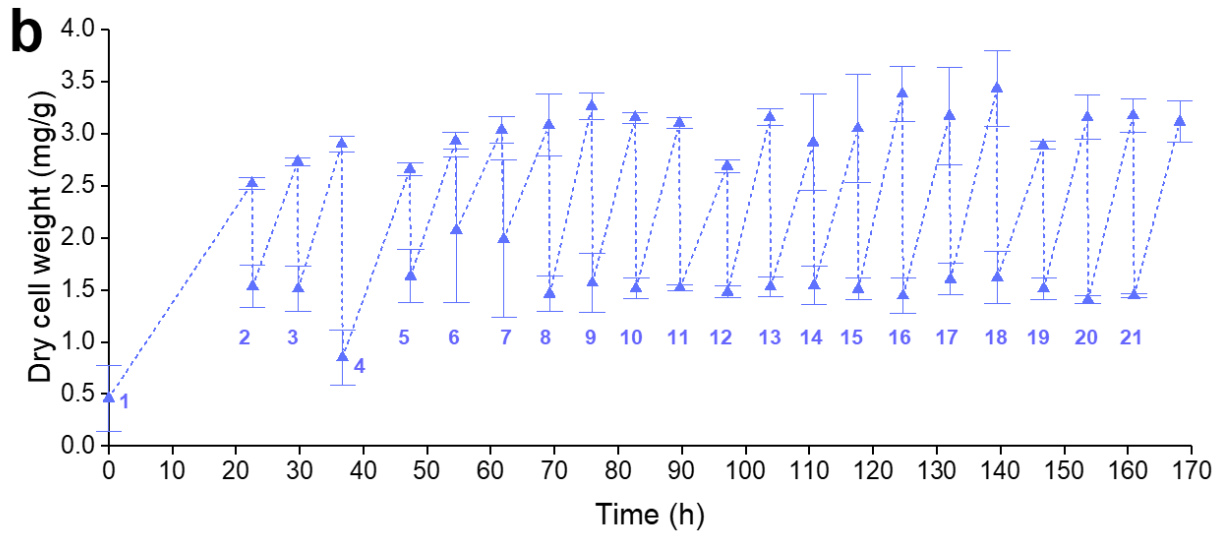
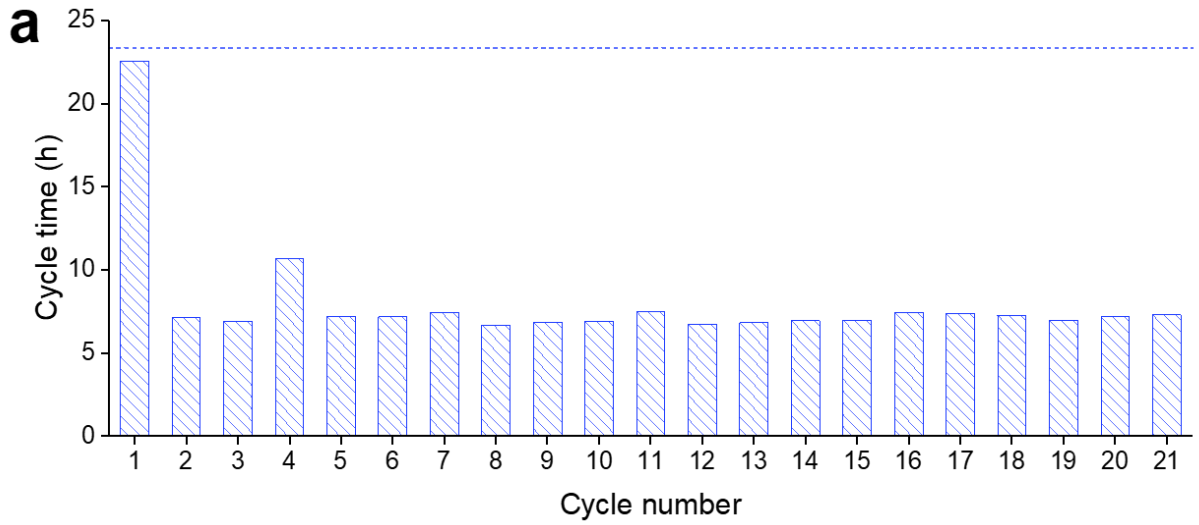
Conversely, when ergosterol and Tween 80 were reintroduced to the system (cycles 15 to 18, and 25 to 28), shorter cycle times, lower final pH values, higher gas flow rates and lower minimum slope values were reinstated (Figure 4.3). When multiple cycles were operated without ergosterol and Tween 80, once the cycle time increase beyond 3 h and the pH plateaued, the slope of the gas flow rate staggered and the minima of slope did not reach the setpoint to trigger cycling (see cycles 3-4, 12-14, and 21-24 in Figure 4.3b and d); in those cases, cycling was manually initiated. Some residual glucose remained at the end of these cycles (between 0.1 and 0.4 g/L), whereas residual glucose was below 0.1 g/L for all other cycles (excluding 15, for which no sample was taken). Thus, cycles 3-4, 12-14, and 21-24 were manually ended earlier than the theoretical completion time, indicating that they would have a longer cycle time than reported (Figure 4.3a). Interestingly, despite these small fluctuations, all cycles ended with similar final ethanol titers, other than cycles 12 and 14 where the values were lower (Additional Figure 2 in Appendix A). In addition, it should be noted that cycle 15 and the early stages of cycle 16 are missing in Figure 4.3a, c and d due to the failure of a pressure regulator in the nitrogen cylinder, which facilitated excessive flow of nitrogen into the fermenter (Figure 4.1) and disrupted the readings of the gas flow meter. The flow rates and slopes for these two cycles are provided in Additional Figure 3a and b (Appendix A), respectively.

4.4.3 Demonstration of automated SCF operation

SCF was operated for 21 consecutive cycles with the supplementation of ergosterol and Tween 80 to test whether the system is stable, robust, and able to improve productivity (Figure 4.4). The agitation and temperature control were interrupted during cycle 4 to evaluate the capacity of the system to recover from disturbances, and the concentrations of ergosterol and Tween 80 were tripled in cycles 18-21 to determine if excess would impact fermentation. A batch experiment with the supplementation of ergosterol and Tween 80 was performed under the same conditions as SCF for comparison (Additional Table 1 and Additional Figure 4 in Appendix A).

Figure 4.4 shows the main parameters analyzed over SCF operation. First, the cycle time (Figure 4.4a) for cycles 2-21 was consistent for all cycles (except cycle 4, for which agitation and temperature control were halted). It ranged from 6.7-7.5 h, which was

approximately 1/3 the duration of cycle 1 and batch experiment (Additional Table 1 in Appendix A). Biomass production, as measured by dry cell weight, was also relatively consistent for all cycles – except cycles 4 and 11 – with a starting concentration of ~1.5 mg/g culture and reaching ~3 mg/g at the end of cycles (Figure 4.4b). As seen in Figure 4.4c and d, the changes in concentrations of glucose and ethanol generated regular patterns. Starting from cycle 2, glucose went from 23.4 to 0 g/L over the duration of a cycle, while ethanol went from 11.5 to 21.9 g/L. Fermentation efficiency was calculated by comparing the ratio of glucose consumption (g/L) through a cycle over its ethanol production (g/L) against a theoretical value of 0.51. As shown in Additional Table 1 (Appendix A), fermentation efficiency fluctuated among SCF cycles, ranging from 80.8~91.2%, but were similar or greater than the efficiency achieved in batch operation ($81.1 \pm 0.8\%$). Note that ~2.2 g ethanol were detected in the gas trap at the end of the whole fermentation, implying that some ethanol evaporated from the culture over the 21 cycles (168.1 h). Thus, the total amount of ethanol produced and the fermentation efficiency could be greater than values found in Figure 4.4d and Additional Table 1 (Appendix A), respectively. In addition, glycerol is commonly produced during ethanol fermentations as a means to balance redox potential in the cell, particularly when yeasts are grown in stressful conditions [19]. Our analytical results showed that glycerol was present at the beginning of cycles 2-21 at a concentration of 1.8-2.0 g/L and accumulated to 3.3-3.5 g/L over a cycle. In comparison, cycle 1 and batch experiment performed with the same medium started with glycerol content below detection limit, yet it accumulated to 3.6 g/L at the end. Finally, high concentrations of organic acids are typically attributed to bacterial contamination [19]. Lactic acid was not detected throughout SCF operation; acetic acid concentration was less than 0.8 g/L; and no contamination was observed under microscope. Thus, contamination was not likely an issue during the long-term fermentation campaigns performed in this study.



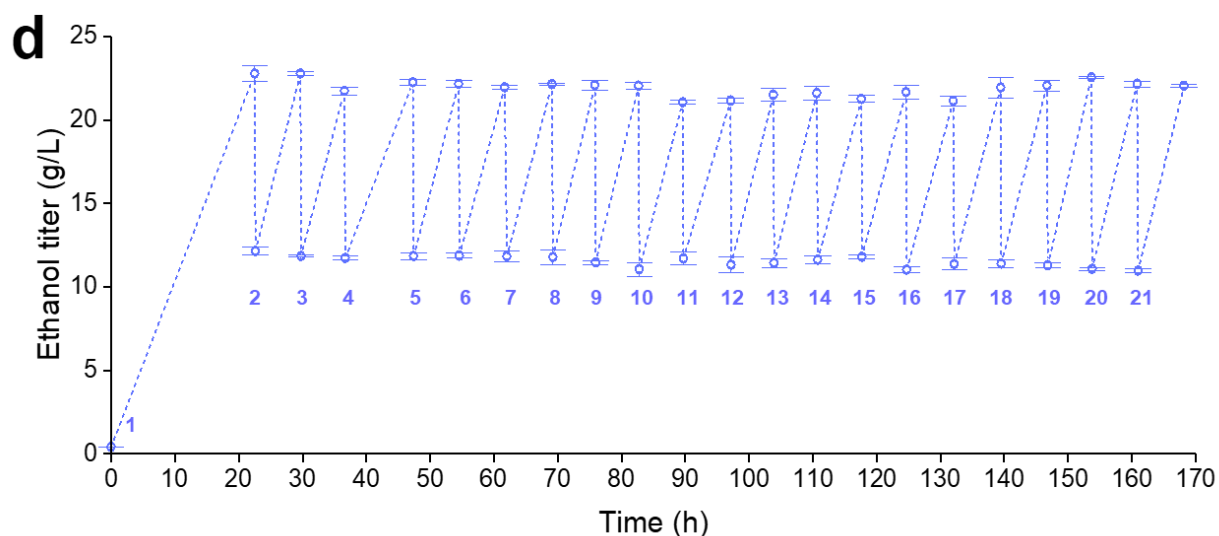
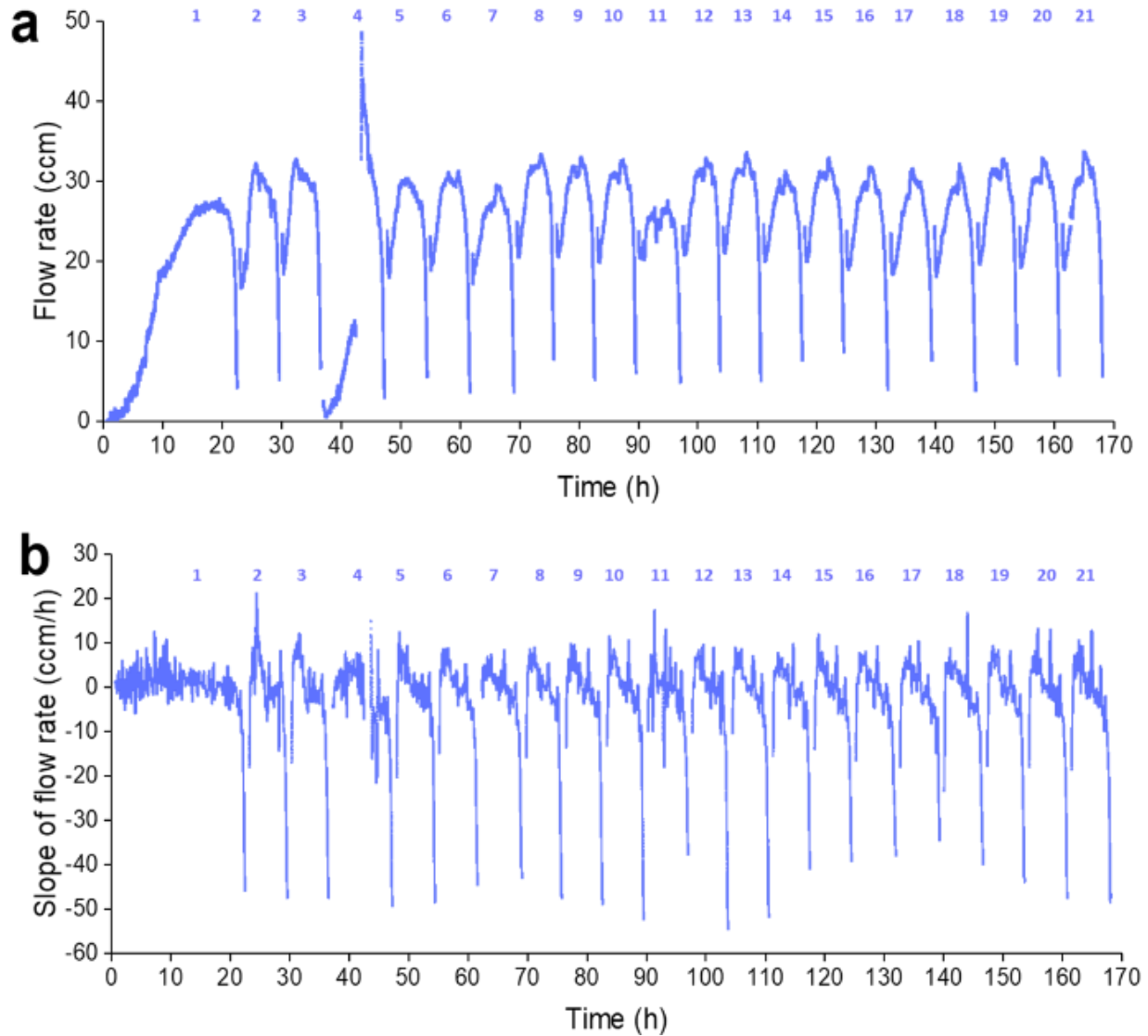


Figure 4.4 Analysis of samples from SCF demonstration. Cycle time (a) amount of biomass (b), and concentrations of glucose (c) and ethanol (d) were plotted for the beginning and end of all cycles. Medium supplemented with ergosterol (0.02 g/L) and Tween 80 (0.8 g/L) was used for cycles 1~17; the concentrations of ergosterol and Tween 80 were tripled for the remaining cycles. Cycle 4 was disrupted by halting agitation and temperature control for ~7 h. Cycle numbers were labeled at the initial stage of each cycle, with the exception of (a) where the cycle number was indicated on the x-axis. The horizontal line in (a) represents the fermentation time for batch operated under similar conditions (Additional Table 1 in Appendix A). In (b-d) data is reported as the average from at least three replicates, with error bars representing standard deviations.

Figure 4.5 shows the online monitoring data related to gas flow rate and pH during SCF operation. Starting from cycle 2, gas flow rate curves (Figure 4.5a), except for cycles 4 and 11, were generally sharper and narrower than that of cycle 1, suggesting a faster production rate of CO₂. It should be noted that the gas flow rate curves for cycles 4 and 11 were considered outliers because of an intentional disruption to the system (see below) and intracycle sampling that relieved system pressure, respectively. For all 21 cycles, after cycle time passed 3 h and pH dropped below 4 (Figure 4.5d), slope values fell below -20 ccm/h and then increased for over 2 min (Figure 4.5b). Therefore, cycling criteria were met, and all the cycles were automatically driven throughout the SCF operation. Total volumes

of gas evolved for cycles 2-21 were approximately half the value for cycle 1 and batch operation (Figure 4.5c). The scale of pH change (Figure 4.5d) observed over a cycle was repeatable for cycles 2-21 throughout the entire fermentation. The reproducibility of these patterns highlights the stability of the system.



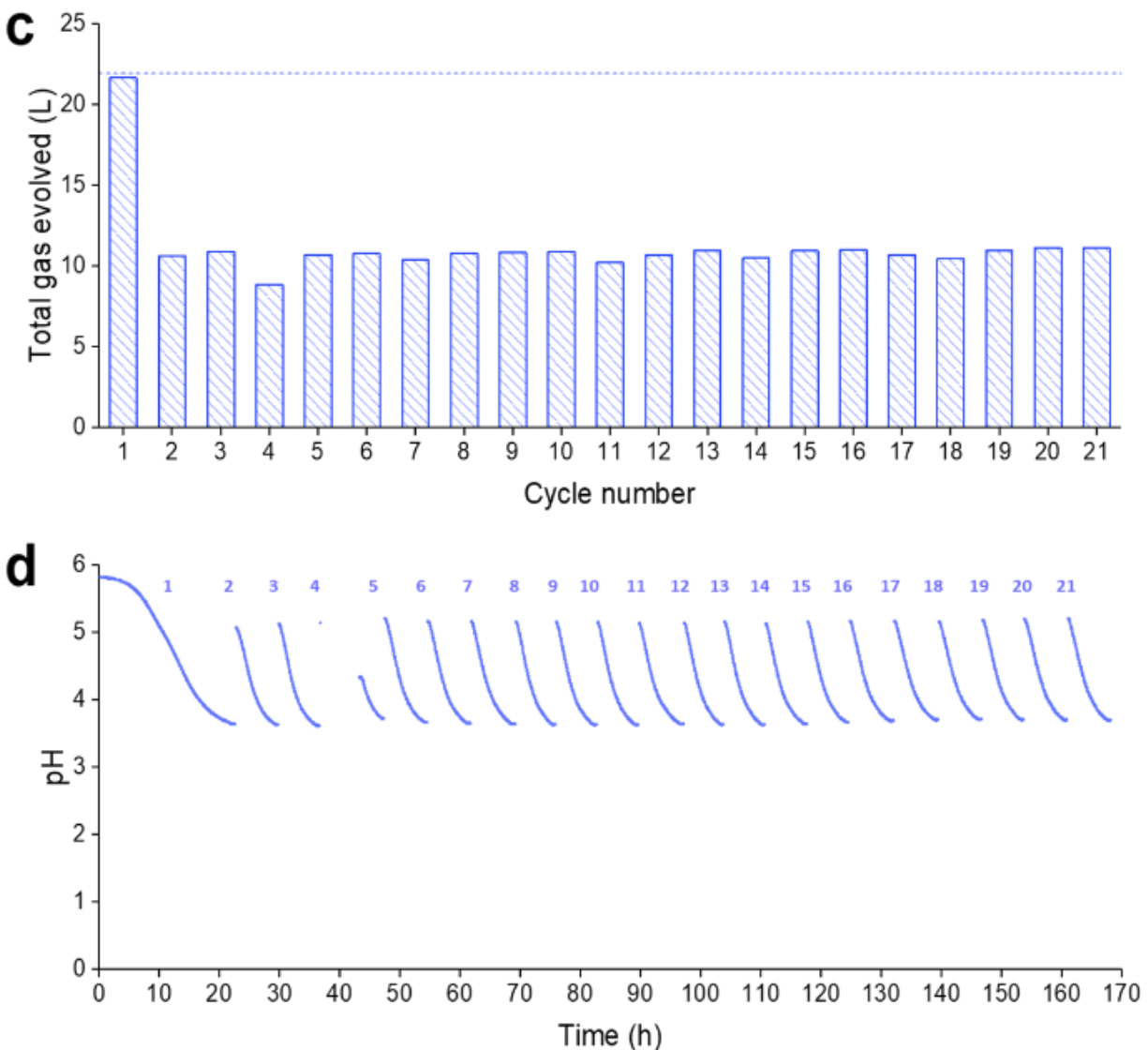


Figure 4.5 Online monitoring parameters from SCF demonstration. Gas flow rate (a), slope of gas flow rate (b), total volume of gas evolved per cycle (c), and pH (d) were monitored throughout SCF operation. Medium supplemented with ergosterol (0.02 g/L) and Tween 80 (0.8 g/L) was used for cycles 1-17; the concentrations of ergosterol and Tween 80 were tripled for the remaining cycles. Cycle 4 was disrupted by halting agitation and temperature control for ~7 h. Cycle numbers were labeled at the top of each figure, with the exception of (c) where the cycle numbers were indicated on the x-axis. The horizontal line in (c) represents the total volume of gas evolved in batch operation conducted under similar conditions (Additional Figure 4c in Appendix A).

As mentioned above, agitation and temperature control were interrupted for ~7 h in cycle 4 to test the capacity of the SCF system to recover from disturbances. This resulted in an abnormal trend of gas flow rate (Figure 4.5a), lower total volume of gas evolved (Figure 4.5c), and a longer cycle time (Figure 4.4a), but the pH (Figure 4.5d) and the slope of the gas flow rate (Figure 4.5b) eventually reached similar levels as other cycles. More importantly, the cycling process was still automatically triggered to initiate cycle 5, which behaved similarly to cycles 2 and 3. This implies that the system is robust enough to withstand interruptions or variations in operating conditions.

Since the addition of ergosterol and Tween 80 was based on concentrations referred by Straver *et al.* [165], starting from cycle 18, the contents of ergosterol and Tween 80 were increased 3-fold to see whether this would have a positive or negative impact on fermentation. No substantial difference in fermentation parameters could be observed (Figures 4.4 and 4.5), indicating that the initial concentrations of ergosterol and Tween 80 were already at or above the optimal levels for cell growth. In addition, as cycle number increased, cells progressively aggregated to the surfaces of probes and fermenter wall above culture and flocculation became obvious (Additional Figure 6 in Appendix A), which was not observed during batch or cycles 1-3 of SCF. This also applied to the previous experiments accessing the requirement of ergosterol and Tween 80 (results shown on Figure 4.3).

To explore the changes occurring during an SCF cycle, intracycle samples were taken throughout cycles 2 and 11. Although more samples at an increased frequency would be needed to better define the details of the kinetics, Additional Figure 5b and d (Appendix A) revealed that the consumption of glucose and production of ethanol were generally linear in both cycles. This would suggest that cells at the end of each SCF cycle were able to quickly uptake nutrients and produce ethanol as the limiting nutrient became available again. However, dry cell weight (Additional Figure 5a and b in Appendix A) did not readily increase at the early stages of the cycles, which might be contributed by the experimental errors related to the measurement and cell flocculation. Future work is needed to investigate the reason for this.

4.4.4 Improvements in productivity

Ethanol volumetric productivity represents the ethanol produced in a cycle per unit volume per cycle time. As seen in Figure 4.6, SCF operation led to improvements of 37.5-75.3% compared to batch, excluding cycles 1 (7%), which was essentially a batch, and 4 (8%), for which agitation and temperature control were interrupted. Annual ethanol productivity (Additional Table 1 in Appendix A) refers to the total amount of ethanol that can be potentially produced over a year, in this case, for a fermenter assumed to be at 10^5 L scale and including conditions such as harvesting time and cleaning time [162]. As seen in Additional Table 1 (Appendix A), switching production from batch to 21-cycle SCF campaigns, annual ethanol productivity could be increased by $75.8 \pm 2.9\%$.

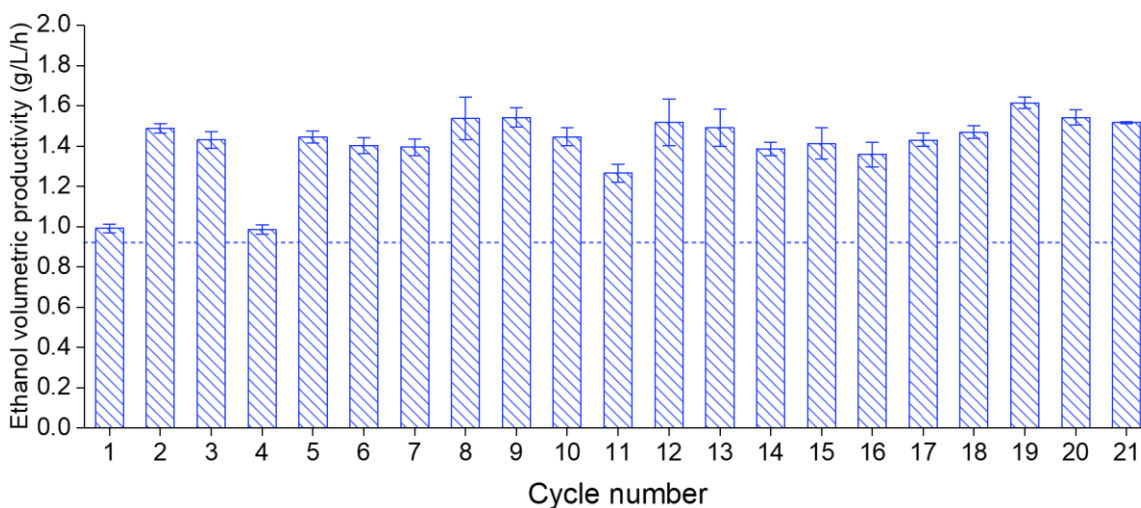


Figure 4.6 Ethanol volumetric productivity during SCF. Medium supplemented with ergosterol (0.02 g/L) and Tween 80 (0.8 g/L) was used for cycles 1~17; the concentrations of ergosterol and Tween 80 were tripled for the remaining cycles. Cycle 4 was disrupted by halting agitation and temperature control for ~7 h. The horizontal line represents the volumetric productivity in batch operation conducted under similar conditions. The data reported is the average from at least three replicates, with error bars representing standard deviations.

4.5 Discussion

4.5.1 The monitoring parameter for anaerobic SCF

In batch fermentation, the production of ethanol, a primary metabolite, showed little change at lag phase and plateaued at stationary phase (Figure 4.2a and b). Hence, the application of SCF operation, in which cycling is triggered at the onset of stationary phase, is expected to minimize the time for which ethanol is not produced. In order to trigger cycling process upon the arrival of stationary phase, it is important to define an appropriate monitoring parameter capable of doing so [24].

Common vibrational spectrosopes for online monitoring of ethanol fermentation have limitations for application in SCF. For instance, for near-infrared and Raman spectroscopic techniques, the fermentation culture needs to be filtered or precipitated to reduce interference from solids present in suspension [130,132], an approach which is not practical in industry. The use of Fourier transform infrared spectroscopy by Veale *et al.* [131] required the installation of an Attenuated Total Reflectance flow cell to the reactor, making part of the fermentation culture continuously circulate between the fermenter and the flow cell. This increases the risk of contaminating cultures and of solids/cells blocking the circulation path. CER has been used as a monitoring parameter for SCFs performed under aerobic conditions [23,143]. Although well studied, CER was mainly determined using infrared radiation sensors assessing the concentration of gaseous CO₂ and dilution of the gas outlet streams was necessary to avoid saturation of the signal. In our anaerobic system, CO₂ was the only gas evolved, which would also saturate the sensor, and these sensors were thus not used in this study.

As an alternative, we used a gas flow meter (Figure 4.1) to record the flow rate of the gas evolved and calculate the slope of flow rate in real time. As can be seen, the slope of the gas flow rate was an appropriate monitoring parameter to identify the onset of stationary phase (Figure 4.2). We demonstrated how these conditions could be used to efficiently automate SCF operation under anaerobic conditions (Figure 4.5). Furthermore, a gas flow meter does not enter in contact with liquid cultures, eliminating probe fouling issues [143] and reducing risks of contamination raised by possible repair/replacement of the meter during fermentation. It is also relatively cheap for industrial purposes and only

needs to be connected to the venting line, without significant changes to existing infrastructure.

It should be noted that the flow rate of gas leaving the reactor recorded by the flow meter may not be equal to the real production rate of CO₂ by yeast. This is primarily because gas CO₂ was mixed with N₂ at the beginning of each SCF cycles to ensure anaerobic conditions. In this case, ~3 L of N₂ left the fermenter in the early stages of the cycles, making the early flow rate readings (Figure 4.2c, 4.3c and 4.5a) approximately 84% of the actual values, since the flow meter was calibrated with pure CO₂ while the gas contained N₂. This influenced the calculation of flow rate by Poiseuille Equation. As the amount of CO₂ produced by the yeast increased during the fermentation (e.g., a total volume of approximately 22 L CO₂ at the end of batch; Additional Figure 1a and 4c in Appendix A), N₂ was driven out of the headspace, eventually nearing zero.

Initially designed to trigger cycling, the monitoring parameter – evolved gas flow rate – was found to have the capability of providing a quick estimation of sugar and ethanol concentrations inside the fermenter, as well as information on different fermentation scenarios. We observed that the concentrations of sugar and ethanol in batch fermentation (Figure 4.2b) correlated well with values predicted from the cumulative gas volume (Additional Figure 1b and c in Appendix A), in spite of N₂ being added to the system at the beginning of the operation. While more data should be gathered to further verify the strength of the correlation, this could provide very useful real-time information on the status of ethanol fermentations. Practically for industry, it shows great promise in helping reduce labor intensity in sampling preparation and analysis, as well as the use of expensive equipment, such as HPLC/GC for fermentation monitoring [20]. In addition to that, SCF cycles 4 and 11 during the demonstration study had lower flow rate peaks than the other cycles (Figure 4.5a). The former saw slower fermentation due to a lower temperature and no agitation, and the latter was disturbed by frequent sampling. Furthermore, SCF cycles without supplementation of ergosterol and Tween 80 (cycles 3-4, 12-14, and 21-24 in Figure 4.3) had less pronounced values in final slopes of flow rate (Figure 4.3d), aligning with slower growth in the absence of ergosterol and fatty acids. Finally, it is worth noting that although one of the cycling criterion employed successfully in these experiments was

the decrease of the flow rate slope below -20 ccm/h, fermentation systems using different organisms or sugars (i.e. sugar types and concentrations) may require alternative values for robust cycling.

4.5.2 Assessing the requirements for ergosterol and Tween 80 in anaerobic SCF

The use of non-supplemented medium in anaerobic SCF of *S. saccharomyces* led to a progressive reduction in growth rate, as seen in the extension of cycle times over multiple cycles (Figure 4.3a). This was not observed in Chapter 3 in which five successive cycles were performed in shake flasks fitted with S-locks for ethanol fermentation. We posit that, because the cycling was performed manually with shake flasks, which briefly exposed the culture to air [162], small amounts of O₂ present at the beginning of each cycle were sufficient for the yeast to synthesize the sterols and unsaturated fatty acids necessary for constructing plasma membrane [118]. In our current study using a 5-L fermenter, the batch experiment and cycle 1 of SCF operation were inoculated with yeast cells that had been cultivated aerobically, and sterols and fatty acids were re-distributed into daughter cells upon division [168]. By the end of batch fermentation or cycle 1 in SCF, cells had divided approximately 6 times (data from cell counts with hemocytometer), which exceeds the 4-5 generation limit for daughter cells to still benefit from parental sterol and fatty acids under anaerobic conditions [168]. Consequently, the yeast cells for subsequent cycles had diminishing levels of sterols and unsaturated fatty acids, putting them under increasing stress and leading to longer cycle times (cycles 2-4 in Figure 4.3a). By supplying ergosterol and Tween 80 (a source of unsaturated fatty acids), the growth rate quickly increased, even for cycle 5, likely due to recovering integrity of the plasma membrane and improving transportation of chemicals. The fact that the absence and supplementation of ergosterol and Tween 80 were directly related to slower and faster growth, respectively, demonstrates the importance of these compounds for sustained SCF operation under anaerobic conditions. It should also be noted that the addition of ergosterol and Tween 80 to batch fermentation did not impact ethanol production (Additional Figure 2 in Appendix A). Finally, the ethanol titers observed for cycles 12 and 14 were lower than for other cycles (Additional Figure 2 in Appendix A). The precise explanation for this is not known. Nevertheless, the ethanol titers reached in these cycles were still high (above 17 g/L).

Interestingly, lower ethanol titers were never observed in cycles where ergosterol and Tween 80 were supplemented.

From an industrial perspective, it would be interesting to conduct studies investigating the addition of small amount of air at the beginning stage of each cycle to initiate the synthesis of sterol and unsaturated fatty acids. This would be a much cheaper option than the addition of ergosterol and Tween 80.

4.5.3 Demonstration of automated SCF operation

The proof-of-concept study in Section 3.4.3 suggested that operating SCF campaigns for ~20 cycles would significantly improve annual ethanol productivity (Figure 3.4), while maintaining a low risk of contamination. Therefore, we performed automated SCF for 21 cycles and tested whether productivity improved accordingly compared to batch.

The first thing to note is that, in comparison to batch fermentation and cycle 1, both the ethanol volumetric productivity (Figure 4.6) and the annual ethanol productivity (Additional Table 1 in Appendix A) are significantly greater under SCF operation. The increase in annual ethanol productivity from SCF operation ($75.8 \pm 2.9\%$, Additional Table 1 in Appendix A) was similar to the value predicted in the lower scale proof-of-concept study ($62.7 \pm 11.9\%$) [162]. It should be noted that annual ethanol productivities were calculated based on operation of the 5-L fermenter. Thus, the value of the reported annual ethanol productivity (Additional Table 1 in Appendix A) may differ for real industrial conditions as many parameters would change upon scale-up. Nevertheless, the significant improvement of SCF over batch operation with regards to annual ethanol productivity highlights the potential of SCF for ethanol production. Furthermore, it is important to point out that both fermentation efficiency (Additional Table 1 in Appendix A) and improvement in productivities confirm the great potential of automated SCF operation at larger scale.

Ethanol volumetric productivity remained relatively stable among cycles 2-21, except for cycle 4 (Figure 4.6). Small discrepancies were likely due to typical processing fluctuations in operating conditions (temperature, concentrations of nutrients, and feeding and harvesting times). Cycle 11 in particular shows variations that were likely due to disturbances from a significantly larger number of samples taken to perform intracycle analysis (Figures 4.4, 4.5, 4.6, and Additional Figure 5 in Appendix A). This disturbed

cultures and readouts and decreased the working volume. Therefore, compared to cycles 2-21 (except 4), a lower value in maximum flow rate (Figure 4.5a), slightly longer cycle time (Figure 4.4a), and lower ethanol volumetric productivity (Figure 4.6) were found for cycle 11. Despite this, SCF operation was stable and robust, and production was reproducible and efficient.

It should be noted that our study used a sugar concentration of 50 g/L, which is lower than the concentrations used in many bioethanol plants. This study thus serves as a stepping stone, providing the first demonstration and establishing the basis for the use of SCF for ethanol production. We expect this study will open the door to future work investigating more parameters and variables affecting SCF operation and ethanol production, such as the use of higher levels of sugars (e.g. 100 g/L) and of real cellulosic hydrolysates.

Unlike in batch and early SCF cycles, cell aggregation – deposition to solid surfaces and flocculation – was observed in later SCF cycles (Additional Figure 6 in Appendix A). This has not been reported in prior studies of any SCF systems using yeast. Although the exact cause of the cell aggregation, which lasted until the end of operation, is not clearly established, Ma *et al.* reported that a repeated-batch method (in which 60% of the culture was drained and refilled every batch) was used to improve flocculation of *S. cerevisiae* [150]. In that study, approximately 18 sequential batches were necessary for yeast to reach high levels of flocculation, compared to the first 10 batches which saw much less flocculation [150]; whereas in our study apparent flocculation was observed as early as cycle 4. It is also interesting that the ethanol volumetric productivity (Figure 4.6) was not affected by flocculation, aligning with results of increasing productivity from Ma *et al.* [150]. According to Guo *et al.*, yeast genes associated with flocculation, such as FLO 1, 5, 9, and 10, are primarily responsible for cell-cell aggregation [87], and it is possible that our SCF process could have activated such genes. As Soares [85] points out, the optimal pH for yeast flocculation is generally between pH 3 and 5, depending on the strain, hence pH may have also played a role in the aggregation observed (Figure 4.5d). Since cell aggregation in SCF rendered biomass quantification by common approaches difficult and unreliable, dry cell weight, rather than OD₆₀₀ and cell counting, was used. Because of this, it was not possible to

clearly assess the level of cell synchrony achieved, which is usually determined by cell counts [143].

Finally, flocculation may have many industrial advantages such as facilitating downstream processing. The quick settling of cells at the end of later SCF cycles improved separation and could lead to great reduction in energy requirements for filtration, which is commonly used before distillation [18]. The recovered cells could be re-used for subsequent fermentation campaigns, enabling cell aggregation in all future SCF cycles, again facilitating downstream processing.

4.6 Conclusions

To our knowledge, this is the first report of successful and sustainable operation of automated SCF under anaerobic conditions, as well as the first SCF operation driven by gas flow measurements. Clearly, this study demonstrates that stable and robust operation of anaerobic SCF is achievable, and leads to improved productivities, primarily due to reduced fermentation time and down time, while maintaining a similar ethanol titer throughout operation. Together with flocculation, this can potentially contribute to significant reductions in capital and operational costs for both fermentation and downstream processes. Overall, with its defined medium and operating conditions, the SCF demonstration in this work can be taken as a starting point from which future investigations and industrial applications can be built.

4.7 Acknowledgements

The project is financially funded by Canada First Research Excellence Fund, Future Energy Systems (T01-P01) at the University of Alberta, BioFuelNet Canada (NCEBFN 3N), and the Natural Sciences and Engineering Research Council of Canada (NSERC, Discovery Grant; RGPIN-2019-04184). We would like to acknowledge Mr. Les Dean (Department of Chemical and Materials Engineering, University of Alberta) for his help on integrating the hardware and developing the Labview® software for our system. Permission for acknowledgement was obtained.

Chapter 5 Application of self-cycling fermentation using wood pulp hydrolysates for improved ethanol productivity*

5.1 Abstract

Although cellulosic ethanol can greatly contribute to mitigate GHG emissions, the rapid expansion of the industry is hindered by economic barriers. A promising approach to address this issue is to improve ethanol productivity to offset overall production costs. In this study, we integrated self-cycling fermentation (SCF), an advanced fermentation approach, with a real lignocellulosic feedstock to improve ethanol productivity. Specifically, wood pulp was enzymatically hydrolyzed to yield sugars, which contained a mixture of glucose and xylose and were then fed to an automated SCF system to produce ethanol for 10 cycles. The SCF system, which was driven by a gas flow meter, facilitated glucose fermentation to ethanol; this was followed by a second fermentation stage that enabled further ethanol production from xylose. SCF achieved regular and stable ethanol production patterns and, more importantly, significantly higher productivity compared to batch operation: ethanol volumetric productivity increased by 54-82% and annual ethanol productivity by $81.2 \pm 4.3\%$. Significantly, the hydrolysate did not display any evidence of impeded ethanol fermentation, which is commonly observed when fermenting enzymatic hydrolysates of lignocellulosic feedstock. Taken together, these results highlight the great potential of using SCF strategy in improving the economics of the cellulosic ethanol industry.

Keywords: self-cycling fermentation, gas flow meter, ethanol productivity, wood pulp, diauxic growth, cellulosic ethanol

5.2 Introduction

Lignocellulose is an abundant feedstock with great promise for biofuel production platforms [5]. This material is primarily composed of cellulose (40-50% of total dry

* A version of this chapter will be submitted for publication. The study in this chapter is a collaborated work with Dawit Beyene, who performed the enzymatic treatment of wood pulp (Beyene *et al.*, Enzymatically-Mediated Co-Production of Cellulose Nanocrystals and Fermentable Sugars. *Catalysts*. 2017). I designed experiments, prepared medium, performed fermentations, conducted sample analysis, analyzed data, and wrote the chapter.

weight), hemicellulose (20-40%), and lignin (15-30%). Cellulose is a linear polysaccharide consisting of glucose monomers linked by β -1,4-glycosidic bonds, leading to highly ordered crystalline regions interspersed with loosely-packed amorphous regions. Conversely, hemicellulose is a branched polysaccharide which wraps around cellulose and predominantly comprised of C5 and C6 sugars. This structure is locked by lignin, an amorphous polymer made of aromatics [5,7,169]. For the production of cellulosic ethanol, the feedstock is first pre-treated to open up its structure, enzymatically hydrolyzed into monomer sugars, fermented into ethanol, and finally distilled into high purity product [5]. Because of the complicated processing steps required, the cellulosic ethanol industry is faced with higher production costs than the starch- or sugar-based ethanol industry [15].

To overcome the economic challenges facing the cellulosic ethanol industry, breakthroughs made in pre-treatment and enzymatic hydrolysis strategies should be supported by the development of advanced ethanol fermentation platforms. Chapter 4 reports the successful development of self-cycling fermentation (SCF) approach for ethanol production which showed a 37.5-75.3% improvement in ethanol volumetric productivity (ethanol produced by a cycle per working volume per cycle time) and an increase of $75.8 \pm 2.9\%$ in potential annual ethanol productivity (ethanol produced per year). Though robust and stable, this system employed a synthetic medium where glucose was the sole carbon source available in the system. Thus, it is not yet known whether improved productivity can be achieved through SCF using hydrolysates from real lignocellulosic materials, which typically contain both C5 and C6 sugars, and, potentially, inhibitors, such as furfural, 5-hydroxymethylfurfural, formic acid, acetic acid, etc. [5].

As an advanced fermentation technique, SCF implements an automated cycling strategy triggered at the onset of stationary phase—half of the culture is automatically harvested from the reactor for downstream processing, and immediately replaced with fresh, sterile medium to start the next cycle in the same reactor [24]. The automation is achieved by using an online sensing parameter that is linked to cell growth, such as dissolved oxygen [29] or carbon dioxide evolution rate [23,143]. This is the standard operation of SCF and has been applied to many microbial cultivation systems with improved productivities [23,29,143], including the demonstration study in Chapter 4.

Another approach involves the combination of SCF operation with a secondary fermentation stage: upon triggering of the cycling procedure in a main reactor, the harvested culture is incubated in a second reactor, while the main reactor begins the next cycle in parallel [145]. Decoupling fermentation into two stages enables a reduction of fermentation time in the primary reactor, as well as the improved flexibility with regards to fermentation conditions in each stage. This was demonstrated for the production of β -galactosidase by a lysogenized bacterial strain. SCF was performed by cultivating the microorganism in the main reactor at 31 °C, and at the end of each cycle the harvested culture was transferred to a secondary fermenter at 42 °C, which induced the prophage and the production of β -galactosidase. This two-stage fermentation strategy displayed significantly reduced fermentation time and improved productivity (40% and 50%, respectively) than batch operation [22].

The present study aimed to improve the economics of cellulosic ethanol production by integrating lignocellulose-derived hydrolysates to an SCF system to improve ethanol productivity. The data presented below highlight the great potential for this advanced fermentation strategy to reduce overall production cost of cellulosic ethanol for the industry.

5.3 Methods

5.3.1 Medium and yeast

The medium used in this study originated from an 8 h enzyme hydrolysis of wood pulp as described elsewhere by Beyene *et al.* [114]. Briefly, northern bleached hardwood kraft pulp was mixed with a solution containing 50 mM sodium citrate buffer (pH 4.8) and 15 FPU/g (filter paper unit) of a cellulase enzyme cocktail (NS 51129; Novozymes, Bagsvaerd, Denmark), and then incubated at 50 °C. After termination of hydrolysis, the mixture was centrifuged and filtered with a particle size retention of 8 μ m (Whatman™ filter paper, Fisher Scientific, ON, Canada) to remove solids. The hydrolysate was then mixed with 6.7 g/L yeast nitrogen base (YNB) without amino acids (Sigma-Aldrich, St. Louis, MO, USA) in volumetric flasks and filter sterilized (Sartolab™ P20 Plus Filter Systems: 0.2 μ m, Thermo Fisher Scientific, Waltham, MA, USA). The addition of YNB provided

nitrogen, vitamins, and minerals, which are commonly required for cellulosic ethanol fermentation [5,18,170]. After supplementation with 0.02 g/L ergosterol and 0.8 g/L Tween 80 (both purchased from Sigma-Aldrich, St. Louis, MO, USA), the medium was ready for fermentation. Under anaerobic conditions, ergosterol and unsaturated fatty acids cannot be produced by yeast, and thus external supplementation was required to facilitate cell growth on a long-term basis (Chapter 4).

Saccharomyces cerevisiae Y128 was kindly provided by Dr. Trey Sato from the University of Wisconsin-Madison, WI, USA. Through genetic engineering and evolution, this yeast strain gained the ability to consume xylose under anaerobic conditions (Parreiras et al., 2014). This was done through the addition of xylose reductase, which converts xylose into xylitol, and xylitol dehydrogenase, which subsequently transforms xylitol into xylulose. Xylulose can be phosphorylated (xylulose-5-phosphate) to enter the pentose phosphate pathway and then merged into glycolysis, before being converted into ethanol [5,60,124,125]. A summary of these pathways can be referred to Figures 2.10 (pathway I) and 2.11. After receiving the yeast strain, glycerol stocks were made, which were later used to plate cells and cultivate seed cultures (Section 3.3.1).

5.3.2 Fermentation

A 5-L fermenter (Infors-HT, Bottmingen, Switzerland) system was used as reported in Figure 4.1 (Section 4.3). Briefly, the fermenter was run anaerobically with a venting line that released gas to a flow meter (Whisper series, MW-200SCCM-D/5M; Alicat Scientific, Inc., Tucson, AZ, USA), with a water trap placed in between to minimize any backflow of gas into the fermenter. Level sensors were used to indicate the culture level inside the fermenter, and the fermenter was connected with peristaltic pumps (Cole-Parmer, Montreal, QC, Canada) to complete the cycling process; this consisted of reducing agitation to 200 rpm, harvesting half the culture from the fermenter, adding fresh medium, increasing agitation to 600 rpm, and adding antifoam (Y-30 emulsion; Sigma-Aldrich, St. Louis, MO, USA) to the fermenter. Moreover, the system used a program developed in the Labview® environment (National Instrument, Austin, Texas, USA) to control temperature and mixing rate, and monitor the pH of the culture (Hamilton Company, Reno, NV, USA), the flow rate of the evolved gas (Whisper series, MW-200SCCM-D/5M; Alicat Scientific, Inc.,

Tucson, AZ, USA), the slope of flow rate, and the cumulative volume of evolved gas at a frequency of 10 s. The gas flow rate was reported as the average value of the measurements taken over the last 15-min period. The slope of the gas flow rate was calculated as a linear regression of averaged flow rate over the same length of time. The volume of evolved gas was calculated as the integral (or cumulative values) of flow rate over time. All flow meter-based values were reported at 25 °C and 1 atm.

Batch fermentation and SCF were operated in the 5-L fermenter with a 2-L working volume. The culture was controlled at 600 rpm and 30.0 °C under anaerobic conditions. The cycling criteria for SCF was set as follows: 1) the slope of gas flow rate is lower than -20 ccm/h and continuously increases for 2 min; 2) the pH is below 4; and 3) the cycle time is greater than 3 h. The latter two conditions helped reduce the impact of noise from intermittent variations in the slope of the gas flow rate. The rationale for setting up these criteria is described in the Results Section 5.4.3. When the cycling criteria were met, cycling process was initiated: the culture was pumped into a 500-mL shake flask until the lower level sensor was triggered to permit continued fermentation (a working volume of 345 ± 38 mL) in the second stage. The shake flasks were fit with an S-lock to eliminate the chance of introducing air during fermentation, and was cultivated at 200 rpm at 30.0 °C in a shaking incubator (Innova 44/44R, New Brunswick Scientific, Edison, NJ, USA). The shake flasks were removed from the incubator when harvesting of the concurrent SCF cycle was completed.

Samples were taken from the fermenter immediately after the addition of fresh medium and antifoam into the SCF system, as well as during harvesting of SCF cultures from the 5-L reactor; corresponding to the beginning and end of a given SCF cycle, respectively. The samples taken during automated harvesting of the SCF culture were also used to assess parameters at the beginning of the second fermentation stage. Furthermore, upon the removal of the shake flasks from the incubator, samples were taken to represent the end of second fermentation stage.

Batch fermentation and SCF shared the same protocols with regards to inoculum preparation (described in Section 4.3.1), with cycle times defined as follows. The cycle time for the batch fermentation comprised the time between inoculation and the timepoint

when the minimum value of the slope of gas flow was reached. This facilitated comparison of batch and SCF cycles, specifically relating to glucose utilization. For SCF, the cycle time for cycle 1 was the length between inoculum and the end of harvesting from the main fermenter; for the following cycles, the cycle time described the time between the beginning of feeding of fresh medium and the end of harvesting from the main fermenter. For the second stage fermentation conducted in shake flasks, the cultivation time for a cycle was equivalent to the length of the cycle time of the concurrent SCF cycle.

5.3.3 Sample analysis

Samples were centrifuged ($10,016 \times g$, 10 min; accuSpin™ 400; Thermo Fisher Scientific, Waltham, MA, USA), and the pellets were used for dry cell weight measurements (Section 4.3.2). The supernatant was used for analysis of sugars and ethanol concentrations. Ethanol titer was measured using a gas chromatograph (GC) (described in Section 3.3.4). Quantification of glucose and xylose was conducted using a high performance liquid chromatograph (HPLC) equipped with an HPX-87P column and a refractive index detector [114]. Residual glucose and xylose below 1 g/L were quantified using a glucose oxidase/peroxidase (GOPOD) (described in Section 3.3.4) and xylose assay kit, respectively. Both assay kits were purchased from Megazyme (Bray, Ireland). The xylose kit measured the concentration of NADH at 340 nm derived from enzymatic reaction of xylose. The concentrations of formic acid, lactic acid, glycerol, acetic acid, furfural, and 5-hydroxymethylfurfural in raw enzymatic hydrolysates and supernatants of fermentation samples were measured using HPLC equipped with an HPX-87H column (described in Section 3.3.4). All chemicals were analyzed using a refractive index detector, except furfural and 5-hydroxymethylfurfural, which were assessed using an ultraviolet detector at wavelengths of 275 and 284 nm, respectively [171].

5.4 Results

To help improve the process economics of the cellulosic ethanol industry, an SCF strategy was applied that would enable the production of ethanol from wood pulp. A schematic of this process, which serves as a foundation for all of the research described below, is shown in Figure 5.1. Briefly, wood pulp is enzymatically digested to generate a

liquid stream containing fermentable sugars. The soluble fermentable sugars can then be integrated into self-cycling fermentation to convert glucose to ethanol, with a secondary fermentation step to facilitate additional ethanol production from xylose.

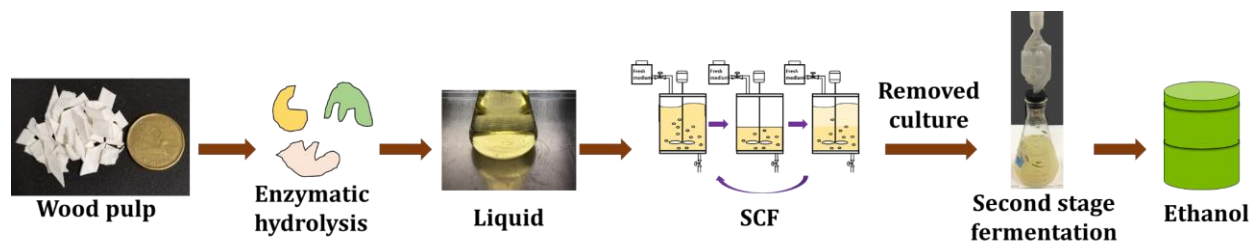


Figure 5.1 Overview of the proposed strategy for producing ethanol from wood pulp. Wood pulp was put together with one Canadian dollar for size comparison.

5.4.1 Hydrolysates from wood pulp

The hydrolysate obtained from enzymatic digestion of wood pulp was analyzed to ascertain the presence of some common inhibitors, which were reported to have a negative influence on subsequent fermentations [5,39]. HPLC analysis showed that formic acid, acetic acid, and 5-hydroxymethylfurfural were not detected. For furfural, the concentration observed was much lower than 0.01 g/L – lower than levels reported for other enzymatic hydrolysates – suggesting that inhibitory effects are not likely to be observed when yeast are cultivated on this sugar stream [170,172].

5.4.2 Batch fermentation using wood pulp hydrolysate

Batch fermentation was conducted under anaerobic conditions to study the kinetics related to yeast performance when grown using the hydrolysate medium. This experiment was also designed to test whether a gas flow meter could be used to indicate any metabolic transitions for *S. cerevisiae* Y128 cultivated in wood pulp hydrolysates comprising both C5 and C6 sugars. As seen in Figure 5.2a, the hydrolysate originally contained approximately 40 g/L glucose and 10 g/L xylose. In the early stages of fermentation, the yeast primarily consumed glucose, as no substantial reduction of xylose was observed until the glucose content became limiting (between 11 and 17 h). Although xylose accounted for 20% of the total initial sugar content, it was consumed very slowly, with 1.6 g/L still remaining after

27 h; 0.5 g/L remained after 32 h. A typical ethanol production curve was observed, characterized by low levels at initial stage, followed by quick increase, and finally plateauing at a final ethanol titer of 22 g/L (Figure 5.2a). The dry cell weight (Additional Figure 7a in Appendix B) observed over the fermentation process did not align well with the consumption of sugars or ethanol production, possibly owing to large variations in measurement caused by cell aggregation. Overall, Figure 5.2a suggests there was a diauxic growth pattern for the strain, with a preference for glucose, which is consistent with previous studies [127].

The pH of the culture (Figure 5.2b) dropped rapidly between 5-15 h of fermentation before reaching relative stability at pH 3.9. As suggested by Figure 5.2c, as the fermentation proceeded, the evolved gas flow rate was initially slow (~0-5 h) but then rapidly increased to a maximum (at ~14 h) before sharply dropping and undergoing a small but long curve between 17 and 30 h. These changes in gas flow were observed in the slope of flow rate (Figure 5.2d), which displayed a significant minimum at 16.02 h (reaching a value lower than -20 ccm/h), that correlated with the time at which glucose neared exhaustion from the growth culture. A similar pattern was observed in our previous work with synthetic media, which established the use of gas flow rate as a trigger to initiate SCF cycling (Chapter 4). Finally, as shown in Additional Figure 7b (Appendix B), the cumulative gas evolved gradually increased until it slowed down between 16 and 17 h of fermentation, stabilizing at a total amount of ~21 L.

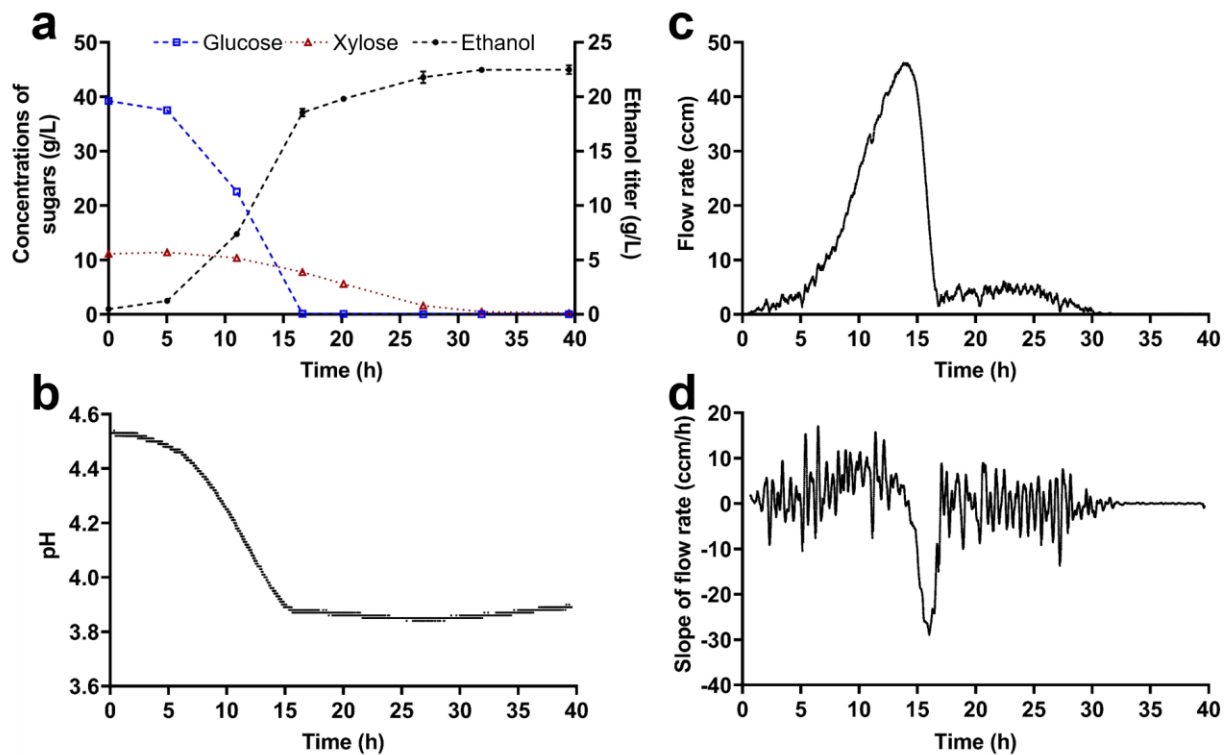


Figure 5.2 Batch fermentation of wood pulp hydrolysate-based medium. Parameters monitored included sugars and ethanol (a), pH (b), evolved gas flow rate (c), and its slope (d). Means from analytical triplicates are reported in panel (a), with error bars representing standard deviation. For panel (c), ccm represents cubic centimeter of gas evolved per minute at 25 °C and 1 atm. For panel (d), the slope of the gas flow rate was reported in cubic centimeter per minute per cycle time (ccm/h).

5.4.3 Incorporation of the wood pulp hydrolysate in SCF

The data obtained through batch fermentation employing the wood pulp hydrolysate confirmed that the slope of the gas flow rate could be used to indicate the timepoint at which glucose is almost depleted from the media. Thus, the cycling criteria employed in the previous SCF study (Chapter 4) were applied to an SCF campaign using wood pulp hydrolysate. In this case, a total of 10 cycles were performed. In general, the SCF cycles achieved similar levels of biomass at the end of each cycle (~2 mg dry cell weight/g culture), which were roughly two-fold higher than values observed at the onset of cycles 2

to 10 (~1 mg/g) (Figure 5.3a). The glucose concentration (Figure 5.3b) at the onset of the SCF campaign (beginning of cycle 1) was ~40 g/L, with each of the subsequent cycles starting with a glucose concentration of ~18-19 g/L, as expected. It is worth noting that the residual glucose content at the end of all cycles was no higher than 1 g/L (averaging 0.5 ± 0.2 g/L). For xylose (Figure 5.3c), cycle 1 started with ~11 g/L, and, as expected based on data from the batch fermentation (Figure 5.2a), a substantial amount (~8 g/L) still remained at the end of the cycle. Similarly, cycles 2-10 started with ~9 g/L of xylose, and ended up with ~8 g/L at the end. Remarkably, despite the differences in residual glucose and xylose content at the end of each stage, similar ethanol titers (around 19 g/L) were observed for the end of the 10 cycles (Figure 5.3d), with cycles 2-10 starting with roughly 10 g/L, slightly higher than half of the final ethanol titer of cycle 1. Overall, the SCF campaign using wood pulp hydrolysate achieved regular and stable patterns.

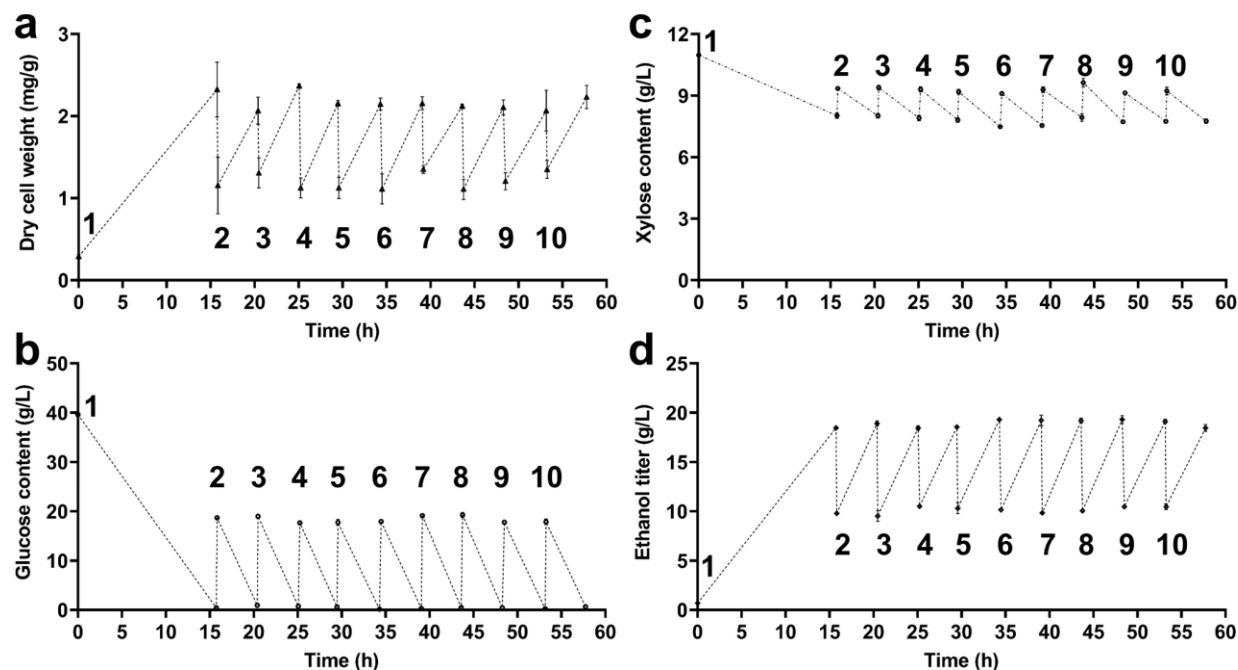


Figure 5.3 SCF operation using wood pulp hydrolysate-based medium. Dry cell weight (a), glucose content (b), xylose content (c), and ethanol titer (d) as a function of fermentation time. Cycle numbers are indicated at the beginning of each cycle. Means from analytical triplicates are reported, with error bars representing standard deviation.

Figure 5.4 shows the growth-related parameters automatically monitored during the SCF campaign. Cycles 2-10 displayed similar repeatable patterns with regards to the peaks for gas flow rate, though the maxima were lower than that of cycle 1 (Figure 5.4a). Despite some overall fluctuations, the slope of the gas flow rate (Figure 5.4b) for all cycles reached values much lower than the -20 ccm/h, as required to trigger cycling. The total gas evolved (Figure 5.4c), which indicated the total volume of gas released over a cycle, confirmed that cycle 1 of the SCF campaign and batch fermentation evolved similar volume of gas, which was roughly two-fold higher than that released by cycles 2-9 (Figure 5.4c). During SCF, the pH in all cycles dropped below 4, with cycles 2-10 starting with lower pH levels than cycle 1. Despite this, similar pH levels were reached at the end of cycles 2-10. Importantly, since all cycles eventually satisfied the cycling criteria (the slope of gas flow rate reached < -20 ccm/h and increased over 2 min, with the $\text{pH} < 4$ and cycle time > 3 h), cycling was automatically triggered, and no manual intervention was required to operate the system.

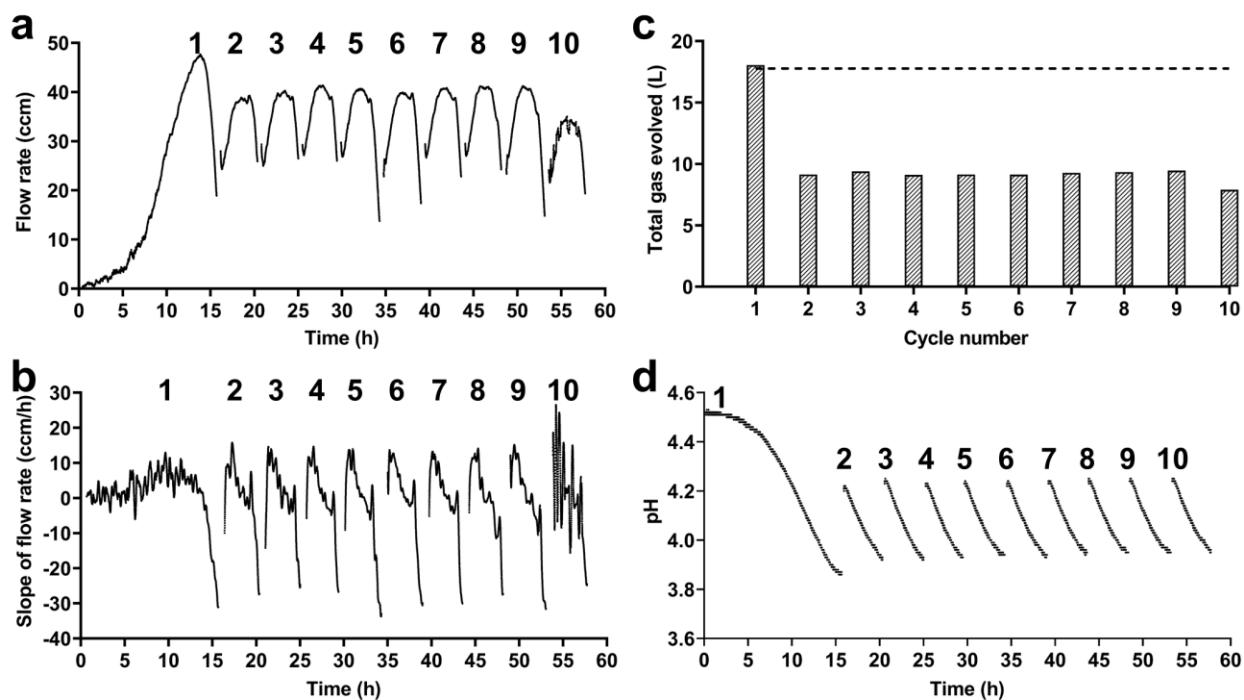


Figure 5.4 Online monitoring parameters during SCF operation using wood pulp hydrolysate. Evolved gas flow rate (a), slope of evolved gas flow rate (b), total volume of

gas produced per cycle (c), and pH (d) as a function of fermentation time. Cycle numbers are indicated at the top of the curves for each cycle, except for panel (c), where cycle numbers were indicated on the x-axis. The horizontal line in panel (c) represents the total gas evolved at the time the minimum in slope is reached during batch operation (Additional Figure 7b in Appendix B) under similar conditions. For panels (a) and (b), ccm represents cubic centimeter of gas evolved per minute.

It is worthwhile to point out that cycle 10 had the lowest peak value in gas flow rate (Figure 5.4a), more fluctuations in the slope of flow rate (Figure 5.4b), and the lowest volume of total gas evolved (Figure 5.4c) among cycles 2-10. This was likely caused by multiple intra-cycle samples that were taken to assess the kinetics of cycle 10 (Figure 5); previous reports have shown that heavy sampling can disturb the patterns in gas flow rate (Figures 4.2 and 4.5 in this thesis) [143]. As seen in Figure 5.5, all parameters examined in the course of cycle 10 – dry cell weight (Figure 5.5a), glucose (Figure 5.5b) and xylose (Figure 5.5c) content, ethanol produced (Figure 5.5d) – did not show a lag or stationary phase and were generally increased or decreased in a linear fashion, implying a faster metabolic rate than batch (Figure 5.2), which typically includes slow growth period such as lag and stationary phases.

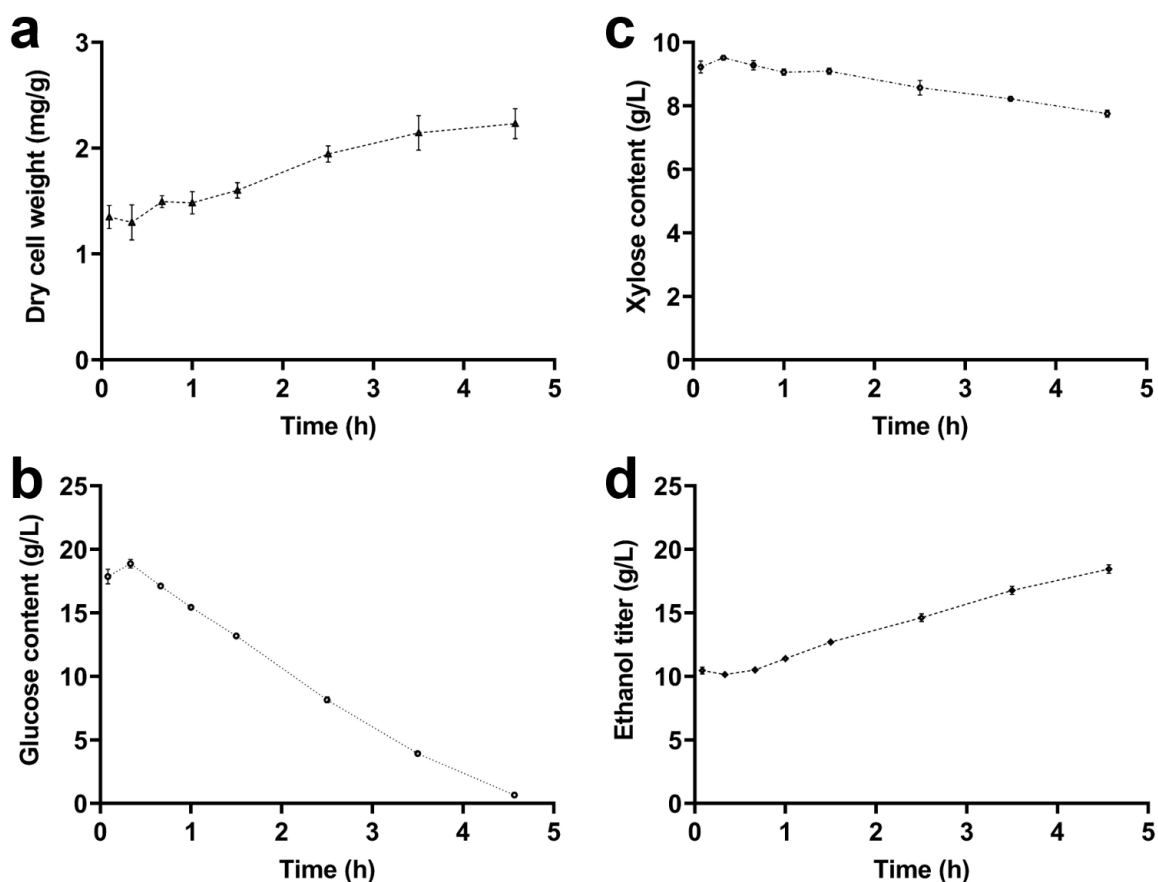


Figure 5.5 Kinetic study of SCF cycle 10. Dry cell weight (a), glucose content (b), xylose content (c), and ethanol titer (d) as a function of cycle time. Means from analytical triplicates are reported, with error bars representing standard deviation.

5.4.4 Improvement in productivity

As implied by Figure 5.6a, the first cycle of SCF displayed a similar fermentation time as batch fermentations, as determined by the timepoint when the minimum slope of the gas flow rate was observed (16.02 h; Figure 5.2d). Conversely, all subsequent cycles had a substantial reduction in cycle time, reaching approximately 1/3 the time of cycle 1 and batch fermentation (Figure 5.6a). The ethanol volumetric productivity was calculated as the amount of ethanol produced by a cycle per working volume per corresponding cycle time. As indicated by Figure 5.6b, the ethanol volumetric productivity in cycle 1 was similar to that of a batch, which is not surprising given that cycle 1 of SCF is essentially a batch

reaction. For all subsequent cycles, improvements of 54-82% were observed for the different cycles.

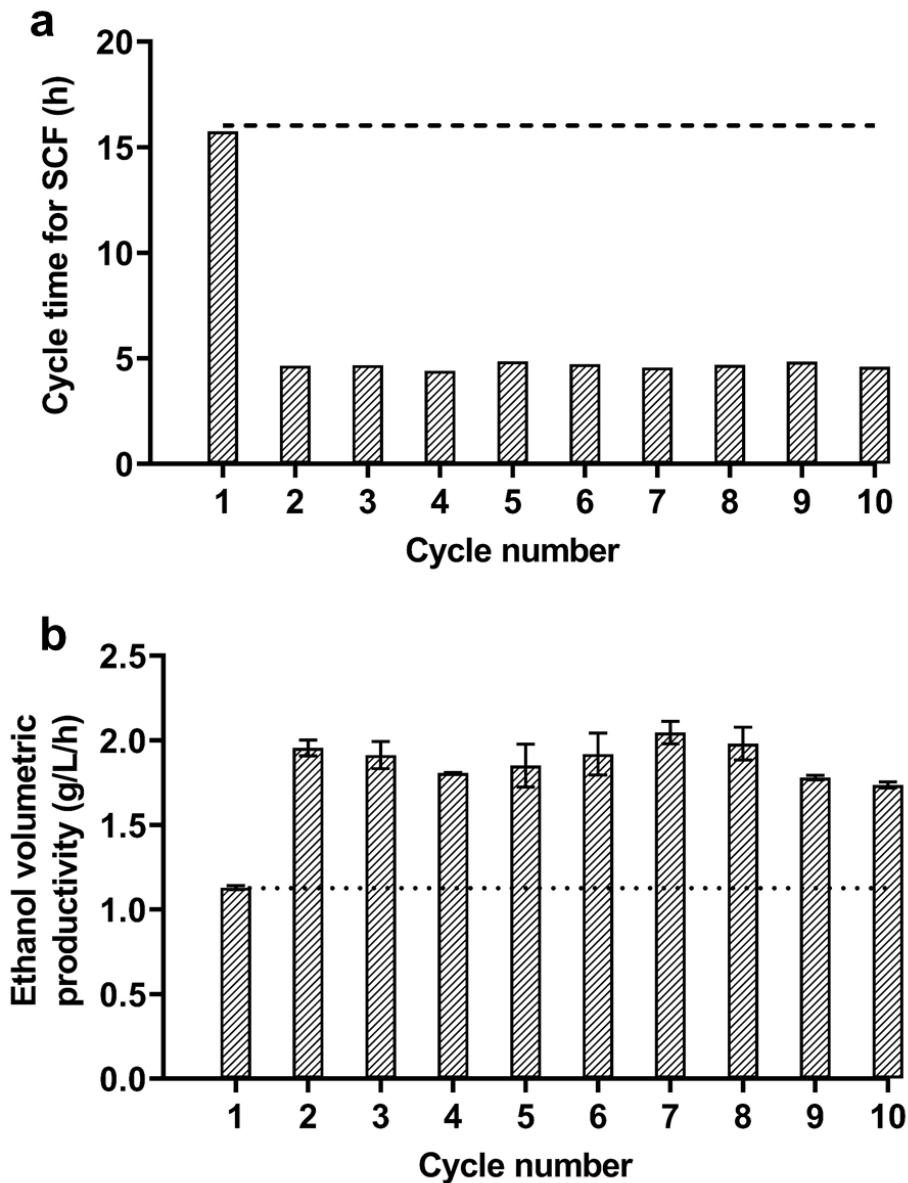


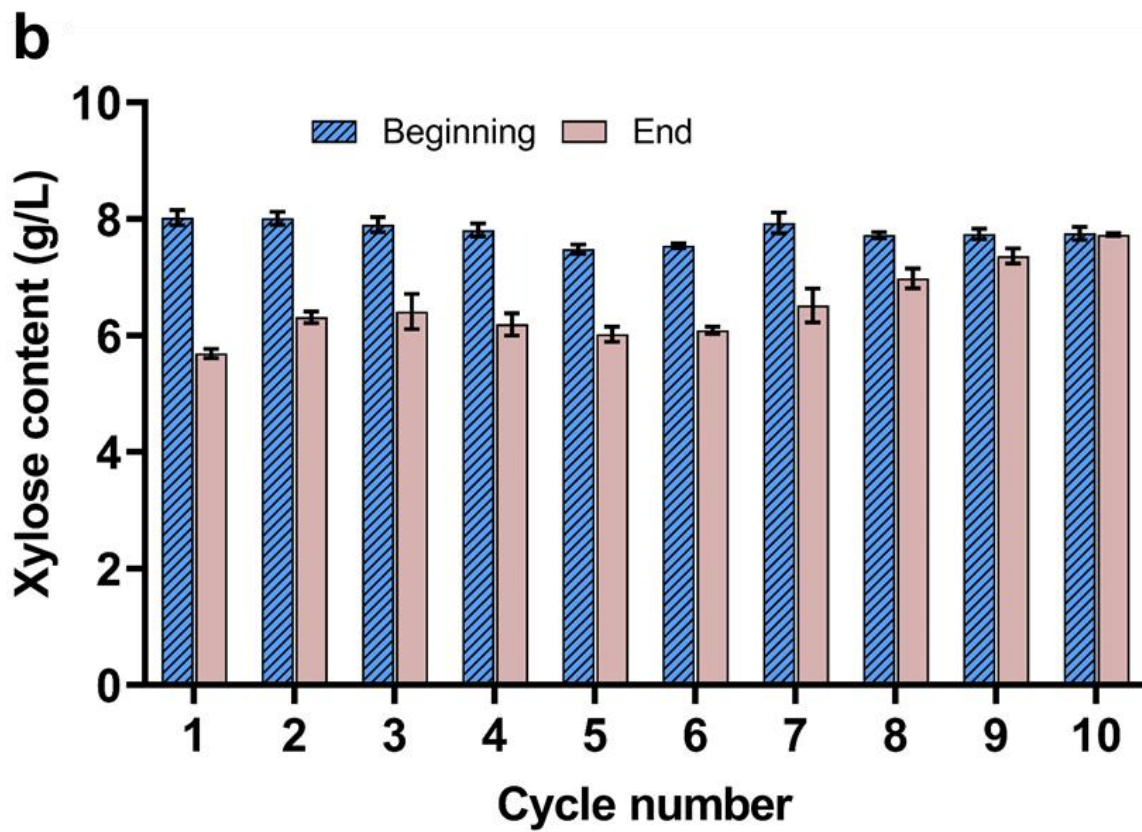
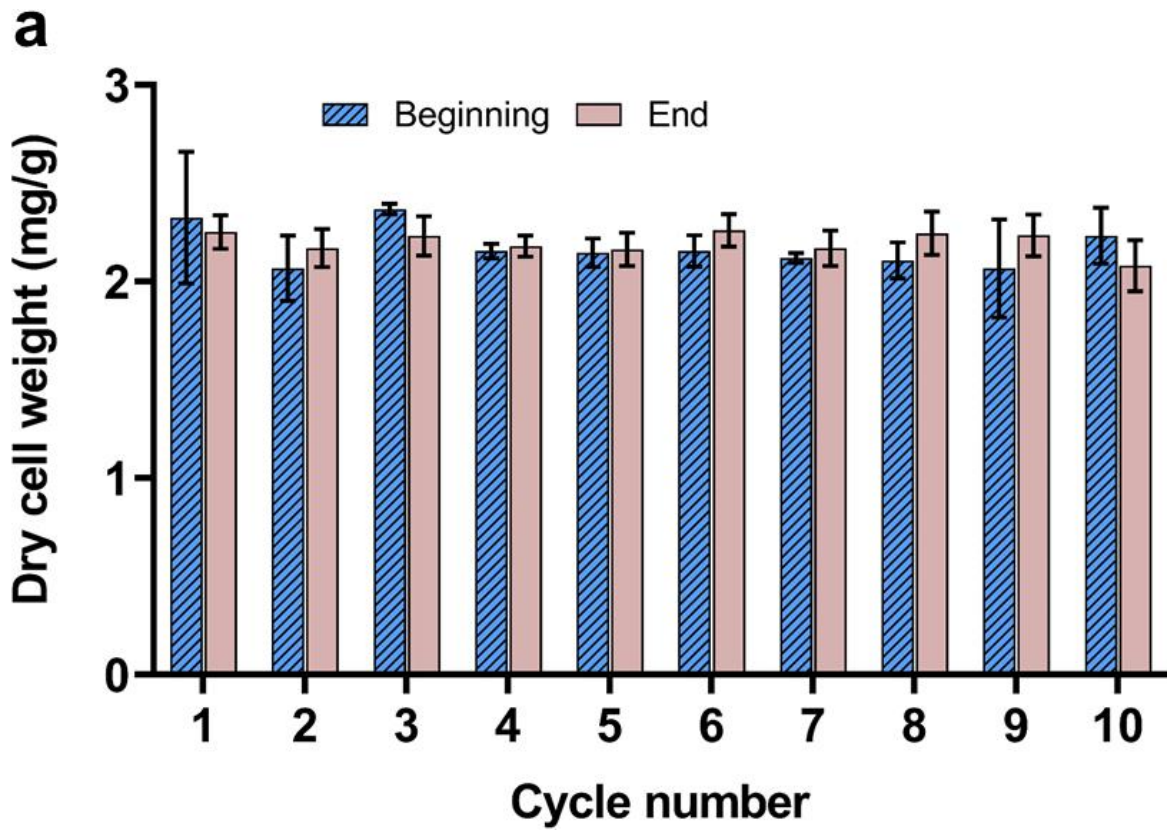
Figure 5.6 Cycle time and ethanol volumetric productivity observed during SCF operation. Cycle time (a) and ethanol volumetric productivity (b) were calculated for each SCF cycle. Horizontal lines for panel (a) and (b) represent the cycle time and ethanol volumetric productivity, respectively, obtained from batch fermentation.

Annual ethanol productivity represents the amount of ethanol that can be potentially produced each year at large scale (10^5 L) under certain industrial conditions [149], and its formula was included in Section 3.4.3 (Equations 3.2 and 3.3). Under these conditions, batch fermentation campaigns, are expected to yield 649 ± 13 tons of ethanol every year. However, using campaigns consisting of 10 SCF cycles into the same industrial settings, the annual ethanol productivity could potentially reach $1.18 \times 10^3 \pm 10$ ton/year, which represents an improvement of $81.2 \pm 4.3\%$ over batch campaign.

5.4.5 Second fermentation stage

Batch fermentation (Figure 5.2) demonstrated that glucose was consumed prior to xylose, and that xylose was still present at high levels when the conditions for SCF cycling were met. Thus, when the SCF campaign was run, at the end of each cycle, part of the harvested culture was sent to a second fermentation stage (shake flask). This was done to determine if the remaining xylose could be converted into ethanol through longer fermentation times.

Since the period of the second fermentation was tied to the cycle time of the concurrent SCF cycle, the length of cycle n of the second stage fermentation was equivalent to that of cycle $n+1$ of SCF (approximately 4.7 h on average; Figure 5.6a). As can be seen in Figure 5.7a, the dry cell weight did not increase noticeably during any of the second fermentation stages. Yet, ethanol titer increased (Figure 5.7c) over the 4-5 h period of continued fermentation, with an average increase of ~ 0.9 g/L (i.e. 4.6% improvement). Substantial amounts of xylose were consumed during the first 7 cycles of the second stage fermentation; though there was a noticeable reduction in xylose utilization starting at cycle 8, with almost no consumption for the following cycles (Figure 5.7b). Despite this, and although further optimization of fermentation conditions is required, these results suggest that a simple second stage fermentation can result in increased production of ethanol.



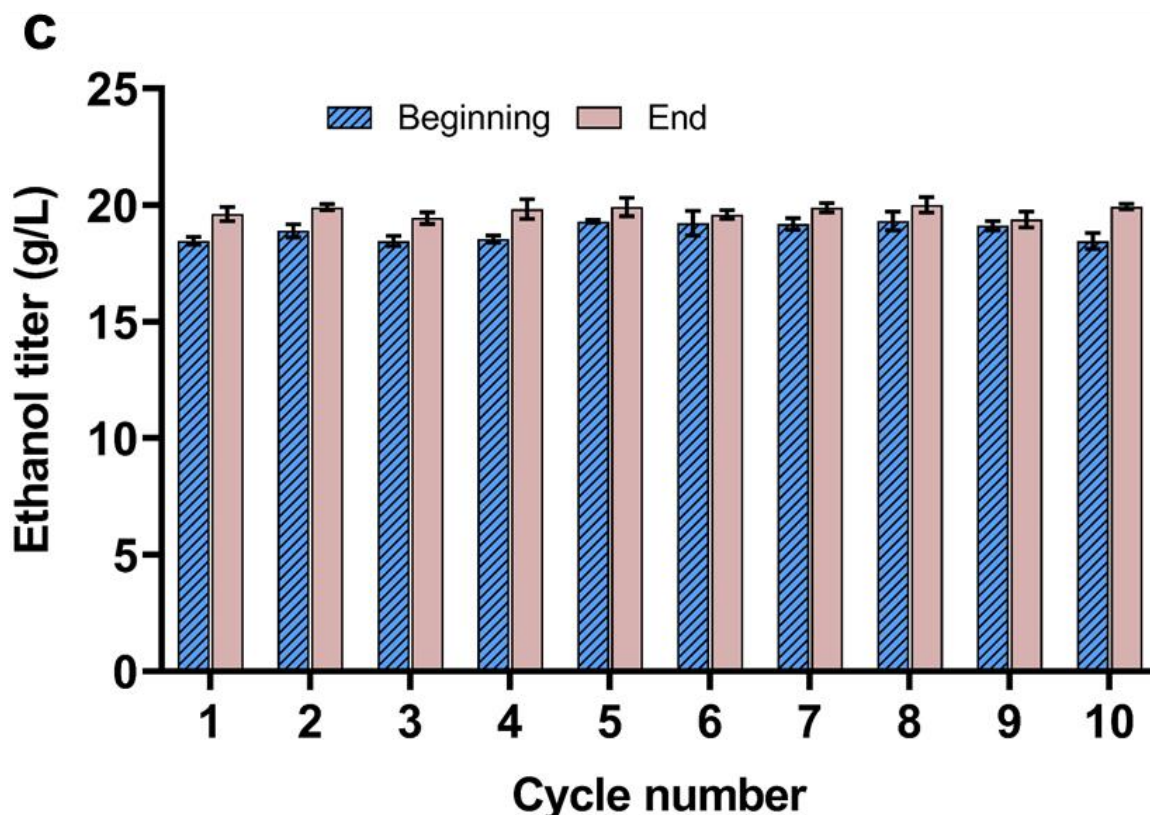


Figure 5.7 Second fermentation stage using wood pulp hydrolysate-based medium. At the end of each SCF cycle, the harvested culture was transferred into shake flasks for a second fermentation stage. This second stage was stopped when the concurrent SCF cycle ended, such that the cycle time was equal for both stages. Dry cell weight (a), xylose content (b), and ethanol titer (c) were analyzed for each cycle of SCF at the beginning and the end of the second fermentation stage.

To further characterize the cycles of both SCF and the second fermentation stage, levels of glycerol and organic acids were assessed. Glycerol is a common by-product generated during ethanol production to balance redox potential in the organism [173], and its accumulation is also associated with cells exposed to stressful environments [19]. On the other hand, high concentrations of organic acids (i.e. acetic and lactic acid) are typically caused by bacterial contamination [19,63,71]. During SCF, cycle 1 produced 2.3 ± 0.2 g/L glycerol, which was similar to levels encountered in the batch fermentation (2.5 ± 0.0 g/L), while cycles 2-10 generally started at ~ 1 g/L glycerol and ended with ~ 2 g/L. No further

increase in glycerol concentration was observed at the end of the second fermentation stages. For all of the fermentations performed in this study, acetic and lactic acid were detected at concentrations below 0.3 g/L. Furthermore, no evidence of contamination was observed in fermentation samples using microscopy.

5.5 Discussion

5.5.1 Hydrolysates from wood pulp

Literature report revealed that an 8 h enzymatic treatment of northern bleached hardwood kraft pulp resulted in the highest recovery of sugars and cellulose nanocrystals (CNCs), a high value by-product derived from the solid residues after enzyme treatment [114]. Hence, a hydrolysate generated under these conditions was chosen for the present study. As the wood pulp used in this study was generated using a kraft process that facilitates use of sodium hydroxide and sodium sulfide, it was possible (albeit unlikely) that chemicals associated with the dried wood pulp could inhibit fermentation, analogous to those that are commonly formed during other pretreatment technologies for lignocellulosic materials [39]. However, our analytical results confirmed that the hydrolysate does not exhibit inhibitory effects during fermentation (Figure 5.2). It is worthwhile to mention that citric acid (0.05 M) was used to buffer enzymatic hydrolysis of lignocellulosic feedstock [154,174]. Although this acid can be an inhibitor of yeast fermentation, negative effects are only observed for *S. cerevisiae* when the concentration is over 0.2 M [175]. Future work will look into incorporating various lignocellulosic feedstocks into the system and using different pretreatment and enzymatic treatments (e.g. enzymes, buffers, and treatment time) to examine whether these changes can influence the ethanol productivity during SCF operation.

5.5.2 Batch fermentation using the wood pulp hydrolysate

Previously, a successful implementation of SCF – automated using gas flow as feedback control parameter – under anaerobic conditions with glucose as the sole carbon source available in a synthetic medium was reported in Chapter 4. When sugar streams are generated from lignocellulosic materials, they often contain both glucose and xylose, the main components of cellulose and hemicellulose, respectively [176]. In the current study,

the wood pulp hydrolysate contained approximately 40 g/L glucose and 10 g/L xylose. Therefore, we used a modified *S. cerevisiae* strain (Y128) that can convert both glucose and xylose into ethanol [127]. Batch fermentations were performed with this strain to assess its behaviour when grown using a wood pulp hydrolysate, as well as to determine whether gas flow could still be used as a real-time monitoring parameter for ensuing SCF campaigns.

As implied by the patterns of glucose and xylose consumption (Figure 5.2a) and by the evolved gas flow rate (Figure 5.2c), the yeast displayed a diauxic growth pattern. This was characterized by preferential glucose consumption, with xylose utilization being initiated only once glucose levels became limiting, and by a bimodal pattern in evolved gas corresponding to the utilization of each sugar. The preferential consumption of glucose in this system aligns well with a previous study in which Y128 was cultivated on hydrolysates from corn stover [127]. Historical research has established diauxic growth as a two-phase growth characterized by sequential metabolism of two sugar substrates, separated by a lag period [177]. The lag observed after depletion of the preferred sugar is generally considered as the time needed for the microorganism to adapt and produce enzymes related to a less-preferred substrate [178]. However, recent research on diauxic growth has shown that the transitional lag period can be reduced when a portion of the cell population starts to produce the enzymes necessary for metabolism of the less preferred substrate prior to consumption of the preferred sugar [179,180]. In the present study, no obvious lag phase was observed between the utilization of glucose and xylose (Figure 5.2a). Thus, it is likely that part of the *S. cerevisiae* Y128 cells had started to express genes related to xylose consumption when glucose reached low levels, rather than once depleted. This is not surprising given that Y128 was selected after a series of evolutionary experiments designed to identify strains that had improved xylose utilization under anaerobic conditions [127].

Simultaneous fermentation of glucose and xylose at comparable rates would be a desirable trait for yeast producing ethanol from lignocellulosic feedstocks; unfortunately, despite numerous attempts to engineer *S. cerevisiae*, the fermentation rate of xylose remains lower than that of glucose [128,129], and a diauxic pattern is commonly observed when both glucose and xylose are present [115,126]. SCF was designed to trigger an

automated cycling process immediately when a limiting nutrient is depleted, avoiding stationary phase [21,23,24,29]. However, although ethanol production and gas flow rate were dramatically reduced when glucose approached depletion, significant amounts of xylose (~8 g/L), which could still contribute to ethanol production, were still present. In this case, stationary phase was not likely achieved until after hour 32 when both glucose and xylose were exhausted from the growth medium (Figure 5.2a). The relatively small amount of ethanol (~4 g/L) generated from xylose in the ~16 hours following glucose depletion would dramatically reduce ethanol productivity if this period were to be included in the SCF cycles. Indeed, switching between different metabolic pathways, which is characteristic of diauxic growth, retards microbial growth and metabolism, resulting in longer SCF cycle times and reduced volumetric productivity [149].

5.5.3 Incorporation of the wood pulp hydrolysate in SCF

To overcome the potential negative impact of the diauxic shift on ethanol productivity in a SCF system using a mixed sugar medium, we proposed to trigger SCF cycling when glucose became almost depleted in the medium and include a second fermentation step to convert the remaining glucose and xylose (Figure 5.1). Based on the results of the batch fermentation (Figure 5.2), the timeframe spanning the beginning of fermentation and the point of glucose approaching depletion is where the bulk of the ethanol is produced (i.e. 0 h to ~16 h). The second stage fermentation served to promote conversion of xylose to ethanol, which was identified as a much slower process (Figure 5.2). This two-stage strategy was proposed to maximize ethanol productivity: maximizing ethanol productivity from glucose in SCF, while allowing the slower xylose fermentation to continue outside of the main fermenter.

The regular patterns achieved in the SCF stage (shown in Figures 5.3 and 5.4) highlighted the stability of the SCF system when wood pulp hydrolysates were employed as feedstock. Of note, a significant reduction in cycle time was observed for cycles 2-10 (Figure 5.6a). In addition, at the end of SCF operation, ~1 g ethanol was detected in the water trap that was placed between the venting line and gas flow meter, which was attributable to ethanol evaporation. This suggested that the ethanol titers reported in Figure 5.3d were slightly lower than the actual ethanol produced. Furthermore, the

difference between the initial pH of cycle 1 and of the subsequent cycles (Figure 5.4d) implied that growth rate and productivity might be further enhanced if the buffer capacity of the growth medium was increased. Taken together, these results demonstrate that SCF can be applied to the bioconversion of hydrolysates from wood pulp.

5.5.4 Improvement in productivity

Since low amounts of ethanol were produced during the second fermentation stage (Figure 5.7c), which was performed in parallel with SCF (Figure 5.1), thus, productivities were calculated using ethanol values and cycle time observed strictly during SCF. Compared to cycle 1 of SCF or batch operation under equivalent conditions, cycles 2 to 10 displayed a substantial improvement in ethanol volumetric productivity (Figure 5.6), which resulted primarily from the reduction of cycle time, while maintaining similar ethanol production. The dramatic reduction in cycle time observed in cycles 2 to 10 of SCF is likely attributable to the quick uptake of nutrients and conversion to ethanol that is characteristic of cells in exponential phase [24]. This is in contrast to batch fermentations, where lag and stationary phases are observed, during which there is no significant production of ethanol (Figure 3.1). Furthermore, the annual ethanol productivity observed in the current study is consistent with previous reports that employed a synthetic medium in SCF operation (Chapter 4). As a result of the productivities improvement, ethanol producers can increase the total amount of ethanol production within a given period of time. This provides a great potential for more replacement of ethanol to fossil fuels, thus contributing to a reduction of greenhouse gas (GHG) emissions for the environment.

5.5.5 Second fermentation stage

Upon harvesting from the SCF reactor, the culture was transferred to shake flasks to facilitate further ethanol production. Interestingly, xylose utilization and ethanol production was indeed observed in this second stage (Figure 5.7), albeit at low levels within the time frame under examination. It is worth noting that since harvesting from the SCF reactor was triggered by the near depletion of glucose, the cells that were transferred to shake flasks were likely undergoing diauxic growth, and were not yet consuming xylose at optimal rates. Indeed, the batch culture (Figure 5.2) showed that following glucose

depletion from the medium, an additional 16 hours was required for near complete utilization of xylose. Since the cycle time of the second fermentation stage employed in our experiments was based on the cycle time of SCF (4-5 h), it is likely that there was not sufficient time for complete xylose utilization to occur. Future work would be needed to determine the growing conditions (i.e. time, shaking rate, incubation temperature, etc.) for optimal xylose-to-ethanol conversion by *S. cerevisiae* Y128 in the second stage. Nevertheless, it should be noted that even in this non-optimized system, analytical triplicates confirmed that 6 of the 10 second stage cycles resulted in elevated production of ethanol.

It is also interesting to point out that while yeast maintained similar fermentation patterns among cycles 2-10 (Figures 5.3, 5.4, and 5.6), including xylose consumption (Figure 5.3c), a gradual reduction in xylose consumption was observed over the final 3 cycles of the second fermentation stage (Figure 5.7b). The reason behind this reduction is not yet known. However, future work to assess differences in gene expression during both SCF and second stage cycles may help reveal the mechanisms responsible for the shift in xylose consumption.

Should optimization experiments reveal that xylose cannot be efficiently converted to ethanol during the second stage fermentation, it may be more valuable to recover and utilize xylose for other applications. Specifically, cells could be harvested from the SCF fermenter, and ethanol distilled from the culture solution, which is a standard practice. The residual aqueous solution, which contains xylose, could be recovered and utilized for the production of high value products. For instance, in the presence of sulfuric acid, xylose can be chemically converted into furfural, a platform compound for the production of various furan-based chemicals [110]. The production of furfural from aqueous xylose solutions originating from lignocellulosic feedstocks has been implemented commercially, as summarized by Cai *et al.*, and attempts have also been made to integrate the process within cellulosic ethanol production schemes [110].

During batch fermentation, it was observed that yeast slightly aggregated to surfaces inside the fermenter, and they settled down quickly during sampling. This phenomenon was also observed during SCF and second stage fermentations, with higher

aggregation and settling rates achieved in later cycles. This pattern was in agreement with our previous report in which SCF was performed using synthetic medium and an industrial yeast strain (Chapter 4). The increased cell aggregation and settling caused non-homogenous distribution of cells during samples, making cell count or optical density measurements inaccurate. As stated in Chapter 4, flocculation of cells could facilitate downstream separation of solids from liquid, and potentially lead to substantial reductions in processing costs incurred by the ethanol industry [18].

5.6 Conclusions

This is the first study to successfully integrate lignocellulosic materials with SCF for ethanol production. It is also the first report of applying an SCF strategy using a mixed sugar medium that promotes diauxic growth of microorganisms. Significant improvements in ethanol volumetric productivity (54-82%) and annual ethanol productivity ($81.2 \pm 4.3\%$) were achieved using fully automated SCF, compared to batch operation. The inclusion of a second stage for the extended fermentation of xylose showed that further improvements in ethanol production could be achieved without impeding on productivity. Finally, such improvements in ethanol productivity could greatly contribute to offsetting the overall production costs for cellulosic ethanol, as well as reducing the GHG emissions for the environment.

5.7 Acknowledgments

We acknowledge Dr. Trey Sato for kindly providing their yeast *Saccharomyces cerevisiae* Y128 for this research. We would also like to acknowledge our funding agencies Canada First Research Excellence Fund, Future Energy Systems (T01-P01) at the University of Alberta, BioFuelNet Canada (NCEBFN 3N), and the Natural Sciences and Engineering Research Council of Canada (NSERC, Discovery Grants; RGPIN-2019-04184) for their financial support of our research.

Chapter 6 Summary, conclusion, and future directions

6.1 Summary and conclusion

This is the first successful report to significantly improve ethanol productivity through an SCF strategy. It is also the first attempt that successfully automated the SCF process under anaerobic conditions; the incorporation of a gas flow meter to monitor the fermentation process is also novel for SCF. This study also identified the necessity to supplement ergosterol and Tween 80 to the SCF system for maintaining short cycle time for long-term runs. Stable and robust, the feedback control conditions developed in this study were effectively applied using real cellulosic feedstock to improve ethanol productivities. Collectively, the work described in this thesis demonstrates the great potential of SCF to reduce production costs for cellulosic ethanol industry.

This work started with defined and controlled conditions to investigate the effects of integrating SCF with ethanol production. Specifically, a synthetic medium was used, where glucose was the sole carbon source available. Shake flasks were used to perform fermentation for five cycles (Chapter 3), and a manual cycling was initiated after the glucose content reached zero. Results showed that, compared to batch fermentation operated under similar conditions, significant improvement in ethanol volumetric productivity was observed, primarily due to the reduction of cycle time and stable ethanol titers at the end of all cycles.

The improvement in productivity observed in shake flasks provided motivation for the construction of an automated SCF system (Chapter 4). A gas flow meter attached to the outlet of a 5-L fermenter facilitated identification of a suitable feedback control parameter (i.e. gas flow rate) to automate the cycling process under anaerobic conditions. The cycle time of SCF operated in this 5-L fermenter, using a synthetic medium, can be dramatically shortened through the addition of ergosterol and Tween 80, which are required to maintain the integrity of cell membranes. SCF was automatically operated in this 5-L fermenter for over 20 cycles, and the system was observed to be stable and robust, with all cycles being automatically driven. In fact, the SCF system was able to quickly recover after

an imposed disturbance. Compared to batch, significantly improved ethanol volumetric productivity (37.5-75.3%) was observed, similar with shake flasks.

Finally, a real lignocellulosic feedstock, wood pulp, was incorporated into the SCF system; 10 consecutive cycles were successfully demonstrated when the hydrolysate of wood pulp was employed in the culture medium (Chapter 5). Since the yeast strain *S. cerevisiae* Y128 showed a diauxic growth pattern on the hydrolysate, a two-stage SCF was performed to minimize the effects of the metabolic switch between glucose and xylose. As a result, the ethanol volumetric productivity was substantially improved (by 54-82%) with the two-stage operation strategy. The improved cellulosic ethanol production per time indicates its great potential to reduce GHG emissions by the partial replacement of fossil fuels. Interestingly, flocculation was consistently observed as SCF cycles moved forward, which can accelerate the downstream process and thus help reduce operational cost.

6.2 Future directions

This thesis set out to explore the potential of introducing SCF approach into ethanol production, with a strong focus on the automation and productivity improvement aspects. To fully understand the system and improve its performance for ethanol production, many interesting studies can be performed in the future.

- **Flocculation and its impact on downstream separations**

This thesis is one of the few reports on the cell aggregation and flocculation achieved through the operation of SCF. Despite its potential benefit to downstream separation, the reason for why flocculation was triggered on a molecular level, need to be explored to better understand the system. For instance, yeast genes such as FLO 1, 5, 9, and 10 are responsible for the production of some cell wall proteins that facilitate the adhesion among cells [87], and it is possible that these genes were activated during the SCF process. The potential internal factors (e.g. pH, nutrients, strain) that contributed to flocculation in this system also need to be studied [85,86].

- **Synchrony of SCF**

A common observation with SCF operation is the synchronization of cells. However, due to flocculation, measurement of cell number using cell counts, the classical way of

quantifying synchrony (Chapter 2, Section 2.4.3), becomes unreliable. Therefore, whether synchrony was achieved in this study, and if it contributed to the improvement of ethanol productivities during the operation remain as questions. Future work is required to find alternative methods to measure the synchrony index of cells in SCF for ethanol production. It will also be very interesting to reveal the mechanism of synchrony from a molecular level.

- **Ergosterol and Tween 80**

As reported in Chapter 4, the addition of ergosterol and Tween 80 helped to reduce the fermentation cycle time for long-term SCF operation. In anaerobic conditions, the cell is unable to generate certain molecules that are integral to cell membranes. The use of ergosterol and Tween 80 has been previously shown to alleviate these effects. Further study needs to be conducted to reveal if the addition of these supplements changed the fatty acids profile of yeast cell membrane. In addition, it may be possible to add a cheap alternative, air, at the beginning of each cycle to replace the supplementation of ergosterol and Tween 80 in an industrial setting. Exposure to a very small amount of air should enable cells to produce the sterols and unsaturated fatty acids necessary for fully functional plasma membranes, while maintaining an anaerobic environment to ensure high ethanol yields.

- **Medium**

This work used low sugars content (~ 50 g/L), and yeast nitrogen base (YNB) was added as a chemically defined source for nitrogen, vitamins, and minerals (Chapters 3-5). Future work can be performed to increase the sugars concentration for a higher ethanol titer at the end of fermentation, which would help reduce the cost for distillation (described in Section 2.2.1.1, Chapter 2) [14,16,76]. In addition, cheap and more industrial relevant sources can be used as alternatives for YNB, for instance, corn steep liquor [18]. Furthermore, inhibitors (e.g. acetic acid, furfural) that are commonly present in lignocellulosic hydrolysate are known to stress the yeast cells, prolong fermentation time, and/or reduce ethanol yield [5]. In the current study, since all of the media in this study had negligible amount of those inhibitors (Chapters 3-5), it will be important to add

inhibitors into the current fermentation media or use hydrolysate that contain them, to test if ethanol productivity can still be elevated by SCF.

- **Increase in solids loading**

The 10% (w/w) solids loading in this study (Chapter 5) can be further improved to increase the final ethanol titer, so that distillation cost can be reduced [14,75]. In a higher solids loading environment, yeast will be faced with much higher stress levels than the current studies [75], and it will be worthwhile to test if SCF can still help improve ethanol productivity under those conditions.

- **Various types of feedstock**

Initially, this work employed a synthetic medium and then proceeded to use a hydrolysate of wood pulp for ethanol production in an SCF fermenter. Future work can expand to various types of feedstock for integration with SCF, including agricultural wastes, other forestry residues, as well as 1st generation feedstocks mentioned previously (Section 2.2, Chapter 2). In the case of grain feedstock, a simultaneous saccharification and fermentation (SSF) strategy as a way to reduce enzyme inhibition and osmotic stress for cells (Section 2.2.1.1, Chapter 2) can be tested with regards to its compatibility with the SCF technique. There is also a great possibility to integrate SSF into SCF for the lignocellulosic feedstocks.

- **Simultaneous co-fermentation of C5 and C6 sugars**

Chapter 5 used a strain of *S. cerevisiae* (Y128) that showed a diauxic growth pattern with a preference for glucose fermentation. Hence, a two-stage SCF was operated to minimize the impact of the metabolic switch between glucose and xylose during the SCF campaign. In the future, providing the improvement in molecular and evolutionary engineering of microorganism, it will be interesting to incorporate SCF with a microorganism that can simultaneously ferment C5 and C6 sugars at similar rate, which would convert both sugars into ethanol in one stage.

- **Compare SCF with fed-batch**

Currently, cellulosic ethanol fermentation is primarily operated in batch, which served as a benchmark for comparison with SCF in this work. Future efforts can look into

the comparison between SCF and a fed-batch approach, which is commonly employed in ethanol production from sugar-based feedstock (discussed in Section 2.2.1.2, Chapter 2). The benefit of a fed-batch system is the slow feeding rate, which results in lower osmotic stress to yeast, especially with a high solids loading system.

- **Scale up and techno-economic analysis**

This thesis started with 500-mL shake flasks for ethanol fermentation and scaled up to a 5-L SCF fermenter with a maximum run of 21 cycles. Up to now, the highest level of fermentation volume in an SCF fermenter reported in the literature is a 10-L reactor [181]. It will be significant if the SCF process developed in this work can be integrated with other types of feedstocks mentioned above, and then scaled up, and tested for its improvement in productivity for around 20 cycles. In addition, a techno-economic analysis can be carried out to compare the discrepancy between SCF and batch/fed-batch with respect to the production cost at the large scale. A life-cycle analysis can also be conducted to access these different fermentation approaches in terms of carbon intensity.

Overall, this work is the first to provide a platform for future fermentation-based production schemes linked to the production of ethanol. The results highlighted the successful automation of the fermentation process and the remarkable improvement in ethanol productivity. With minor changes required for existing infrastructure to adapt to SCF, this accomplishment offers great potential to reduce cost and help boost the profitability of cellulosic ethanol industry, as well as to reduce GHG emissions.

Bibliography

1. Balat M, Balat H. Recent trends in global production and utilization of bio-ethanol fuel. *Appl. Energy*. 2009;86:2273–82.
2. Rosales-Calderon O, Arantes V. A review on commercial-scale high-value products that can be produced alongside cellulosic ethanol. *Biotechnol. Biofuels*. 2019;12:240.
3. Binder JB, Raines RT. Fermentable sugars by chemical hydrolysis of biomass. *Proc. Natl. Acad. Sci. U. S. A.* 2010;107:4516–21.
4. Jarvis M. Chemistry: cellulose stacks up. *Nature*. 2003;426:611–2.
5. Santos LV dos, Grassi MC de B, Gallardo JCM, Pirolla RAS, Calderón LL, Carvalho-Neto OV de, et al. Second-generation ethanol: the need is becoming a reality. *Ind. Biotechnol.* 2016;12:40–57.
6. Lee S. Ethanol from lignocellulosics. *Handb. Altern. Fuel Technol.* 2007.
7. Branco RHR, Serafim LS, Xavier AMRB. Second generation bioethanol production: on the use of pulp and paper industry wastes as feedstock. *Fermentation*. 2019;5:4.
8. Kang Q, Appels L, Tan T, Dewil R. Bioethanol from lignocellulosic biomass: current findings determine research priorities. *Sci. World J.* 2014;2014.
9. Tao L, Schell D, Davis R, Tan E, Elander R, Bratis A, et al. NREL 2012 achievement of ethanol cost targets: biochemical ethanol fermentation via dilute-acid pretreatment and enzymatic hydrolysis of corn stover. Golden, CO (NREL/TP-5100-61563); 2014.
10. Mohd Azhar SH, Abdulla R, Jambo SA, Marbawi H, Gansau JA, Mohd Faik AA, et al. Yeasts in sustainable bioethanol production: a review. *Biochem. Biophys. Reports*. 2017;10:52–61.
11. De Bhowmick G, Sarmah AK, Sen R. Lignocellulosic biorefinery as a model for sustainable development of biofuels and value added products. *Bioresour. Technol.* 2018;247:1144–54.
12. POET-DSM. POET-DSM achieves cellulosic biofuel breakthrough. 2017. [cited 2019 Jul 31]. Available from: <http://poet-dsm.com/pr/poet-dsm-achieves-cellulosic-biofuel-breakthrough>
13. Brunecky R, Donohoe BS, Yarbrough JM, Mittal A, Scott BR, Ding H, et al. The multi domain Caldicellulosiruptor bescii CelA cellulase excels at the hydrolysis of crystalline cellulose. *Sci. Rep.* 2017;7:9622.

14. Koppram R, Tomás-Pejó E, Xiros C, Olsson L. Lignocellulosic ethanol production at high-gravity: challenges and perspectives. *Trends Biotechnol.* 2014;32:46–53.
15. Zhao X, Liu D. Multi-products co-production improves the economic feasibility of cellulosic ethanol: a case of formiline pretreatment-based biorefining. *Appl. Energy.* 2019;250:229–44.
16. Jin M, Sousa L da C, Schwartz C, He Y, Sarks C, Gunawan C, et al. Toward lower cost cellulosic biofuel production using ammonia based pretreatment technologies. *Green Chem. Royal Society of Chemistry;* 2016;18:957–66.
17. Chen M, Smith PM, Wolcott MP. US biofuels industry: a critical review of opportunities and challenges. *Bioprod. Bus.* 2016;1:42–59.
18. Humbird D, Davis R, Tao L, Kinchin C, Hsu D, Aden A, et al. Process design and economics for biochemical conversion of lignocellulosic biomass to ethanol. Golden, CO (No. NREL/TP-5100-47764); 2011.
19. Ingledew WM, Kelsall DR, Austin GD, Kluhspies C. The alcohol textbook. A reference for the beverage, fuel and industrial alcohol industries. 5th ed. Ingledew WM, Kelsall DR, Austin GD, Kluhspies C, editors. Nottingham, United Kingdom: Nottingham University Press; 2009.
20. Ewanick SM, Thompson WJ, Marquardt BJ, Bura R. Real-time understanding of lignocellulosic bioethanol fermentation by Raman spectroscopy. *Biotechnol. Biofuels.* 2013;6:28.
21. Brown WA, Cooper DG. Self-cycling fermentation applied to *Acinetobacter calcoaceticus* RAG-1. *Appl. Environ. Microbiol.* 1991;57:2901–6.
22. Storms ZJ, Brown T, Sauvageau D, Cooper DG. Self-cycling operation increases productivity of recombinant protein in *Escherichia coli*. *Biotechnol. Bioeng.* 2012;109:2262–70.
23. Agustin RV. The impact of self-cycling fermentation on the production of shikimic acid in populations of engineered *Saccharomyces cerevisiae*. University of Alberta; 2015.
24. Brown WA. The self-cycling fermentor: development, applications, and future opportunities. *Recent Res. Dev. Biotechnol. Bioeng. Research Signpost;* 2001;4:61–90.
25. Sheppard JD, Cooper DG. Development of computerized feedback control for the

- continuous phasing of *Bacillus subtilis*. *Biotechnol. Bioeng.* 1990;36:539–45.
26. Sheppard JD, Cooper DG. The response of *Bacillus subtilis* ATCC 21332 to manganese during continuous-phased growth. *Appl. Microbiol. Biotechnol.* 1991;35:72–6.
27. Sarkis BE, Cooper DG. Biodegradation of aromatic compounds in a self-cycling Fermenter (SCF). *Can. J. Chem. Eng.* 1994;72:874–80.
28. Hughes SM, Cooper DG. Biodegradation of phenol using the self-cycling fermentation (SCF) process. *Biotechnol. Bioeng.* 1996;51:112–9.
29. Wentworth SD, Cooper DG. Self-cycling fermentation of a citric acid producing strain of *Candida lipolytica*. *J. Ferment. Bioeng.* 1996;81:400–5.
30. BP p.l.c. BP Energy Outlook: 2019 edition. BP Energy Outlook 2019. 2019.
31. International Energy Agency. 2018 World Energy Outlook: Executive Summary. 2018.
32. Sharma S, Ghoshal SK. Hydrogen the future transportation fuel: from production to applications. *Renew. Sustain. Energy Rev.* 2015;43:1151–8.
33. Intergovernmental Panel on Climate Change. Mitigation of climate change. *Contrib. Work. Gr. III to Fifth Assess. Rep. Intergov. Panel Clim. Chang.* 2014.
34. Rogelj J, Den Elzen M, Höhne N, Fransen T, Fekete H, Winkler H, et al. Paris Agreement climate proposals need a boost to keep warming well below 2 °C. *Nature.* 2016;534:631–9.
35. Demirbas A. Biofuels sources, biofuel policy, biofuel economy and global biofuel projections. *Energy Convers. Manag.* 2008;49:2106–16.
36. Pandiyan K, Singh A, Singh S, Saxena AK, Nain L. Technological interventions for utilization of crop residues and weedy biomass for second generation bio-ethanol production. *Renew. Energy.* 2019;132:723–41.
37. IEA. Renewables 2018. Market analysis and forecast from 2018 to 2023. *Int. Energy Agency.* 2018
38. Schill SR. IEA says 3-fold or greater increase in biofuels possible by 2040. *Ethanol Prod. Mag.* 2015 [cited 2019 Sep 10]. Available from: <http://ethanolproducer.com/articles/12776/iea-says-3-fold-or-greater-increase-in-biofuels-possible-by-2040>
39. Jönsson LJ, Alriksson B, Nilvebrant N. Bioconversion of lignocellulose: inhibitors and detoxification. *Biotechnol. Biofuels.* 2013;6:16.

40. U.S. National Library of Medicine. PubChem Database. Ethanol, CID=702. Natl. Cent. Biotechnol. Inf. [cited 2019 Sep 5]. Available from:
<https://pubchem.ncbi.nlm.nih.gov/compound/Ethanol>
41. Balat M. Production of bioethanol from lignocellulosic materials via the biochemical pathway: a review. *Energy Convers. Manag.* 2011;52:858–75.
42. Iodice P, Langella G, Amoresano A. Ethanol in gasoline fuel blends: effect on fuel consumption and engine out emissions of SI engines in cold operating conditions. *Appl. Therm. Eng.* 2018;130:1081–9.
43. Demirbaş A. Bioethanol from cellulosic materials: a renewable motor fuel from biomass. *Energy Sources.* 2005;27:327–37.
44. Koehler N, Mccaherty J, Rfa CW, Cooper G. 2019 Ethanol industry outlook. 2019.
45. Ludwig D, Mangel M, Haddad B. Fuel ethanol: background and public policy issues. In: Leland WP, editor. *Alcohol fuels policies, Prod. potential.* 1982. p. 33–56.
46. Wang Y, Cheng M-H. Greenhouse gas emissions embedded in US-China fuel ethanol trade: a comparative well-to-wheel estimate. *J. Clean. Prod.* 2018;183:653–61.
47. Stout SA, Douglas GS, Uhler AD. Automotive gasoline. In: Morrison RD, Murphy BL, editors. *Environ. Forensics Contam. Specif. Guid.* Elsevier; 2010. p. 465–531.
48. Wang M, Han J, Dunn JB, Cai H, Elgowainy A. Well-to-wheels energy use and greenhouse gas emissions of ethanol from corn, sugarcane and cellulosic biomass for US use. *Effic. Sustain. Biofuel Prod. Environ. Land-Use Res.* 2015;249–80.
49. Choi JH, Jang SK, Kim JH, Park SY, Kim JC, Jeong H, et al. Simultaneous production of glucose, furfural, and ethanol organosolv lignin for total utilization of high recalcitrant biomass by organosolv pretreatment. *Renew. Energy.* 2019;130:952–60.
50. Zhou Z, Lei F, Li P, Jiang J. Lignocellulosic biomass to biofuels and biochemicals: a comprehensive review with a focus on ethanol organosolv pretreatment technology. *Biotechnol. Bioeng.* 2018;115:2683–702.
51. Rosillo-Calle F, Walter A. Global market for bioethanol: historical trends and future prospects. *Energy Sustain. Dev.* 2006;X:20–32.
52. OECD/FAO. *Biofuels. OECD-FAO Agric. Outlook 2018-2027.* 2018.
53. Bai FW, Anderson WA, Moo-Young M. Ethanol fermentation technologies from sugar

and starch feedstocks. *Biotechnol. Adv.* 2008;26:89–105.

54. DOE. U.S. Production, Consumption, and Trade of Ethanol. U.S. Dep. Energy. 2019 [cited 2019 Sep 11]. Available from: <https://afdc.energy.gov/data/10323>

55. Vasconcelos JN de. Ethanol Fermentation. In: Santos F, Borém A, Caldas C, editors. *Sugarcane Agric. Prod. bioenergy ethanol*. London: Academic Press; 2015. p. 311–40.

56. Barros S, Berk C. Brazil biofuels annual. *Glob. Agric. Inf. Netw.* Washington, DC (BR18017); 2018.

57. Trading Economics. Ethanol stock price. *Trading Econ.* 2019 [cited 2019 Sep 10]. Available from: <https://tradingeconomics.com/commodity/ethanol>

58. Axelsson L, Franzén M, Ostwald M, Berndes G, Lakshmi G, Ravindranath NH. Time to rethink cellulosic biofuels? *Biofuels, Bioprod. Biorefining.* 2018;12:5–7.

59. Friedl A. Bioethanol from sugar and starch. In: Kaltschmitt M, editor. *Energy from Org. Mater. A Vol. Encycl. Sustain. Sci. Technol.* 2nd ed. New York: Springer; 2019. p. 905–24.

60. Ingledew WMM, Lin Y-H. Ethanol from starch-based feedstocks. In: Moo-Young M, editor. *Compr. Biotechnol.* 3rd ed. Elsevier; 2011. p. 37–49.

61. Kim TH, Kim TH. Overview of technical barriers and implementation of cellulosic ethanol in the U.S. *Energy.* 2014;66:13–9.

62. Naik SN, Goud V V., Rout PK, Dalai AK. Production of first and second generation biofuels: a comprehensive review. *Renew. Sustain. Energy Rev.* 2010;14:578–97.

63. Robertson GH, Wong DWS, Lee CC, Wagschal K, Smith MR, Orts WJ. Native or raw starch digestion: a key step in energy efficient biorefining of grain. *J. Agric. Food Chem.* 2006;54:353–65.

64. Bothast RJ, Schlicher MA. Biotechnological processes for conversion of corn into ethanol. *Appl. Microbiol. Biotechnol.* 2005;67:19–25.

65. Jacques KA, Lyons TP, Kelsall DR, editors. *The alcohol textbook. A reference for the beverage, fuel and industrial alcohol industries.* 4th ed. Nottingham, United Kingdom: Nottingham University Press; 2003.

66. Maity SK. Opportunities, recent trends and challenges of integrated biorefinery: Part I. *Renew. Sustain. Energy Rev.* 2015;43:1427–45.

67. Ai Y, Jane JL. Macronutrients in corn and human nutrition. *Compr. Rev. Food Sci. Food*

Saf. 2016;15:581–98.

68. Rojas OJ, Stein HH. Effects of reducing the particle size of corn grain on the concentration of digestible and metabolizable energy and on the digestibility of energy and nutrients in corn grain fed to growing pigs. *Livest. Sci.* 2015;181:187–93.

69. Gibreel A, Sandercock JR, Lan J, Goonewardene L a., Zijlstra RT, Curtis JM, et al. Fermentation of barley by using *Saccharomyces cerevisiae*: examination of barley as a feedstock for bioethanol production and value-added products. *Appl. Environ. Microbiol.* 2009;75:1363–72.

70. Wang P, Singh V, Xue H, Johnston DB, Rausch KD, Tumbleson ME. Comparison of raw starch hydrolyzing enzyme with conventional liquefaction and saccharification enzymes in dry-grind corn processing. *Cereal Chem.* 2007;84:10–4.

71. Parashar A, Jin Y, Mason B, Chae M, Bressler DC. Incorporation of whey permeate, a dairy effluent, in ethanol fermentation to provide a zero waste solution for the dairy industry. *J. Dairy Sci.* 2015;99:1859–67.

72. Lopes ML, Paulillo SC de L, Godoy A, Cherubin RA, Lorenzi MS, Giometti FHC, et al. Ethanol production in Brazil: a bridge between science and industry. *Brazilian J. Microbiol.* 2016;47s:64–76.

73. Jin Y. Co-Fermentation of wheat and whey permeate for ethanol production and chemical characteristics of the resulting dried distillers' grains with solubles. University of Alberta; 2014.

74. Devantier R, Pedersen S, Olsson L. Characterization of very high gravity ethanol fermentation of corn mash. Effect of glucoamylase dosage, pre-saccharification and yeast strain. *Appl. Microbiol. Biotechnol.* 2005;68:622–9.

75. Puligundla P, Smogrovicova D, Obulam VSR, Ko S. Very high gravity (VHG) ethanolic brewing and fermentation: a research update. *J. Ind. Microbiol. Biotechnol.* 2011;38:1133–44.

76. Zacchi G, Axelsson A. Economic evaluation of preconcentration in production of ethanol from dilute sugar solutions. *Biotechnol. Bioeng.* 1989;34:223–33.

77. Puligundla P, Smogrovicova D, Mok C, Obulam VSR. A review of recent advances in high gravity ethanol fermentation. *Renew. Energy.* 2019;133:1366–79.

78. Basso LC, Basso TO, Rocha SN. Ethanol production in Brazil: the industrial process and its impact on yeast fermentation. In: Bernardes MADS, editor. *Biofuel Prod. Recent Dev. Prospect.* Rijeka, Croatia: InTech; 2011. p. 85–100.
79. Dalena F, Senatore A, Iulianelli A, Paola L Di, Basile M, Basile A. Ethanol from biomass: future and perspectives. *Ethanol.* Elsevier; 2019. p. 25–59.
80. Abud AKDS, Silva CEDF. Bioethanol in Brazil: status, challenges and perspectives to improve the production. *Bioethanol Prod. from Food Crop.* Elsevier; 2019. p. 417–43.
81. Dias MOS, Cunha MP, Jesus CDF, Scandiffio MIG, Rossell CE V, Filho RM, et al. Simulation of ethanol production from sugarcane in Brazil: economic study of an autonomous distillery. *Comput. Aided Chem. Eng.* 2010;28:733–8.
82. Vallejo JA, Sánchez-Pérez A, Martínez JP, Villa TG. Cell aggregations in yeasts and their applications. *Appl. Microbiol. Biotechnol.* 2013;97:2305–18.
83. Verstrepen KJ, Klis FM. Flocculation, adhesion and biofilm formation in yeasts. *Mol. Microbiol.* 2006;60:5–15.
84. Westman JO, Mapelli V, Taherzadeh MJ, Franzén CJ. Flocculation causes inhibitor tolerance in *Saccharomyces cerevisiae* for second-generation bioethanol production. *Appl. Environ. Microbiol.* 2014;80:6908–18.
85. Soares E V. Flocculation in *Saccharomyces cerevisiae*: a review. *J. Appl. Microbiol.* 2011;110:1–18.
86. Verstrepen KJ, Derdelinckx G, Verachtert H, Delvaux FR. Yeast flocculation: what brewers should know. *Appl. Microbiol. Biotechnol.* 2003;61:197–205.
87. Guo B, Styles CA, Feng Q, Fink GR. A *Saccharomyces* gene family involved in invasive growth, cell–cell adhesion, and mating. *Proc. Natl. Acad. Sci.* 2000;97:12158–63.
88. Kim M, Day DF. Composition of sugar cane, energy cane, and sweet sorghum suitable for ethanol production at Louisiana sugar mills. *J. Ind. Microbiol. Biotechnol.* 2011;38:803–7.
89. Hettinga WG, Junginger HM, Dekker SC, Hoogwijk M, McAloon AJ, Hicks KB. Understanding the reductions in US corn ethanol production costs: an experience curve approach. *Energy Policy.* 2009;37:190–203.
90. Goldemberg J, Coelho ST, Nastari PM, Lucon O. Ethanol learning curve - the Brazilian experience. *Biomass and Bioenergy.* 2004;26:301–4.

91. Hassan SS, Williams GA, Jaiswal AK. Moving towards the second generation of lignocellulosic biorefineries in the EU: drivers, challenges, and opportunities. *Renew. Sustain. Energy Rev.* 2019;101:590–9.
92. Smeets EMW, Faaij APC, Lewandowski IM, Turkenburg WC. A bottom-up assessment and review of global bio-energy potentials to 2050. *Prog. Energy Combust. Sci.* 2007;33:56–106.
93. NREL. NREL Proves cellulosic ethanol can be cost competitive. Golden, CO (NREL/FS-6A42-60663); 2014.
94. Gray K a, Zhao L, Emptage M. Bioethanol. *Curr. Opin. Chem. Biol.* 2006;10:141–6.
95. Pirani S, Hashaikeh R. Nanocrystalline cellulose extraction process and utilization of the byproduct for biofuels production. *Carbohydr. Polym.* 2013;93:357–63.
96. Mosier N, Wyman C, Dale B, Elander R, Lee YY, Holtzapple M, et al. Features of promising technologies for pretreatment of lignocellulosic biomass. *Bioresour. Technol.* 2005;96:673–86.
97. Yang B, Wyman CE. Pretreatment: the key to unlocking low-cost cellulosic ethanol. *Biofuels, Bioprod. Biorefining.* 2008;2:26–40.
98. Sindhu R, Binod P, Pandey A. Biological pretreatment of lignocellulosic biomass - an overview. *Bioresour. Technol.* 2016;199:76–82.
99. Sims REH, Mabee W, Saddler JN, Taylor M. An overview of second generation biofuel technologies. *Bioresour. Technol.* 2010;101:1570–80.
100. Prasad S, Singh A, Joshi HC. Ethanol as an alternative fuel from agricultural, industrial and urban residues. *Resour. Conserv. Recycl.* 2007;50:1–39.
101. Canilha L, Chandel AK, Suzane Dos Santos Milessi T, Antunes FAF, Luiz Da Costa Freitas W, Das Graças Almeida Felipe M, et al. Bioconversion of sugarcane biomass into ethanol: an overview about composition, pretreatment methods, detoxification of hydrolysates, enzymatic saccharification, and ethanol fermentation. *J. Biomed. Biotechnol.* 2012;2012.
102. Phitsuwan P, Laohakunjit N, Kerdchoechuen O, Kyu KL, Ratanakhanokchai K. Present and potential applications of cellulases in agriculture, biotechnology, and bioenergy. *Folia Microbiol.* 2013;58:163–76.

103. Liu CG, Xiao Y, Xia XX, Zhao XQ, Peng L, Srinophakun P, et al. Cellulosic ethanol production: progress, challenges and strategies for solutions. *Biotechnol. Adv.* 2019;37:491–504.
104. Larsen J, Øtergaard Petersen M, Thirup L, Li HW, Iversen FK. The IBUS process - lignocellulosic bioethanol close to a commercial reality. *Chem. Eng. Technol.* 2008;31:765–72.
105. Chen X, Kuhn E, Jennings EW, Nelson R, Tao L, Zhang M, et al. DMR (deacetylation and mechanical refining) processing of corn stover achieves high monomeric sugar concentrations (230 g L⁻¹) during enzymatic hydrolysis and high ethanol concentrations (>10% v/v) during fermentation without hydrolysate purification or concentration. *Energy Environ. Sci.* 2016;9:1237–45.
106. Merino ST, Cherry J. Progress and challenges in enzyme development for biomass utilization. *Adv. Biochem. Eng. Biotechnol.* 2007. p. 95–120.
107. Novozymes. Novozymes Cellic® CTec3 - Secure your plant's lowest total cost. 2012.
108. Mohagheghi A, Linger JG, Yang S, Smith H, Dowe N, Zhang M, et al. Improving a recombinant *Zymomonas mobilis* strain 8b through continuous adaptation on dilute acid pretreated corn stover hydrolysate. *Biotechnol. Biofuels.* 2015;8:55.
109. Zhang K, Wells P, Liang Y, Love J, Parker DA, Botella C. Effect of diluted hydrolysate as yeast propagation medium on ethanol production. *Bioresour. Technol.* 2019;271:1–8.
110. Cai CM, Zhang T, Kumar R, Wyman CE. Integrated furfural production as a renewable fuel and chemical platform from lignocellulosic biomass. *J. Chem. Technol. Biotechnol.* 2014;89:2–10.
111. Ragauskas AJ, Beckham GT, Biddy MJ, Chandra R, Chen F, Davis MF, et al. Lignin valorization: improving lignin processing in the biorefinery. *Science.* 2014;344:1246843.
112. Moon R, Beck S, Rudie A. Cellulose nanocrystals—a material with unique properties and many potential applications. In: Postek MT, Moon RJ, Rudie A, Bilodeau MA, editors. *Prod. Appl. Cellul. Nanomater.* Peachtree Corners, GA, USA: TAPPI Press; 2013. p. 9–12.
113. George J, Sabapathi S. Cellulose nanocrystals: synthesis, functional properties, and applications. *Nanotechnol. Sci. Appl.* 2015;8:45–54.
114. Beyene D, Chae M, Dai J, Danumah C, Tosto F, Demesa AG, et al. Enzymatically-

mediated co-production of cellulose nanocrystals and fermentable sugars. *Catalysts*. 2017;7:322.

115. Moysés DN, Reis VCB, de Almeida JRM, de Moraes LMP, Torres FAG. Xylose fermentation by *Saccharomyces cerevisiae*: challenges and prospects. *Int. J. Mol. Sci.* 2016;17:1–18.

116. Russell I. Yeast. In: Stewart GG, Priest FG, editors. *Handb. Brew.* 2nd ed. Boca Raton, FL, the United States: CRC Press; 2006. p. 281–332.

117. Lagunas R. Sugar transport in *Saccharomyces cerevisiae*. *FEMS Microbiol. Lett.* 1993;104:229–42.

118. Zamora F. Biochemistry of alcoholic fermentation. In: Moreno-Arribas MV, Polo MC, editors. *Wine Chem. Biochem.* New York: Springer; 2009. p. 3–26.

119. Zoecklein BW, Fugelsang KC, Gump BH, Nury FS. Oxygen, carbon dioxide, and nitrogen. In: Zoecklein BW, Fugelsang KC, Gump BH, Nury FS, editors. *Wine Anal. Prod.* New York: Chapman & Hall; 1999. p. 216–27.

120. Patiño MA, Ortiz JP, Velásquez M, Stambuk BU. D-Xylose consumption by nonrecombinant *Saccharomyces cerevisiae* : a review. *Yeast*. 2019;1–16.

121. Bajwa PK, Shireen T, D’Aoust F, Pinel D, Martin VJJ, Trevors JT, et al. Mutants of the pentose-fermenting yeast *Pichia stipitis* with improved tolerance to inhibitors in hardwood spent sulfite liquor. *Biotechnol. Bioeng.* 2009;104:892–900.

122. Delgenes JP, Moletta R, Navarro JM. Effects of lignocellulose degradation products on ethanol fermentations of glucose and xylose by *Saccharomyces cerevisiae*, *Zymomonas mobilis*, *Pichia stipitis*, and *Candida shehatae*. *Enzyme Microb. Technol.* 1996;19:220–5.

123. Hou X. Anaerobic xylose fermentation by *Spathaspora passalidarum*. *Appl. Microbiol. Biotechnol.* 2012;94:205–14.

124. McMillan JD. Xylose fermentation to ethanol: a review. Golden, CO (No. NREL/TP-421-4944); 1993.

125. Sato TK, Tremaine M, Parreiras LS, Hebert AS, Myers KS, Higbee AJ, et al. Directed evolution reveals unexpected epistatic interactions that alter metabolic regulation and enable anaerobic xylose use by *Saccharomyces cerevisiae*. *PLoS Genet.* 2016;12:e1006372.

126. Kim SR, Kwee NR, Kim H, Jin YS. Feasibility of xylose fermentation by engineered

Saccharomyces cerevisiae overexpressing endogenous aldose reductase (GRE3), xylitol dehydrogenase (XYL2), and xylulokinase (XYL3) from *Scheffersomyces stipitis*. *FEMS Yeast Res.* 2013;13:312–21.

127. Parreiras LS, Breuer RJ, Narasimhan RA, Higbee AJ, La Reau A, Tremaine M, et al. Engineering and two-stage evolution of a lignocellulosic hydrolysate-tolerant *Saccharomyces cerevisiae* strain for anaerobic fermentation of xylose from AFEX pretreated corn stover. *PLoS One.* 2014;9:e107499.

128. Verhoeven MD, De Valk SC, Daran JMG, Van Maris AJA, Pronk JT. Fermentation of glucose-xylose-arabinose mixtures by a synthetic consortium of single-sugar-fermenting *Saccharomyces cerevisiae* strains. *FEMS Yeast Res.* 2018;18:foy075.

129. Turner TL, Kim H, Kong II, Liu JJ, Zhang GC, Jin YS. Engineering and evolution of *Saccharomyces cerevisiae* to produce biofuels and chemicals. In: Zhao H, Zeng A-P, editors. *Synth. Biol. Eng.* Springer; 2017. p. 175–216.

130. Pinto ASS, Pereira SC, Ribeiro MPA, Farinas CS. Monitoring of the cellulosic ethanol fermentation process by near-infrared spectroscopy. *Bioresour. Technol.* 2016;203:334–40.

131. Veale EL, Irudayaraj J, Demirci A. An on-line approach to monitor ethanol fermentation using FTIR spectroscopy. *Biotechnol. Prog.* 2007;23:494–500.

132. Iversen JA, Ahring BK. Monitoring lignocellulosic bioethanol production processes using Raman spectroscopy. *Bioresour. Technol.* 2014;172:112–20.

133. Gray SR, Peretti SW, Lamb HH. Real-time monitoring of high-gravity corn mash fermentation using in situ raman spectroscopy. *Biotechnol. Bioeng.* 2013;110:1654–62.

134. Moo-Young M, editor. *Comprehensive Biotechnology*. 2nd ed. Elsevier; 2011.

135. Godoy A, Amorim H V, Lopes ML, Oliveira AJ. Continuous and batch fermentation processes: advantages and disadvantages of these processes in the Brazilian ethanol production. *Int. sugar J.* 2008;110:175–82.

136. Rattanapan A, Limtong S, Phisalaphong M. Ethanol production by repeated batch and continuous fermentations of blackstrap molasses using immobilized yeast cells on thin-shell silk cocoons. *Appl. Energy.* 2011;88:4400–4.

137. Yu J, Zhang X, Tan T. An novel immobilization method of *Saccharomyces cerevisiae* to sorghum bagasse for ethanol production. *J. Biotechnol.* 2007;129:415–20.

138. Brethauer S, Wyman CE. Review: continuous hydrolysis and fermentation for cellulosic ethanol production. *Bioresour. Technol.* 2010;101:4862–74.
139. Moon SK, Kim SW, Choi GW. Simultaneous saccharification and continuous fermentation of sludge-containing mash for bioethanol production by *Saccharomyces cerevisiae* CHFY0321. *J. Biotechnol.* 2012;157:584–9.
140. Xu TJ, Zhao XQ, Bai FW. Continuous ethanol production using self-flocculating yeast in a cascade of fermentors. *Enzyme Microb. Technol.* 2005;37:634–40.
141. De Oliva-Neto P, Dorta C, Azevedo F, Gomes V, Fernandes D. The Brazilian technology of fuel ethanol fermentation – yeast inhibition factors and new perspectives to improve the technology. *Formatex.* 2013;371–9.
142. Brown WA, Cooper DG. Hydrocarbon degradation by *Acinetobacter calcoaceticus* RAG-1 using the self-cycling fermentation technique. *Biotechnol. Bioeng.* 1992;40:797–805.
143. Sauvageau D, Storms Z, Cooper DG. Synchronized populations of *Escherichia coli* using simplified self-cycling fermentation. *J. Biotechnol.* 2010;149:67–73.
144. Brown WA, Cooper DG, Liss SN. Adapting the self-cycling fermentor to anoxic conditions. *Environ. Sci. Technol.* 1999;33:1458–63.
145. Sauvageau D, Cooper DG. Two-stage, self-cycling process for the production of bacteriophages. *Microb. Cell Fact.* 2010;9:81.
146. Blumenthal LK, Zahler SA. Index for measurement of Synchronization of cell populations. *Science.* 1962. p. 724.
147. Kida K, Morimura S, Kume K, Suruga K, Sonoda Y. Repeated-batch ethanol fermentation by a flocculating yeast, *Saccharomyces cerevisiae* IR-2. *J. Ferment. Bioeng.* 1991;71:340–4.
148. Kida K, Kume K, Morimura S, Sonoda Y. Repeated-batch fermentation process using a thermotolerant flocculating yeast constructed by protoplast fusion. *J. Ferment. Bioeng.* 1992;74:169–73.
149. Feng S, Srinivasan S, Lin YH. Redox potential-driven repeated batch ethanol fermentation under very-high-gravity conditions. *Process Biochem.* 2012;47:523–7.
150. Ma K, Wakisaka M, Sakai K, Shirai Y. Flocculation characteristics of an isolated mutant flocculent *Saccharomyces cerevisiae* strain and its application for fuel ethanol production

- from kitchen refuse. *Bioresour. Technol.* 2009;100:2289–92.
151. Ma KD, Wakisaka M, Kiuchi T, Praneetrattananon S, Morimura S, Kida K, et al. Repeated-batch ethanol fermentation of kitchen refuse by acid-tolerant flocculating yeast under the non-sterilized condition. *Japan J. Food Eng.* 2007;8:275–9.
152. Goldemberg J. Ethanol for a sustainable energy future. *Science.* 2007;315:808–10.
153. Kumar R, Tabatabaei M, Karimi K, Horváth IS. Recent updates on lignocellulosic biomass derived ethanol - a review. *Biofuel Res. J.* 2016;3:347–56.
154. Chen X, Shekiri J, Pschorn T, Sabourin M, Tao L, Elander R, et al. A highly efficient dilute alkali deacetylation and mechanical (disc) refining process for the conversion of renewable biomass to lower cost sugars. *Biotechnol. Biofuels.* 2014;7:98.
155. Teter SA. DECREASE Final Technical Report: Development of a Commercial Ready Enzyme Application System for Ethanol. Davis CA; 2012.
156. Bamforth CW. pH in brewing: an overview. *Tech. Quarterly-Master Brew. Assoc. Am.* 2001;38:1–9.
157. Shuler M, Filkret K. *Bioprocess engineering: basic concepts.* 2nd ed. Upper Saddle River, NJ: Prentice Hall; 2002.
158. Bai FW, Anderson WA, Moo-Young M. Ethanol fermentation technologies from sugar and starch feedstocks. *Biotechnol. Adv.* 2008;26:89–105.
159. Tomás-pejó E, Olsson L. Influence of the propagation strategy for obtaining robust *Saccharomyces cerevisiae* cells that efficiently co-ferment xylose and glucose in lignocellulosic hydrolysates. *Microb. Biotechnol.* 2015;8:999–1005.
160. 110th United States Congress, H.R.6: Energy Independence and Security Act of 2007. [cited 2019 Oct 3]. Available from: <https://www.congress.gov/bill/110th-congress/house-bill/6>
161. Nguyen TY, Cai CM, Kumar R, Wyman CE. Overcoming factors limiting high-solids fermentation of lignocellulosic biomass to ethanol. *Proc. Natl. Acad. Sci.* 2017;114:11673–8.
162. Wang J, Chae M, Sauvageau D, Bressler DC. Improving ethanol productivity through self-cycling fermentation of yeast: a proof of concept. *Biotechnol. Biofuels.* 2017;10:193.
163. Liu CG, Liu LY, Lin YH, Bai FW. Kinetic modeling for redox potential-controlled repeated batch ethanol fermentation using flocculating yeast. *Process Biochem.* 2015;50:1–

7.

164. Sablayrolles JM, Barre P, Grenier P. Design of a laboratory automatic system for studying alcoholic fermentations in anisothermal enological conditions. *Biotechnol. Tech.* 1987;1:181-4.

165. Straver MH, Aar PCVD, Smit G, Kijne JW. Determinants of flocculence of brewer's yeast during fermentation in wort. *Yeast.* 1993;9:527-32.

166. Andreasen AA, Stier TJB. Anaerobic nutrition of *Saccharomyces cerevisiae*. I. Ergosterol requirement for growth in a defined medium. *J. Cell. Comp. Physiol.* 1953;41:23-36.

167. Andreasen AA, Stier TJB. Anaerobic nutrition of *saccharomyces cerevisiae*. II. Unsaturated fatty and requirement for growth in a defined medium. *J. Cell. Comp. Physiol.* 1954;43:271-81.

168. Zoecklein BW, Fugelsang KC, Gump BH, Nury FS. *Wine analysis and production*. New York: Chapman & Hall; 1999.

169. Gray K a., Zhao L, Emptage M. *Bioethanol.* *Curr. Opin. Chem. Biol.* 2006;10:141-6.

170. Almario MP, Reyes LH, Kao KC. Evolutionary engineering of *Saccharomyces cerevisiae* for enhanced tolerance to hydrolysates of lignocellulosic biomass. *Biotechnol. Bioeng.* 2013;110:2616-23.

171. Zhang H, Ping Q, Zhang J, Li N. Determination of furfural and hydroxymethyl furfural by UV spectroscopy in ethanol-water hydrolysate of Reed. *J. Bioresour. Bioprod.* 2017;2:170-4.

172. Modig T, Almeida JRM, Gorwa-Grauslund MF, Lidén G. Variability of the response of *Saccharomyces cerevisiae* strains to lignocellulose hydrolysate. *Biotechnol. Bioeng.* 2008;100:423-9.

173. Brumm PJ, Hebeda RE. Glycerol production in industrial alcohol fermentations. *Biotechnol. Lett.* 1988;10:677-82.

174. Chen X, Shekiro J, Pschorn T, Sabourin M, Tucker MP, Tao L. Techno-economic analysis of the deacetylation and disk refining process: characterizing the effect of refining energy and enzyme usage on minimum sugar selling price and minimum ethanol selling price. *Biotechnol Biofuels.* 2015;8:173.

175. Nielsen MK, Arneborg N. The effect of citric acid and pH on growth and metabolism of anaerobic *Saccharomyces cerevisiae* and *Zygosaccharomyces bailii* cultures. *Food Microbiol.* 2007;24:101–5.
176. Cunha JT, Romaní A, Costa CE, Sá-Correia I, Domingues L. Molecular and physiological basis of *Saccharomyces cerevisiae* tolerance to adverse lignocellulose-based process conditions. *Appl. Microbiol. Biotechnol.* 2019;103:159–75.
177. Monod J. The growth of bacterial cultures. *Annu. Rev. Microbiol.* 1949;3:371–94.
178. Epstein W, Naono S, Gros F. Synthesis of enzymes of the lactose operon during diauxic growth of *Escherichia coli*. *Biochem. Biophys. Res. Commun.* 1966;24:588–92.
179. Venturelli OS, Zuleta I, Murray RM, El-Samad H. Population diversification in a yeast metabolic program promotes anticipation of environmental shifts. *PLoS Biol.* 2015;13:1–24.
180. Boulineau S, Tostevin F, Kiviet DJ, ten Wolde PR, Nghe P, Tans SJ. Single-cell dynamics reveals sustained growth during diauxic shifts. *PLoS One.* 2013;8:e61686.
181. Dawson PS. A pilot plant apparatus for continuous phased culture--some observations on oxygen usage by *Candida utilis* during the cell cycle. *Biotechnol Bioeng.* 1971;13:877–92.

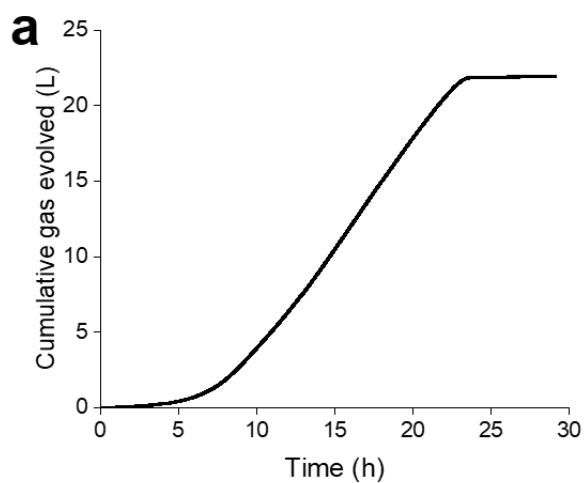
Appendix A: supplementary material for Chapter 4

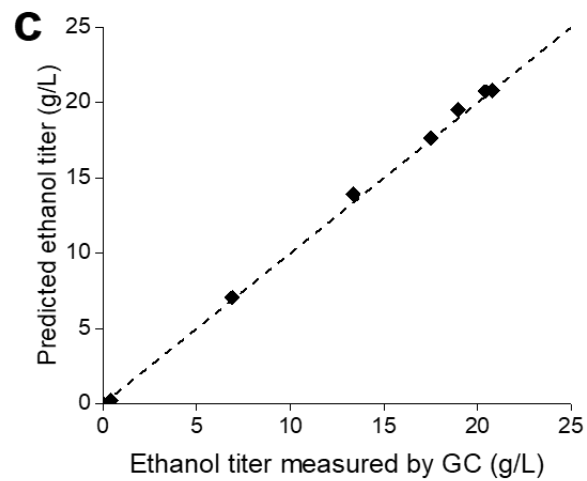
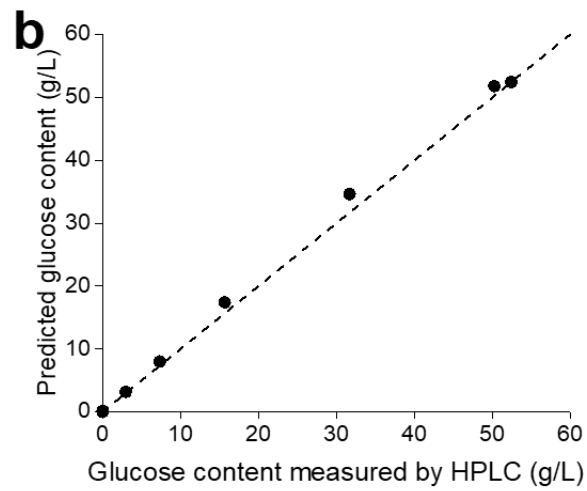
Additional Table 1. Comparison between batch and SCF operation under similar conditions.

Operation mode	Cycle time (h)	Ethanol produced (g/L)	Fermentation efficiency (%)	Annual ethanol productivity* (ton/year)
Batch	23.4	21.5 ± 0.1	81.1 ± 0.8	580 ± 3
SCF				
Cycle 1	22.6	22.4 ± 0.5	80.8-91.2	1020 ± 16
Cycle 4	10.7	10.5 ± 0.3		
Cycles 2,3,5-21	6.7-7.5	9.5-11.2		

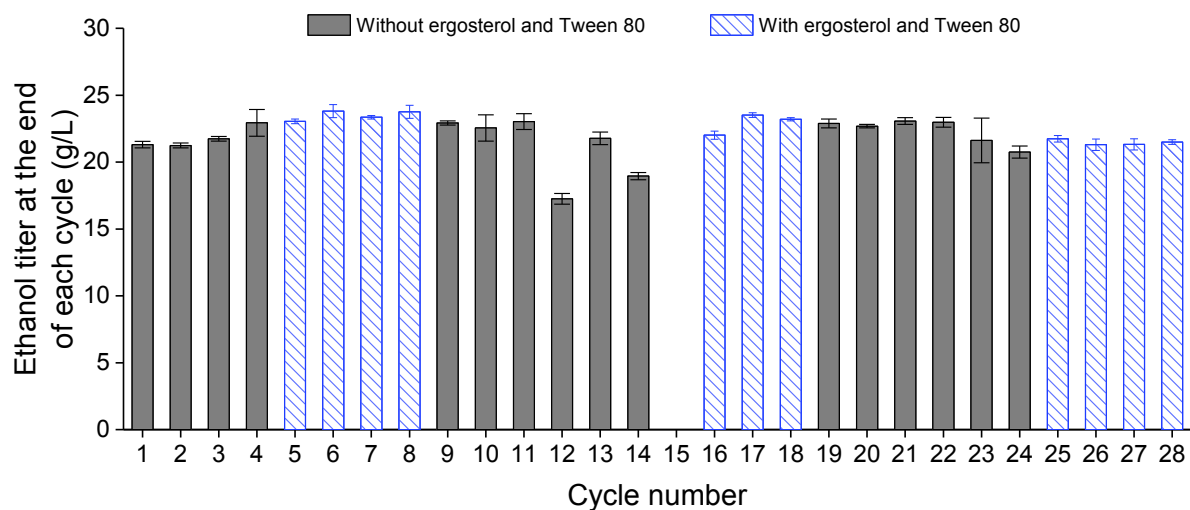
*Based on a fermenter of volume 10⁵ L.

Mean values from triplicate analysis ± standard deviation.

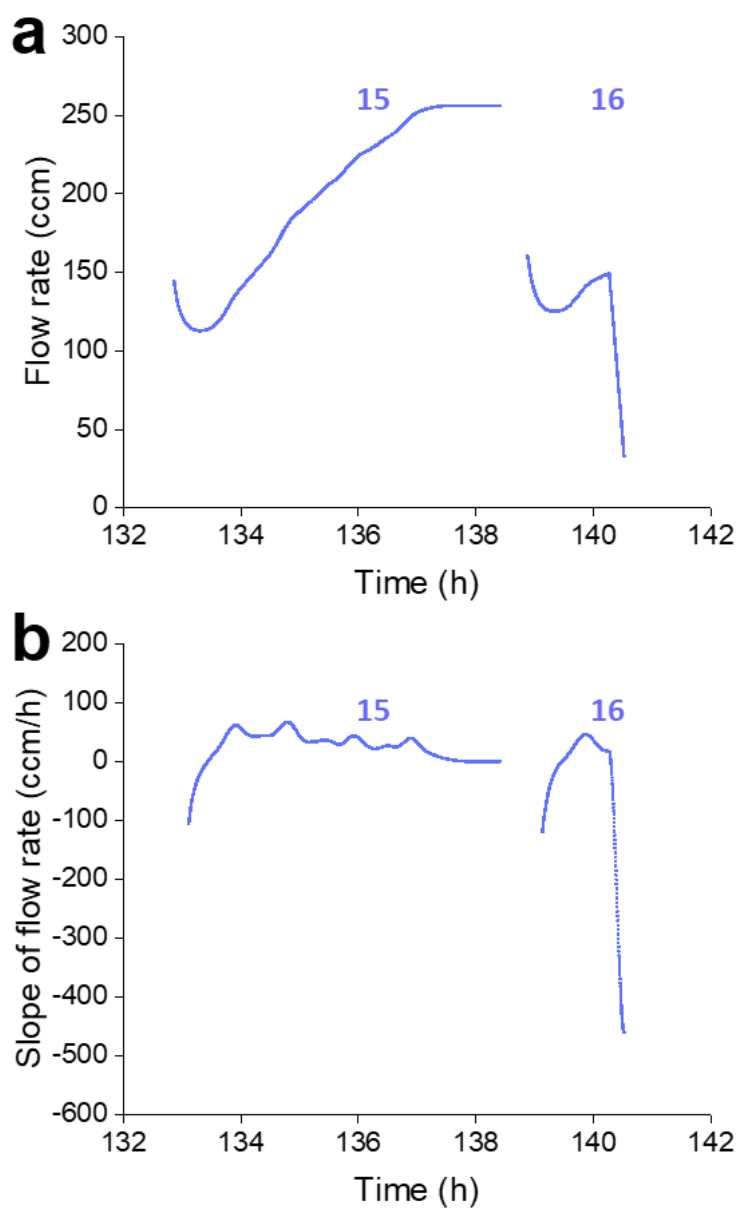




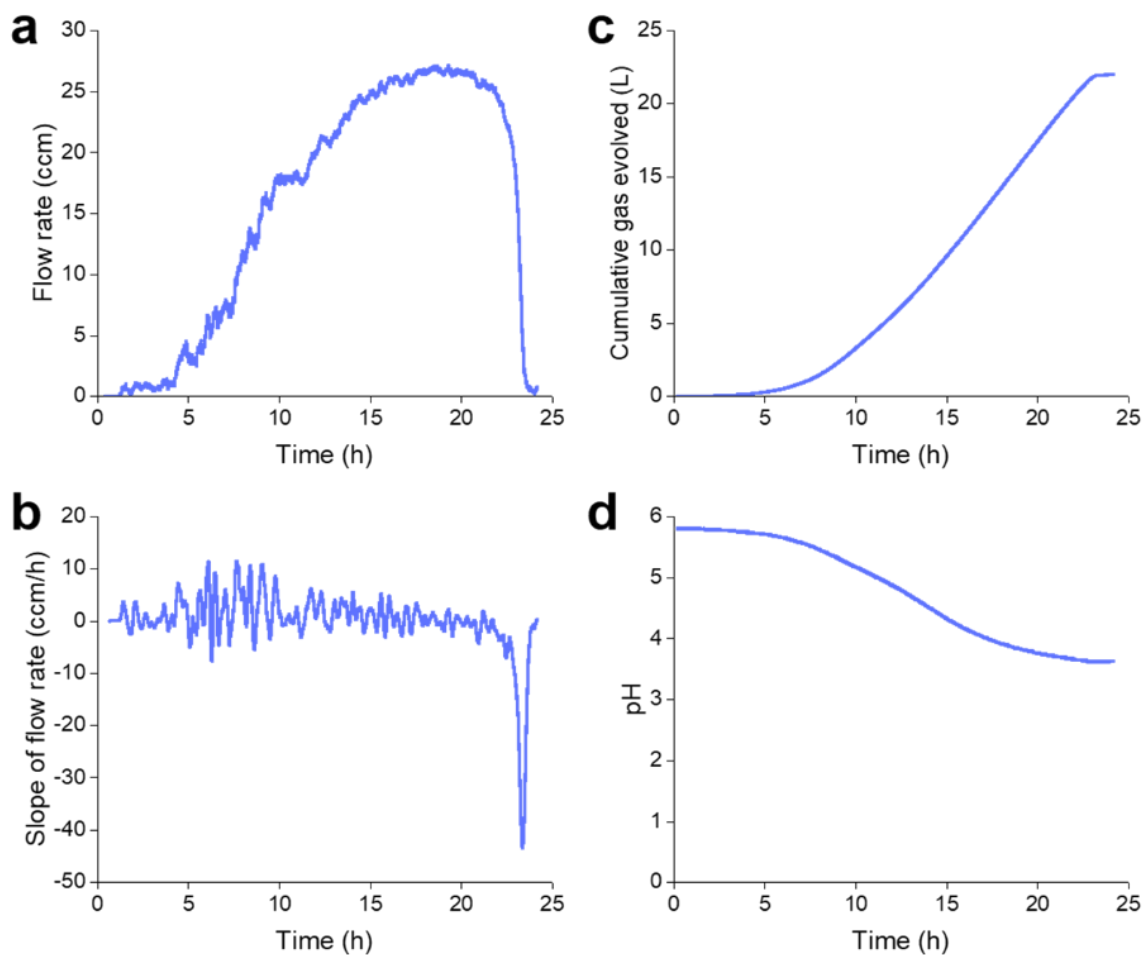
Additional Figure 1. Relationship between cumulative gas flow and fermentation parameters. The cumulative gas flow (a), as well as the predicted and measured contents of glucose (b) and ethanol (c) were plotted. The dotted lines in (b) and (c) represent ideal scenario where predicted values were equal to the measured ones.



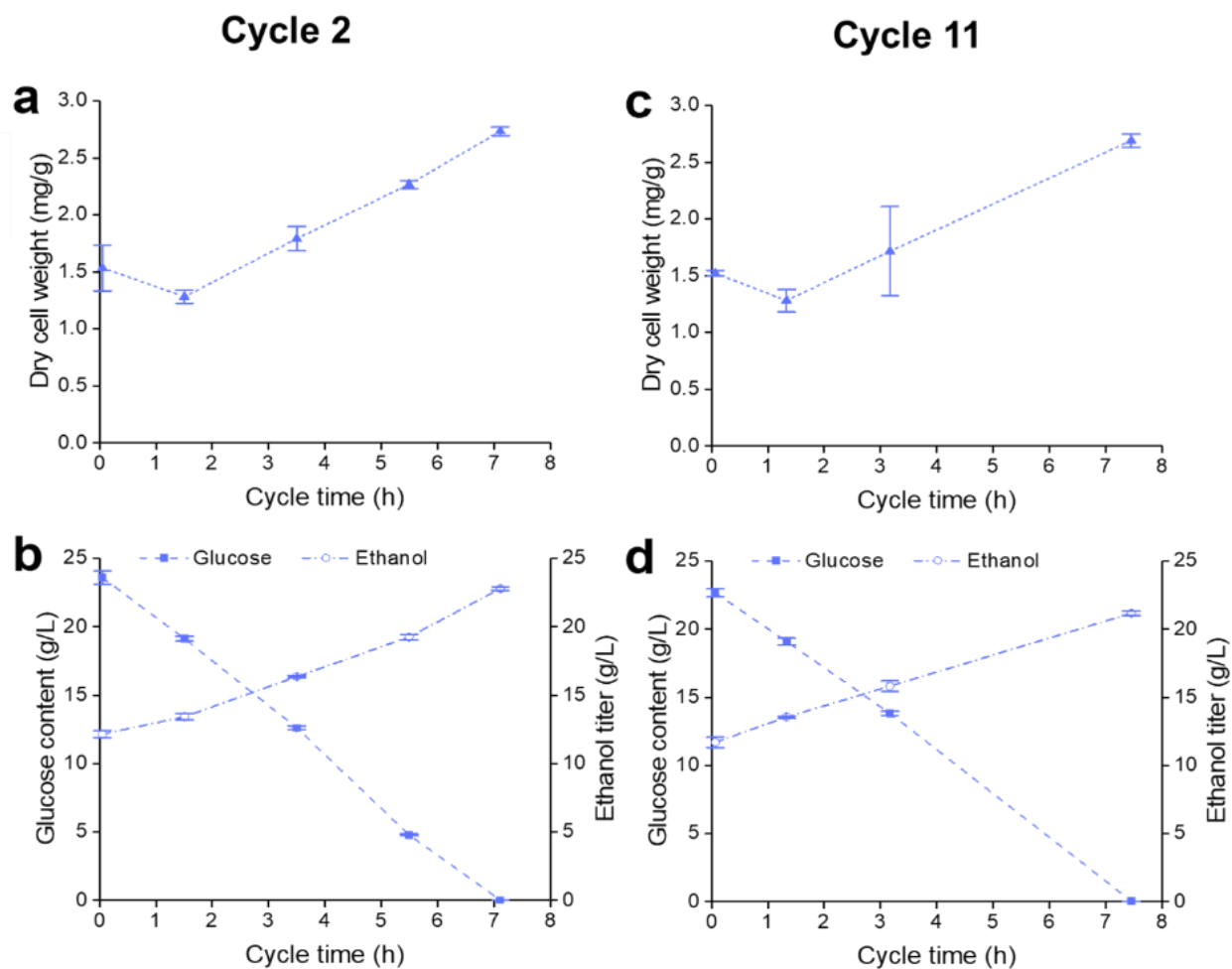
Additional Figure 2. Final ethanol titer at the end of each SCF cycle. SCF was performed using medium without or with the supplementation of ergosterol (0.02 g/L) and Tween 80 (0.8 g/L). The data reported is the average of triplicates, with error bars representing standard deviations. No samples were collected for the end of cycle 15.



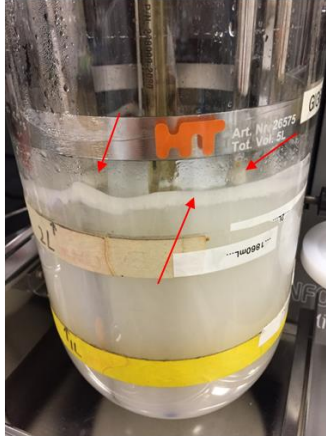
Additional Figure 3. Ergosterol and Tween 80 supplementation for cycle 15 and 16. Medium with supplementation of ergosterol (0.02 g/L) and Tween 80 (0.8 g/L) was used for these two cycles. Cycle numbers were labeled at the top of each figure. Cycle 15 and part of cycle 16 were removed from Figure 3c and d, due to excessive flow of nitrogen to the fermenter as a result of nitrogen regulator failure; however, they are displayed here for gas flow rate (a) and slope of gas flow rate (b).



Additional Figure 4. Batch fermentation with supplements. Medium supplemented with ergosterol (0.02 g/L) and Tween 80 (0.8 g/L) was used. Gas flow rate (a), slope of gas flow rate (b), total gas captured per cycle (c), and pH (d) were monitored throughout SCF operation.



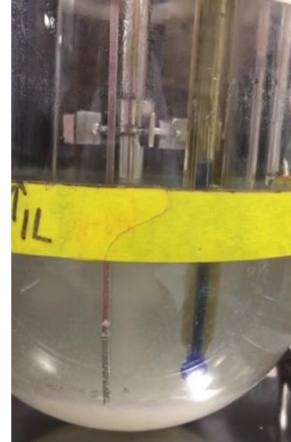
Additional Figure 5. Intracycle sampling during SCF demonstration. Biomass dry cell weight, glucose and ethanol concentrations were plotted for cycle 2 (a and b) and 11 (c and d). Medium supplemented with ergosterol (0.02 g/L) and Tween 80 (0.8 g/L) was used. The data reported is the average of triplicates, with error bars representing standard deviations.



a. Cell aggregated and deposited to fermenter wall and probes above the culture



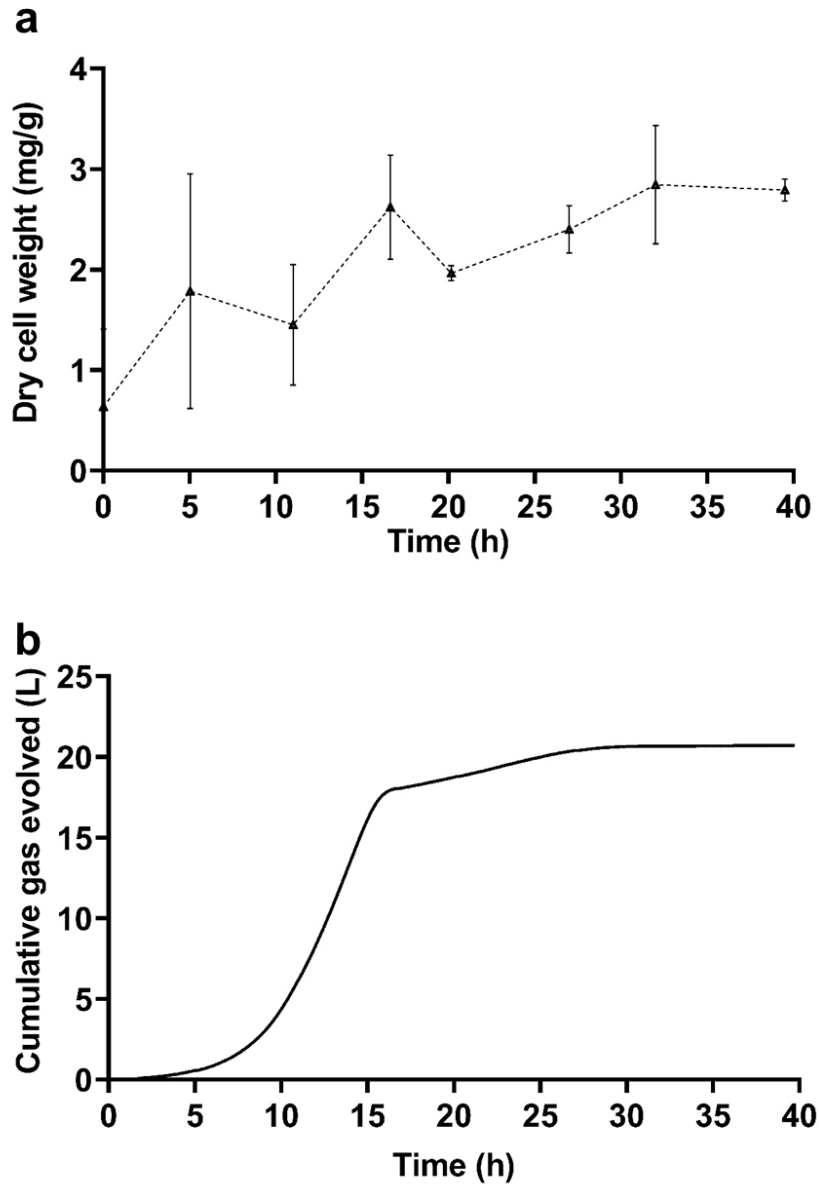
b. 0 s after impellor was completely stopped



c. 30 s after impellor was completely stopped

Additional Figure 6. Cell deposition and flocculation observed during SCF. A picture was taken at the end of cycle 21 (cycle time of 6.4 h) for a demonstration of cell deposition (a). Pictures were also taken at 0 s (b) and 30 s (c) after the impellor was completely stopped for cycle 21 to show the effect of flocculation.

Appendix B: supplementary material for Chapter 5



Additional Figure 7. Parameters monitored during batch fermentation. Dry cell weight (a) was measured at different time intervals during fermentation, while the cumulative gas evolved (b) was calculated in real time. Means from analytical triplicates are reported for panel (a), with error bars representing standard deviation.